論文 / 著書情報
Article / Book Information

題目(和文)	ガラスレンズ成形金型材料用Ni基アモルファス合金のコンビナトリアル探索
Title(English)	Combinatorial Approach of Ni-based Amorphous Alloys for Glass Lens Molding Die Materials
著者(和文)	Jiang Shengxian
Author(English)	Jiang Shengxian
出典(和文)	学位:博士(工学), 学位授与機関:東京工業大学, 報告番号:甲第9656号, 授与年月日:2014年9月25日, 学位の種別:課程博士, 審査員:秦　誠一,横田　眞一,香川　利春,初澤　毅,吉岡　勇人
Citation(English)	Degree:Doctor (Engineering), Conferring organization: Tokyo Institute of Technology, Report number:甲第9656号, Conferred date:2014/9/25, Degree Type:Course doctor, Examiner:,,,,
学位種別(和文)	博士論文
Type(English)	Doctoral Thesis

Combinatorial Approach of Ni-based Amorphous Alloys for Glass Lens Molding Die Materials

Supervised by

Prof. Seiichi Hata

Tokyo Institute of Technology

Department of Mechano-Micro Engineering

11D55193

JIANG Shengxian

Index

Chapter 1 Introduction and background

1.1Glass lenses with complex shape

1.1.1 Diffractive optical element

Along with the development of new technology, optical elements with precise microstructures occupy an increasingly important role in industry. Optical elements with microstructures can realize multiple optical functions which make it possible to miniaturize and optimize the design of optical components for systems and devices with small dimensions. Diffractive optical elements are usually designed to produce predetermined distribution of light by means of interference and diffraction or to optimize and miniaturize optical systems since they can perform many optical functions simultaneously.

Diffractive optical elements can also be applied in glass lens to mitigate chromatic aberration since they have opposite dispersion properties to that of ordinary convex lens. When a beam of parallel light comes pass a glass lens with diffraction gratings presented as Figure 1.1, the refractive index increases with the wavelength, which means that light with longer wavelength will focus closer to lens, meanwhile light with shorter wavelength will focus further from lens. However, this is totally contrary to the refraction condition of ordinary convex lens. Therefore, combining these two optical elements can lead to cancel out each other's chromatic aberration and lights with different wavelength can focus at

same point. According to this, glass lenses with diffraction gratings can be applied not only to the optical system in disk player which is able to read data written by different wavelengths of light, as well as camera lenses to optimize the optical system and improve image quality.

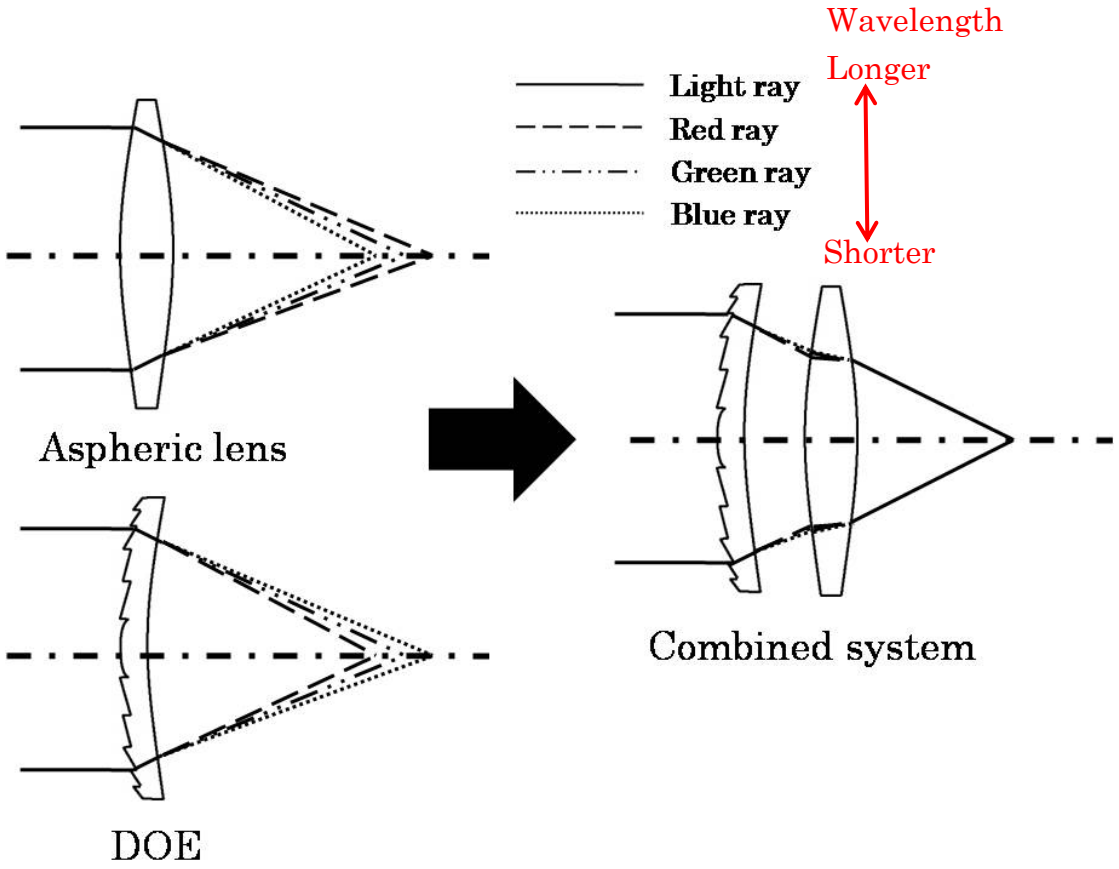

Fig.1.1 Application of DOE

However, conventional glass grinding and polishing method becomes unsuitable to produce optical components with precise microstructures due to time consuming and high cost. Therefore new molding method needs to be developed for glass lens with diffraction gratings.

1.1.2 Molding method for glass lens with diffraction gratings

For glass lens with diffraction gratings, precision glass molding process, as no post-processing such as grinding or polishing is necessary, is much more suitable than conventional glass grinding and polishing method, which makes it possible to fabricate high volume, high precision optics elements with complex shape [1-2].

Compression glass molding is a promising manufacturing process with high precision which is shown as Figure 1.2. At first, the lower mold with prefabricated diffraction gratings is heated to certain temperature. Then melt glass drops into the lower mold and is pressed by the upper mold. After being cooled for a predetermined time, glass lens with diffraction gratings is blown away from the mold.

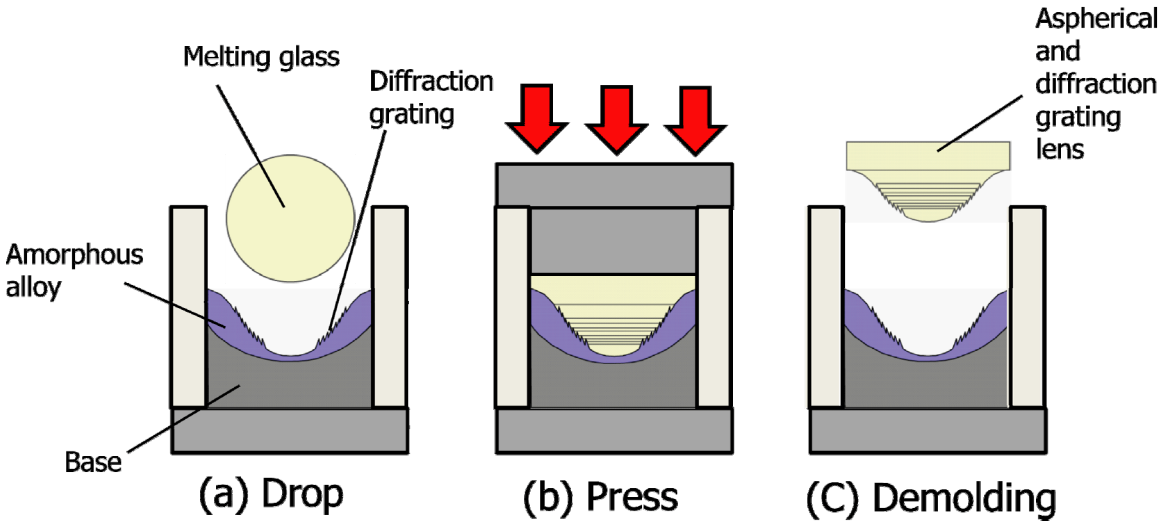

Fig. 1.2 Glass lens molding process

Although this method can save the post processing, it requires that the mold materials can withstand extremely harsh molding conditions,

such as, high temperature up to 723 K (723 K for commonly known glass material BK7 (Schott AG))[3], long time contact with inorganic glasses and high compression force during molding process.

1.2 Mold materials for glass lens with gratings

1.2.1 Requirements for mold materials of glass lens with gratings

As mold material for glass lens with microstructures, it requires not only excellent mechanical properties, high thermal stability and oxidation resistance, low adherence to glass, but also satisfying machinability.

1) Mechanical properties

In order to make sure that microstructures on the surface of mold will be not tore or wore during molding process, mold material is demanded to possess high strength and hardness, which, referring to the mechanical properties of Pd-Cu-Si system as mold material for plastic lens (σf: 1 GPa, H: 6.7 GPa [4]), is determined to be tensile strength over 1GPa; hardness over 7 GPa.

2) High thermal stability and oxidation resistance

In this research, BK7 (Schott AG) is chosen as the material of glass lens, which is currently widely applied as common lens material. As said before, during molding process, mold should be isothermally heated at some temperature, which is 723 K for BK7. For the application in real

industry world, a mold should, at least, be able to produce 10,000 pieces of glass lens to fulfill its value, which means mold materials need to withstand high temperature totally for 100 h. Moreover, during molding process at high temperature, oxidation as well is expected not to appear, which might bring about shape error of microstructures on mold. So the materials we search for glass lens mold are required with the capability to resist oxidation, even after being heated for 100h at temperature 723 K.

3) Low adherence to glass

The sticking behavior between glass and mold could result in surface quality deterioration of mold and potentially destroy the mold during demolding step, which is harmful especially to the mold with microstructures. Mold materials need to have low adherence to glass.

4) Machinability

Due to the optical characteristics, mold materials are required not just to be able to fabricate diffraction gratings, but as well to be with low surface roughness (Ra) less than 5 nm in our case. Machinability is a quite important requirement for mold material for glass lens with gratings.

1.2.2 Common mold materials

Ceramics, metals cermets and composites have all been used as molding tool materials over the years [5-7]. The most commonly used material for precision glass molding tools is still the cemented tungsten

carbide. Unfortunately, due to the high hardness, it is pretty difficult to fabricate microstructures on those materials. What's more, the cobalt binder in cemented tungsten carbide is easy to fall off, which brings about shape errors in manufactured microstructures. For its good machinability, nickel also has been using as mold material. However, its application is limited to the material with low molding temperature, because nickel mold cannot withstand the high temperature for common optical glass [8].

Therefore, our group is devoted to search for special materials which meet all the requirements for glass lens mold with microstructures.

1.2.3 Amorphous alloy

Recently, amorphous alloys are commonly regarded as promising candidate for glass lens mold materials, due to their homogeneous and isotropic structure with high machinability.

An amorphous metal is non-crystalline metallic material with no long-range ordered atomic-scale structure, as shown as Figure 1.3(a), in contrast to the highly long-range ordered arrangement of atoms of crystalline metals, as shown as Figure 1.3(b).

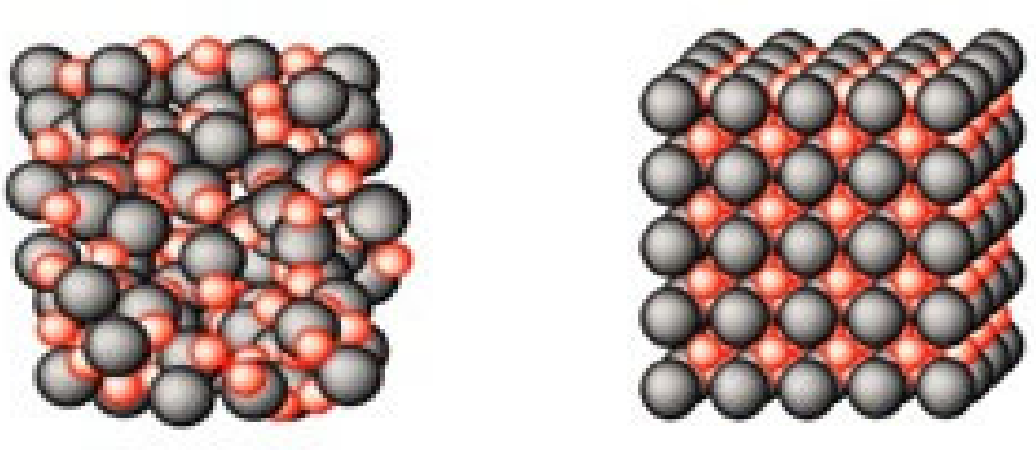

(a) Amorphous phase (b) Crystalline phase

Fig.1.3 Amorphous and crystalline phase

The disordered structure of amorphous metal can be produced directly by cooling the liquid state materials with a steep cooling rate so that atoms cannot travel to their lattice sites before they lose their mobility. In order to obtain amorphous phase instead of crystalline phase, the cooling rate should be larger than a certain value regarded as critical cooling rate which depends on the composition of the alloys. The phase conversion process is explained in Figure 1.4

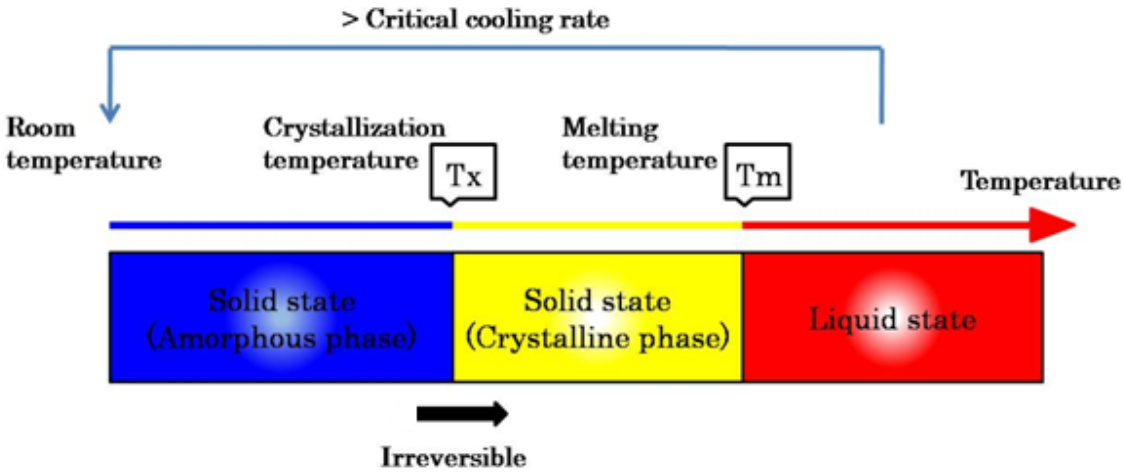

Fig. 1.4 Phase of amorphous alloy

However, there are several ways besides extremely rapid cooling by which amorphous metals can be produced, including physical vapor deposition, solid-state reaction, ion irradiation, melt spinning, and mechanical alloying. In this research, amorphous alloys are obtained by arc plasma deposition.

1.2.4 Advantages and disadvantages of amorphous alloy

Without long-range orderly repeating pattern, amorphous alloys possess homogeneous and isotropic structure, without grain boundaries which tend to decrease electrical and thermal conductivity of material. These features endow amorphous alloys with good mechanical properties [9-10], functional physical properties and excellent corrosion and oxidation resistance and high machinability.

Advantages of amorphous alloy are listed as following:

1) Mechanical properties

Generally, amorphous alloys are considered as materials with high tensile strength, low Young's modulus and high elastic strain about 2% [11] which enable them to be potential die materials for compression glass molding. Comparing to crystalline metals, most amorphous alloys have high compression and tensile strength over 1GPa. Recently, Co-Fe-Ta-B alloy system has been found out with high compression strength about 5GPa [12].

2) Machinability

In contrast to crystalline materials with different types of crystalline lattices to which many fundamental mechanical properties can be attributed, amorphous alloys with homogeneous structure can be able to be cut with high precision without effect of grain boundaries existing in crystalline materials, which usually lead to strength varying. This strength variety induced by grain boundaries, referring to Hall-Petch relationship [13-14], makes an unfavorable impact on machining accuracy during cutting process. As a result, amorphous alloys are much more appropriate as the mold materials for glass lenses with microstructures.

In spite of those advantages, amorphous alloys, of course, bear some disadvantages as following when acting as mold materials:

As demonstrated as Figure 1.4, if the temperature over Tx (Crystallization temperature), amorphous materials will turn into

crystalline materials, which indicates that amorphous materials cannot be applied under high temperature condition. Even at the temperature lower than Tx, as long as being heated for a long time, crystallization can take place as well. Once the thermal energy increases above activation energy caused by the long-time heating, amorphous materials in nonequilibrium state will be transformed to crystalline materials in equilibrium state. Consequently, in order to avoid this transformation and maintain excellent properties presenting in amorphous phase, it requires that amorphous alloys as glass lens mold materials should possess high thermal stability to withstand long time heating.

1.2.5 Previous research in our laboratory

Serving as molding die materials for glass lens with precise microstructures, amorphous alloys are demanded to possess not only excellent mechanical properties which can prevent molding die from breaking during whole molding process, high thermal stability which enables it to maintain amorphous state at molding temperature, high oxidation resistance which prevents amorphous alloy from oxidation even being heated in the air at molding temperature 723 K, but also good machinability which makes sure that microstructures can be fabricated [15-16]. Our laboratory has conducted a lot of experiments to search for the suitable amorphous alloys for glass lens mold materials, and results are summarized as following:

1) Pt-based system

i. Pt-Hf-Zr-Ni system

In this system, composition of $Pt_{51}Hf_{20}Zr_{17}Ni_{12}$ at.% demonstrated satisfying properties, Tx temperature 992 K, tensile strength 0.9 GPa, hardness 9.9GPa[17]. Unfortunately, when being heated in a vacuuming chamber, 10 hours later, crystallization came into being, which displayed its disappointing thermal stability. Moreover, it is unable to be cut as expected.

ii. Pt-Zr-Ni system

Composition of $Pt_{50}Zr_{36}Ni_{14}$ at.% in this system manifested excellent mechanic properties, Tx temperature 985 K, tensile strength 2.12 GPa, hardness 8.2 GPa[18], as well as low adherence to glass and good machinability. As shown in Figure 1.5, it can be successfully fabricated to glass lens mold with diffraction gratings. However, the thermal stability of this composition was not good enough and application of Pt, a very expensive material, sharply increases manufacture cost. Then another element was considered to substitute Pt to decrease the cost.

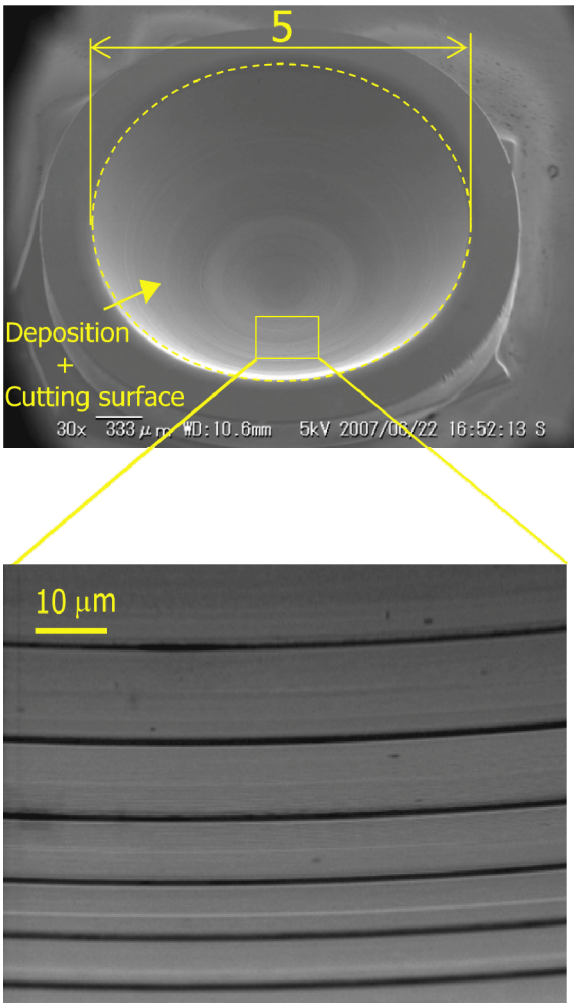

Fig. 1.5 Pt-Zr-Ni glass lens mold

2) Ni-Nb-Zr system

Our research on Ni-Nb-Zr alloy system found out that one amorphous alloy composition ($Ni_{35}Nb_{40}Zr_{25}$ at.%) met almost all the requirements for glass lens mold material: high thermal stability, maintaining in amorphous state even being heated for 100 hours in vacuuming chamber at temperature 723 K; suitable tensile strength, 1.71

GPa; high oxidation resistance, without oxidation even be heated for 100 hours in the air at temperature 723 K. Unfortunately, when fabricating gratings on the mold, the immense wear of bit which might be caused by high hardness (10 GPa) made it impossible to cut precise gratings. Consequently, the forth element Ti was considered to be added to decrease the hardness, in order to improve machinability [19].

1.3 Combinatorial research method

Along with the development of technology, the requirements on material become extremely high. A lot of properties have to be measured and compared. Search for the material which meets all the requirements is a huge project. As a result, combinatorial approach with high efficiency becomes the center of attention especially in the scientific research.

The combinatorial approach applied in this research is demonstrated as Figure 1.6. Multiple samples are integrated onto one substrate to do the experiments. The results of many samples can be obtained just by one time experiment. In this research, the amorphous samples are fabricated by arc plasma deposition. The combinatorial arc plasma deposition method (CAPD) is adopted to make thin film library for the composition measurement, thermal stability test and others. Parallel-plate sputtering system is used to make thin film samples with

grading compositions by a special target for machinability test. These will be specifically explained in the later chapters.

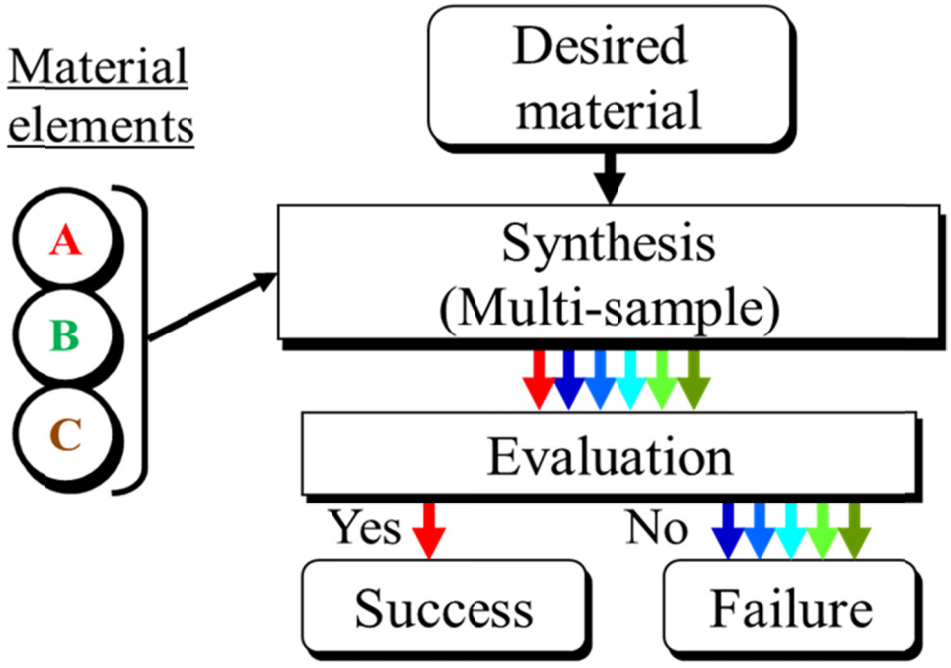

Fig. 1.6 Combinatorial approach

1.4 Objective of this research

As mold materials for glass lenses with diffraction gratings, it requires not merely excellent mechanic properties, like tensile strength over 1 GPa, hardness over 7 GPa, high thermal stability to endure to be heated for 100 h at temperature 723 K, but even eligible machinability to process gratings. Among those requirements, experiments to evaluation machinability and thermal stability are time-consuming and costly. As a result, the main objective of this research is to develop combinatorial

evaluation method to efficiently find out desirable composition which can best meet those described requirement. Moreover, it is to apply the method to the search for glass lens mold material candidate.

The structure of this thesis is explained in Figure 1.7. Ni-Nb-Ti amorphous alloy is chosen as research subject, based on the evaluation results demonstrated in Chapter 2. The machinability of Ni-Nb-Ti amorphous alloy is going to be measured by the novel high-throughput evaluation method explained in Chapter 3, and results are shown in Chapter 4. The crystallization property of material with good machinability is examined in Chapter 5 to confirm it is qualified as mold material or not. The summary of each chapter is displayed as following.

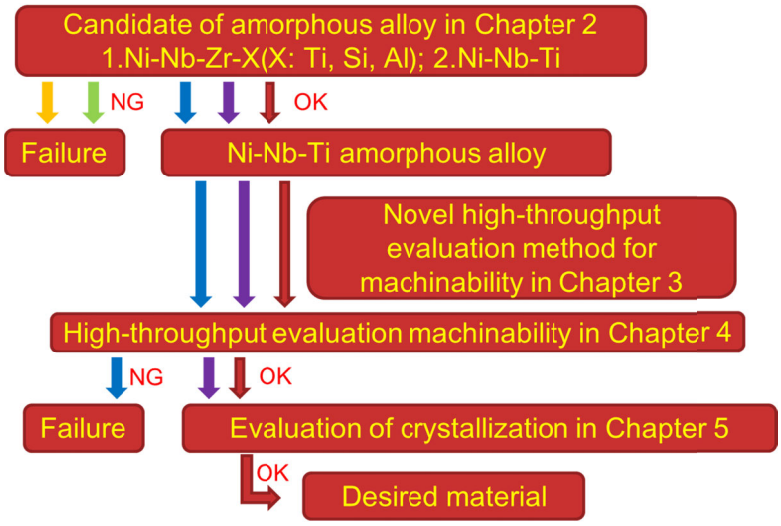

Fig.1.7 The structure of thesis

In Chapter 2, based on the result of research on $Ni_{35}Nb_{40}Zr_{25}$ at.%, Ti is added to substitute Ni-Nb to make thin film samples. Among them, for the sample with composition $Ni_{28}Nb_{32}Zr_{25}Ti_{15}$ at.%, machinability improves

but not enough, and it tends to increase with Ti's content level. However, when Ti's content level increases to 20%, crystallization begins to appear during thermal stability test, which may be induced by the great decrease of Ni-Nb.

In order to improve the machinability, meanwhile preserve the high thermal stability, in this research, instead of Ni-Nb-Zr system, Ni-Nb-Ti system is determined as the research subject, which can provide the possibility to fabricate thin film samples with high Ti content level without decreasing Ni-Nb to exceed the desired range.

The thin film libraries of Ni-Nb-Ti were made by CAPD for the thermal stability test. According to the results, thin film samples exhibit high thermal stability when compositions belong to this area, Ni,40-58 at.%; Nb, 24-46 at.%; Ti, 5-20 at.%, which can withstand high temperature 723K for 100h. This area becomes the research subject.

Chapter 3 proposes a novel combinatorial evaluating method for machinability, in the concept of which, a sample with grading composition is indispensable. New special targets for parallel-plate type sputtering machine were designed to obtain samples with grading composition. At first, Zr was applied for trial experiment, instead of Ni-Nb, due to the nearly same sputtering rate and lower price. This trial experiment was carried out to determine the relationship between two factors, size of target, distance from target to substrate, and compositions of sample.

Finally, a sample made by inner target $Ni_{15}Nb_{20}Ti_{65}$ and outer target $Ni_{60}Nb_{40}$ was fabricated for cutting test. Although the lowest roughness value of this sample is still higher than the requirement, it confirms the feasibility of this novel combinatorial method of machinability. Moreover, based on the composition results, the inner targets were decided to be Nb-Ti alloy.

In Chapter 4, the results of experiments using Nb-Ti inner targets were explained in detail. Using the designed targets, the samples can almost cover the entire target area with high thermal stability. The sample made by inner target $Nb_{50}Ti_{50}$ and outer target $Ni_{70}Nb_{30}$ was used for cutting test. However, the roughness of surface is larger than the requirement. In order to further improve the efficiency, a cover mask was designed to integrate three samples onto one substrate. The results for three samples can be attained by one cutting test. The samples made by using this cover mask were cut and roughness of surface was measured. Finally, a composition with roughness less than 5nm was found to be $Ni_{51}Nb_{33}Ti_{16}$.

In Chapter 5, another property of $Ni_{51}Nb_{33}Ti_{16}$ was examined. As mentioned before, the mold material for glass lens with gratings has to be not only with good machinability but also high thermal stability which can withstand high temperature during molding process. The crystallization temperature of $Ni_{51}Nb_{33}Ti_{16}$ was found to be 865K which was higher than

723 K as required and it can also maintain the amorphous state for a long time at high temperature.

Chapter 6 draw a conclusion of this research and proposed the future work.

Chapter 2 Selection of the research subject

2.1 Evaluation on Ni-Nb-Zr-X(X: Al, Si and Ti) alloys

We have been searching for suitable materials for glass lens molds by applying a combinatorial method [3, 20]. Until now, two alloy systems had been evaluated and used to fabricate molding dies: a Pt-based amorphous alloy [3, 20-22] and a Ni-Nb-Zr alloy [23-25]. The problem with the $Pt_{50}Zr_{36}Ni_{14}$ at.% was the insufficient thermal stability. Additionally, the manufacturing cost was increased because of the use of Pt. Our previous research on the Ni-Nb-Zr alloy system suggested $Ni_{35}Nb_{40}Zr_{25}$ at.% as a potential glass lens mold material. However, for $Ni_{35}Nb_{40}Zr_{25}$at.%, the significant wear on the bit caused by its high hardness affected the roughness of the mold surface [24]. As a result, the addition of a fourth element was considered to decrease the hardness without destroying the other properties.

Generally speaking, for metal alloys the greater the number of delocalized electrons it has, the stronger the bonding tends to be [26]. By substituting Zr with other elements which have fewer valence electrons, it should be possible to obtain alloys with lower hardness. Another consideration is that the hardness of alloys tends to reduce with the alloy's melting temperature. Based on the values of these two factors, as shown in Table 2.1, Al, Si and Ti were selected as candidates to decrease the hardness while not destroying the other properties .

Table 2.1 Properties of the additional element candidates

Element	Atomic radius(nm)	Melting point(◦C)	Number of valence electrons
Ni	0.125	1453	10 (3d84s2)
Nb	0.143	2468	5 (4d45s1)
Zr	0.16	1852	4 (4d25s2)
Ti	0.145	1660	4 (3s23p2)
Al	0.143	660	3 (3s23p1)
Si	0.117	1410	4 (3s23p2)

In our previous research on the Ni-Nb-Zr system, when the Zr content was in the range of 9% to 25%, the corresponding thin film samples showed excellent thermal stability. Accordingly, the fourth element was considered as a substitute for Zr. As a result, $Ni_{35}Nb_{40}Zr_{15}X_{10}$ (X: Al, Si, Ti) at.% target alloys were made, and thin film samples were fabricated for testing.

Ni-Nb-Zr-X alloy targets were fabricated in an arc furnace (ACM-S01T, Diavac Limited). Those targets were assembled to a conventional parallel-plate sputtering system which is shown in Figure 2.1

respectively to make thin film samples for evaluation of their properties, such as tensile strength, thermal stability, hardness, machinability, etc.

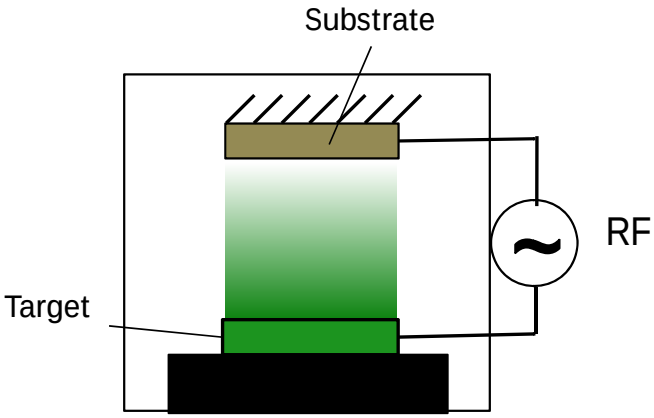

Fig. 2.1 Parallel- plate sputtering system

The nano-indentation method was applied to do the hardness test using the equipment with atomic force microscope (SPI-3000, Seiko Instruments) and a nonoindenter (Triboscope, Hysitron). Figure 2.2 displays the result of hardness test. It becomes apparent that only the sample with Ti successfully attained the goal to reduce hardness.

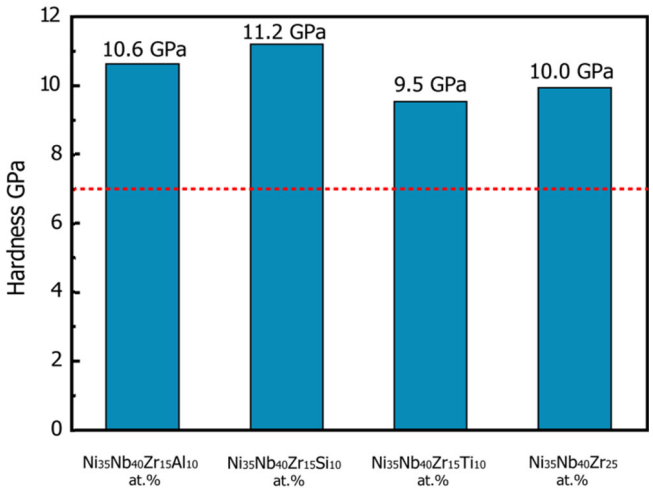

Fig. 2.2 Hardness of $Ni_{35}Nb_{40}Zr_{15}X_{10}$ (X : Al, Si, Ti) samples

Besides the hardness test an ultra-precision diamond machining system (Nanoform 350, Precitech) was used for the cutting tests to characterize the machinability of the alloy samples. First, as shown in Figure 2.3, the sample with the substrate was fixed to the work holder, which rotated at a speed of 200 rpm. Then, the cutting tool with a single crystal diamond radial bit (radius=0.5 mm) was used to cut the sample into a taper shape, with a radial feeding rate of 1 µm/rev and a axial feeding rate of 1 nm/rev. The radial feeding distance was 2 to 3 mm. Subsequently, the cutting surface was examined, and the cutting removal rate was calculated.

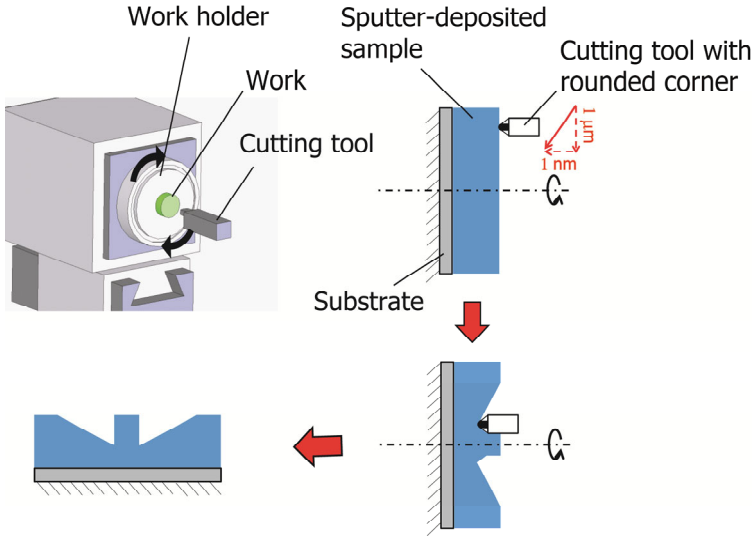

Fig. 2.3. Concept of the taper cutting test

In addition to the above taper cutting test, the material for the glass lens mold with gratings needs to be compatible with micro-cutting. The concept for the micro-cutting test is shown in Figure 2.4. Firstly, a plane was roughly cut using a diamond radial bit (Fig. 2.4 (a, b, c)). Secondly, a

sword bit was applied for the micro-cutting on this plane with a constant axial feeding distance of 0.1 µm and a radial feeding rate of 0.1 mm/min. The cutting process did not cease until the radial feeding distance reached 1 mm. The same cutting movement was then repeated 50 times. Finally, the cutting surface was examined to measure the cutting depth.

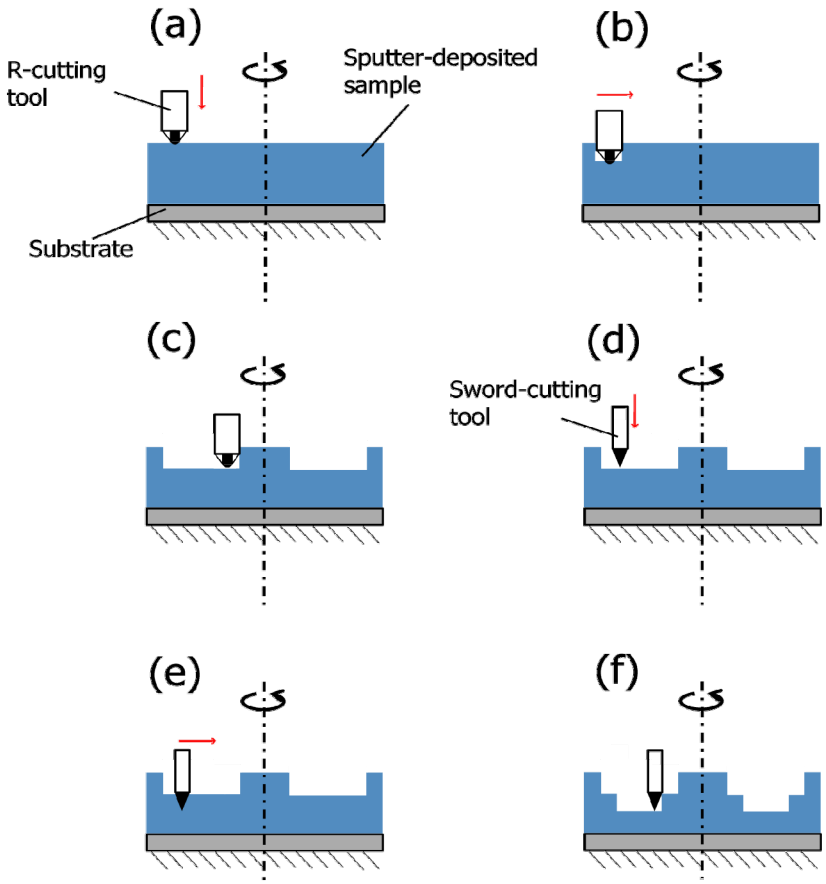

Fig. 2.4 Concept of the micro-cutting test with the sword tool

During taper cutting tests, the samples with Al and Si could not be cut at start points, shown as Figure 2.5, which denied their capabilities for micro-cutting. Therefore, our research was focused on Ni-Nb-Zr-Ti system.

However, cutting removal rate of $Ni_{35}Nb_{40}Zr_{15}Ti_{10}$at.% (67%) was lower than that of $Ni_{35}Nb_{40}Zr_{25}$at.% (94%).

However, the micro-cutting test's result of $Ni_{35}Nb_{40}Zr_{15}Ti_{10}$at.% presented in Figure 2.6, failed. If Ti content would be increased, better results of micro-cutting test may be expected. But the thermal stability of sample may be destroyed if Zr content would be further decreased. Consequently, Ti was considered to substitute for Ni-Nb system instead of Zr.

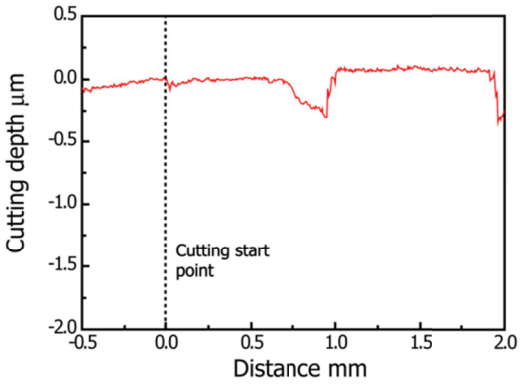

(a) $Ni_{35}Nb_{40}Zr_{15}Al_{10}$

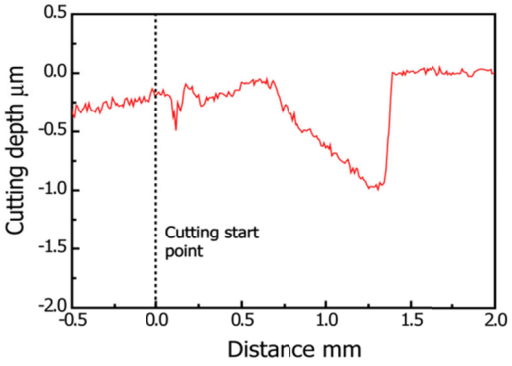

(b) $Ni_{35}Nb_{40}Zr_{15}Si_{10}$

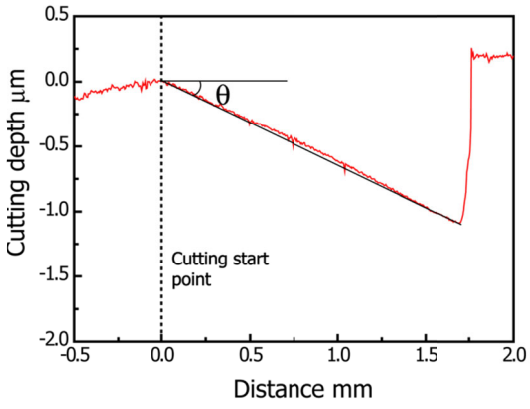

(c) $Ni_{35}Nb_{40}Zr_{15}Ti_{10}$

Fig. 2.5 Cutting profiles in radius feed direction of $Ni_{35}Nb_{40}Zr_{15}X_{10}$ (X: Al, Si, Ti) samples

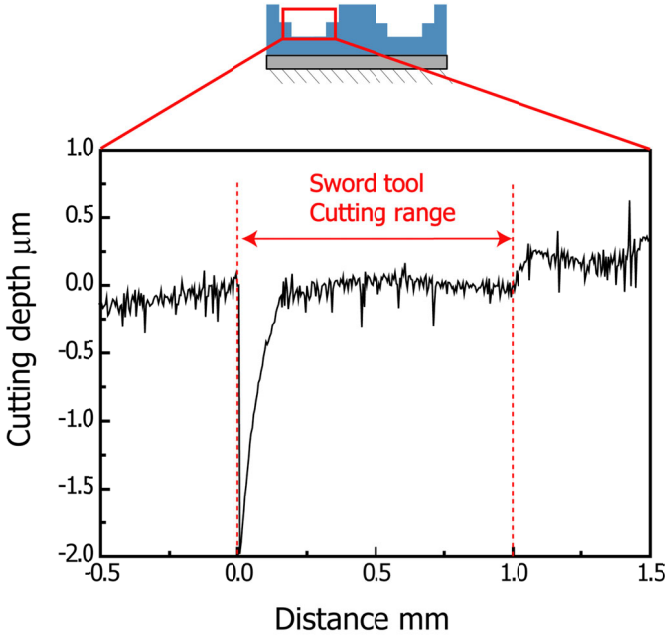

Fig. 2.6 Cutting profiles in radius feed direction of $Ni_{35}Nb_{40}Zr_{15}Ti_{10}$ sample

2.2 Evaluation on Ni-Nb-Zr-Ti alloys

Three different Ni-Nb-Zr-Ti target alloys were used to sputter thin film samples for testing: $Ni_{30}Nb_{35}Zr_{25}Ti_{10}$ at.% , $Ni_{28}Nb_{32}Zr_{25}Ti_{15}$ at.% and $Ni_{25}Nb_{30}Zr_{25}Ti_{20}$ at.%.

In order to measure the tensile strength, alloy samples were sputtered on Cu foils, which were dissolved in HNO_2+H_2O (1:1). Left samples were cut into 1 mm x 7 mm shape by a diamond wire saw (Musashino Electron) for tensile tests which were performed using a thermal mechanical analyzer (TMA; TMA-60, Shimadzu) with a strain rate of $1.42x10^{-4}$/s.

From the tensile test results, stress-strain curves were drawn and are shown in Figure 2.7. All the samples fractured during the tests, and the fracture stresses of the samples are higher than desired (1.0 GPa) for glass lens mold materials. Moreover, from this figure, we can deduce that further increasing the Ti content to over 20% may lower the stress to the desired value (1.0 GPa).

For the hardness test, using Ti (with 4 valence electrons) to substitute Ni (10 valence electrons) and Nb (5 valence electrons), the attraction between the nuclei and electrons will decrease, meaning the cohesion inside of the alloy will also decrease [27]. As shown in Figure 2.8, all the samples, as expected, displayed lower hardness values than $Ni_{35}Nb_{60}Zr_{25}$ at.% (10.0 GPa), as follows: $Ni_{30}Nb_{35}Zr_{25}Ti_{10}$ at.% (9.1 GPa), $Ni_{28}Nb_{32}Zr_{25}Ti_{15}$ at.% (9.2 GPa) and $Ni_{25}Nb_{30}Zr_{25}Ti_{20}$ at.% (9.1 GPa). Therefore, the goal of decreasing hardness was achieved. Because there may be little impact on the hardness when the Ti content is low, the samples with Ti content below 10% were not tested.

During the thermal stability test, the maximum annealing time was fixed at 100 h, which is the desired lifetime for a glass lens mold. The test results for the Ni-Nb-Zr-Ti samples isothermally heated at 723 K for different times are displayed in Figure 2.9. Several sharp peaks in the XRD profiles are attributed to the Al_2O_3 substrate. The halo patterns due to the amorphous phase in each XRD profile establish that the thermal stabilities of the three samples are sufficient.

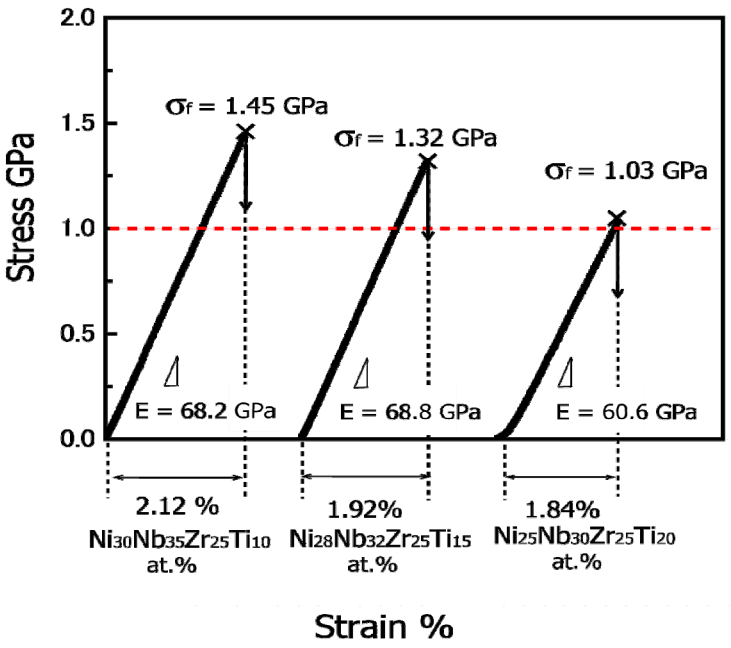

Fig. 2.7 Stress-strain curves of the Ni-Nb-Zr-Ti samples

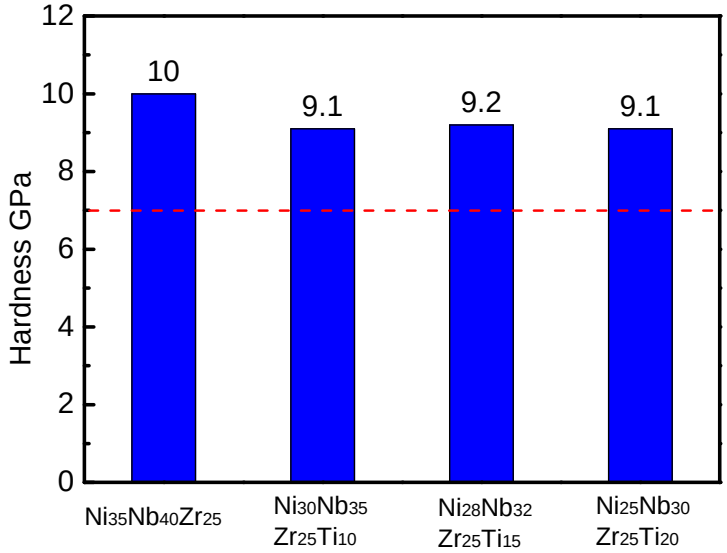

Fig. 2.8 Hardness of the Ni-Nb-Zr-Ti and $Ni_{35}Nb_{40}Zr_{25}$ samples

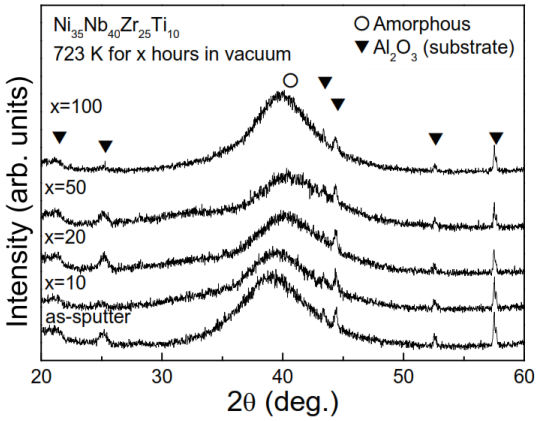

(a) $Ni_{30}Nb_{35}Zr_{25}Ti_{10}$ at.%

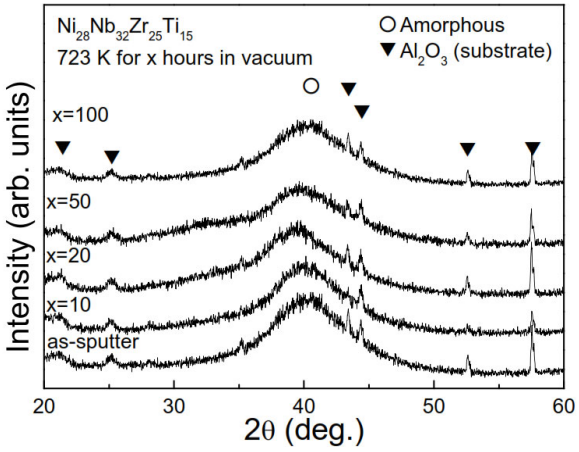

(b) $Ni_{28}Nb_{32}Zr_{25}Ti_{15}$ at.%

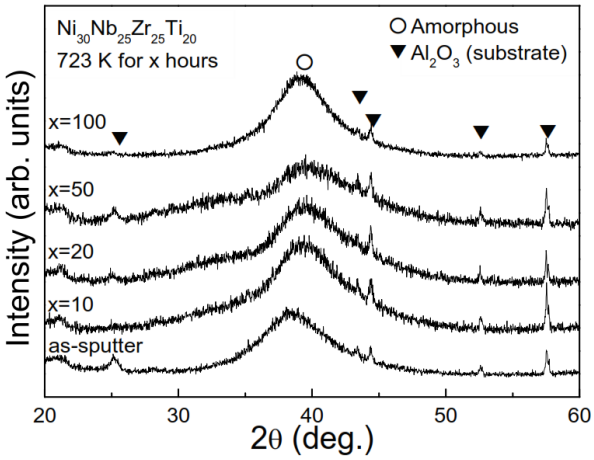

(c) $Ni_{25}Nb_{30}Zr_{25}Ti_{20}$ at.%

Fig. 2.9 XRD profiles of the Ni-Nb-Zr-Ti samples

Figure 2.10 shows the results of the taper cutting process. All the samples can be cut into a tapered shape, and the cutting removal rates were calculated, which were improved to78%, and 75% when the Ti content was 15 at.% and 20 at.%, respectively.

Furthermore, two of the samples were able to be micro-cut. The cutting profiles are presented in Figure 2.11. The $Ni_{30}Nb_{35}Zr_{25}Ti_{10}$ sample cannot be micro-cut. For the other two samples, the cut surface of $Ni_{25}Nb_{30}Zr_{25}Ti_{20}$ is much smoother than that of $Ni_{28}Nb_{32}Zr_{25}Ti_{15}$; the roughness values of these two cut surface are 18 nm and 53 nm, respectively.

Although the hardness values of these three samples are almost the same, as shown in Figure 2.8, the results of micro-cutting test differ greatly. This is because the machinability does not depend on the hardness alone. Other factors, such as the microstructure, composition, modulus of elasticity, thermal conductivity, and so on, also have a great impact on the machinability.

Although the max cutting depth in Figure 2.11 is 0.75 μm, which is smaller than the desired depth of 5 μm, the addition of Ti makes micro-cutting a possibility. Moreover, the cutting depth and machined surface conditions improved with increased Ti content.

While not expecting to be held to any particular theory, it is considered that the improvement of machinability of these samples is due to the low heat conductivity of titanium, which causes temperature accumulation in the cutting zone, combined with another property of titanium, the fact that it loses material strength at elevated temperatures

[28-29]. These properties make the material much easier to be machined. This is also in accordance with the results of the tensile test presented in Figure 2.7; the stress of the samples decreases with increasing Ti content. Moreover, based on the results, it is possible to draw the conclusion that if the Ti content is increased further, the machinability of the thin film samples will improve even further. However, there is a limitation to the increase of Ti, as pure Ti has a poor machinability [28]. This limit will be investigated in future experiments.

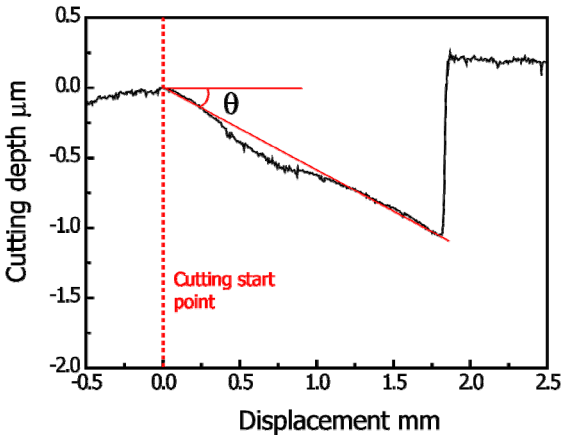

(a) $Ni_{30}Nb_{35}Zr_{25}Ti_{10}$ at.%

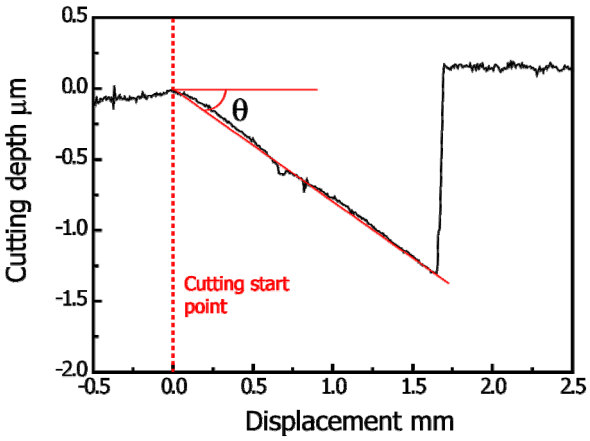

(b) $Ni_{28}Nb_{32}Zr_{25}Ti_{15}$ at.%

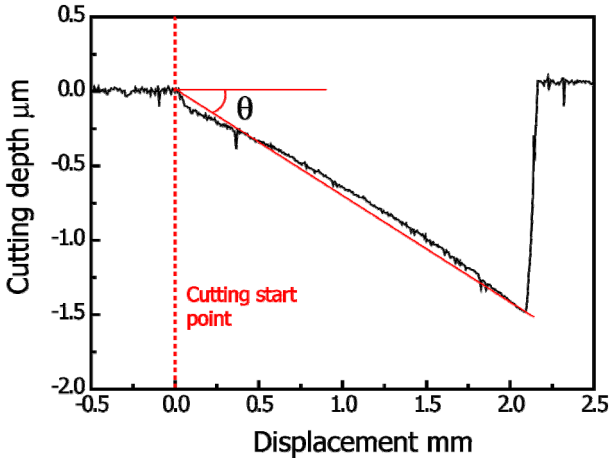

(c) $Ni_{25}Nb_{30}Zr_{25}Ti_{20}$ at.%

Fig. 2.10 Cutting profiles in the radial direction of the Ni-Nb-Zr-Ti samples

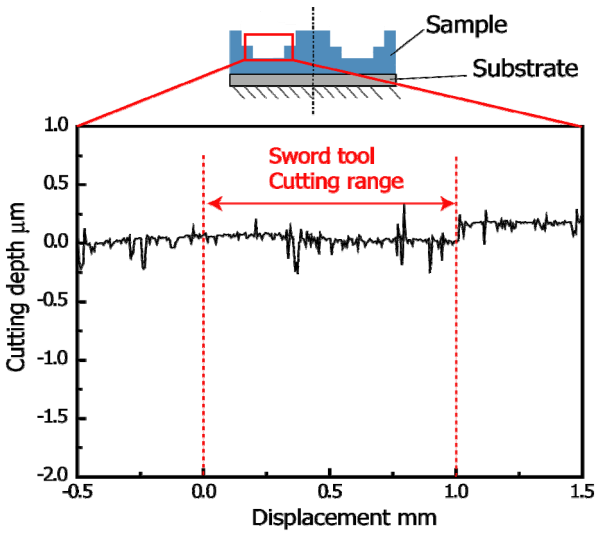

(a) $Ni_{30}Nb_{35}Zr_{25}Ti_{10}$ at.%

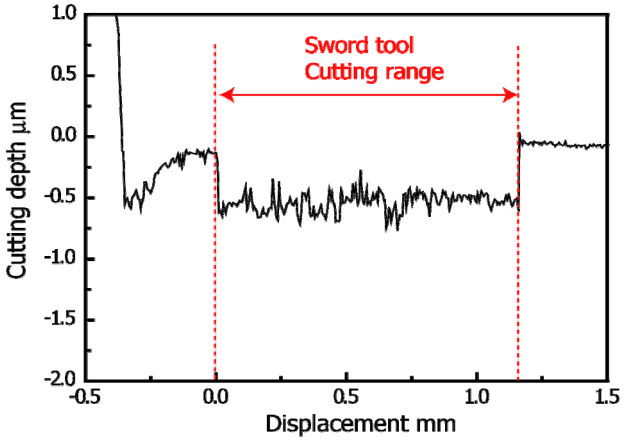

(b) $Ni_{28}Nb_{32}Zr_{25}Ti_{15}$ at.%

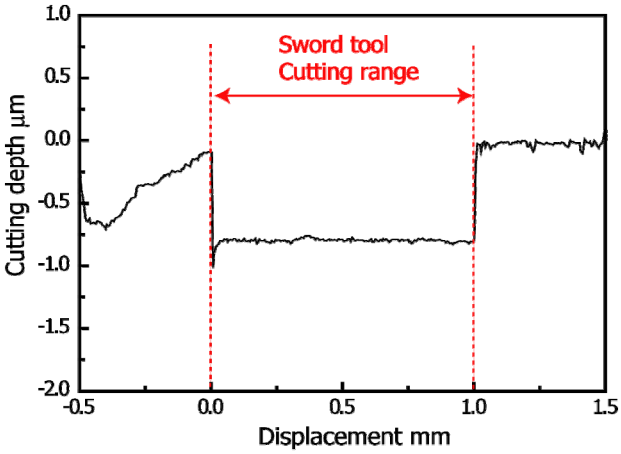

(c) $Ni_{25}Nb_{30}Zr_{25}Ti_{20}$ at.%

Fig.2.11 Cutting profiles of the Ni-Nb-Zr-Ti samples for micro-cutting

We evaluated several properties of the Ni-Nb-Zr-Ti system and the results are summarized in Table 2.2. Some conclusions were drawn as follows:

1. Adding Ti decreased the hardness of the amorphous alloy thin films and made it possible for the samples to not only be taper cut but also micro-cut

2. When the Ti content was increased to 20 at.%, the high tensile stress and excellent thermal stability maintained the amorphous state, and the machinability of the sample was improved. Moreover, if the Ti content would be further increased, better machinability may be expected. Meanwhile, to retain the other properties (e.g., tensile stress), we will focus on the evaluation of Ni-Nb-Ti alloys with higher Ti contents in the research.

Table 2.2 Properties of the Ni-Nb-Zr-Ti and Ni-Nb-Zr samples

Sample (at.%)	$Ni_{30}Nb_{35}Zr_{25}Ti_{10}$	$Ni_{28}Nb_{32}Zr_{25}Ti_{15}$	$Ni_{25}Nb_{30}Zr_{25}Ti_{20}$	$Ni_{35}Nb_{40}Zr_{25}$
Thermal stability	Amorphous	Amorphous	Amorphous	Amorphous
Tension strength (GPa)	1.45	1.32	1.03	1.71
Hardness (GPa)	9.1	9.2	9.1	10.0
Removal rate (%)	58	78	75	94
Cutting depth (μm)	0	0.46	0.75	0

2.3 Evaluation on Ni-Nb-Ti alloys

2.3.1 Fabrication of Ni-Nb-Ti thin film library

On the basis of arc plasma deposition, combinatorial arc plasma deposition is developed in our laboratory to be able to fabricate thin film libraries for evaluation [30].

Arc plasma gun (APG) is adopted in arc plasma deposition to make thin film samples, the structure of which is displayed as figure 2.12. Cathode, which is also the target material, and anode are connected by a circuit with a capacitor. A large current pulse will be generated, which will ionize and emit the cathode material, when the trigger turns on [31]. Then, emitted plasma is guided onto substrate to deposit thin film of cathode material, by magnetic field of the permanent magnet placed under substrate. The thickness of thin film can be adjusted by the number of current pulses (shots) and the value of current strength that is proportional to the capacitance.

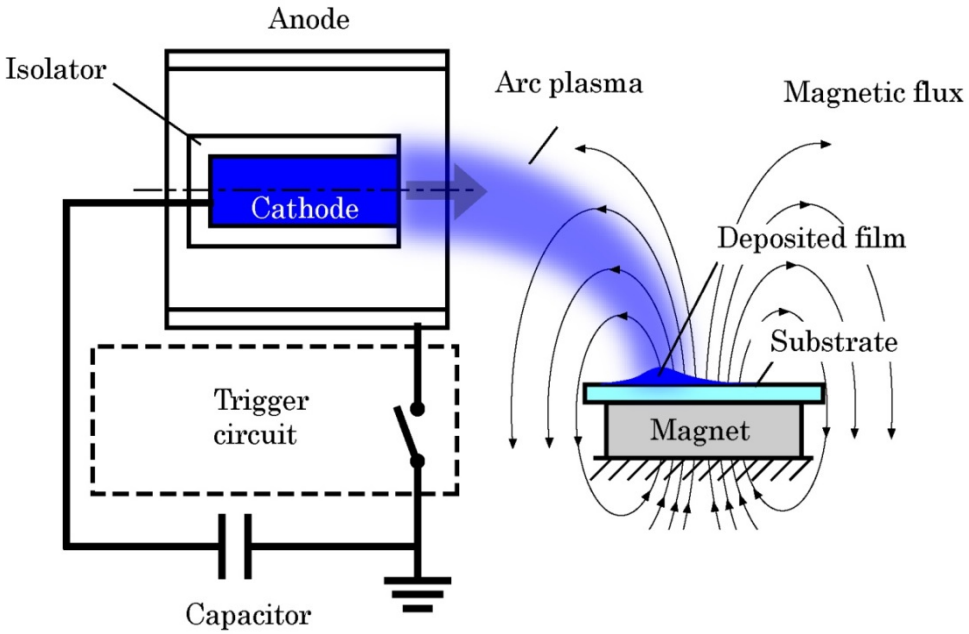

Fig. 2.12 The schematic of the APG

In contrast to the thin film with single composition produced by Arc plasma deposition, a thin film library with different compositions can be obtained by combinatorial arc plasma deposition method, the principle of which is presented as Figure 2.13. Tree APGs are adopted with various materials, from which three elements' atoms are emitted and mix to make a thin film library with grading compositions. This thin film library lays the foundation for our research to utilize a combinatorial approach with high throughput, since one library contains so many different compositions.

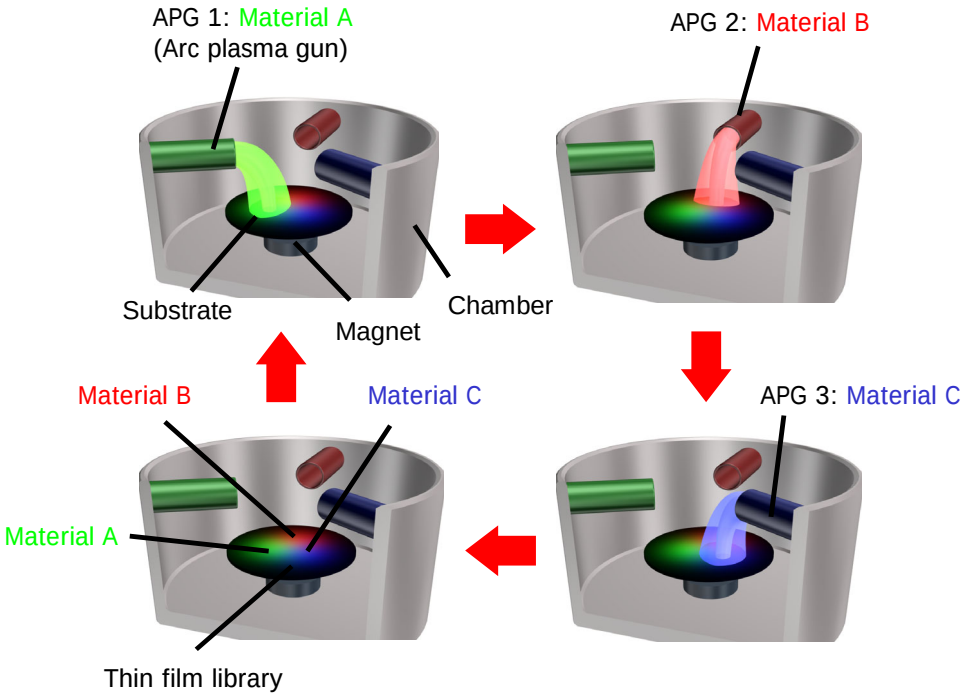

Fig. 2.13 The principle of CAPD

Combinatorial arc plasma deposition (CAPD) was applied to produce thin film library, while MEMS process was employed to separate thin film library, in order to record position information of each composition by 5-bit method. Figure 2.14 demonstrates the specific process of how to fabricate thin film library. First, a MEMS grid with a size of 39.4 mm x 39.4 mm, which can provide 1089 small samples with a size of 1 mm x 1 mm, was fabricated onto the surface of an Al_2O_3 substrate with a diameter 3 inch, a thickness 500 um. Then, by using CAPD, thin film library was deposited on MEMS grid, which would be lifted off later and leave a group of samples with position marks as shown in Figure 2.15.

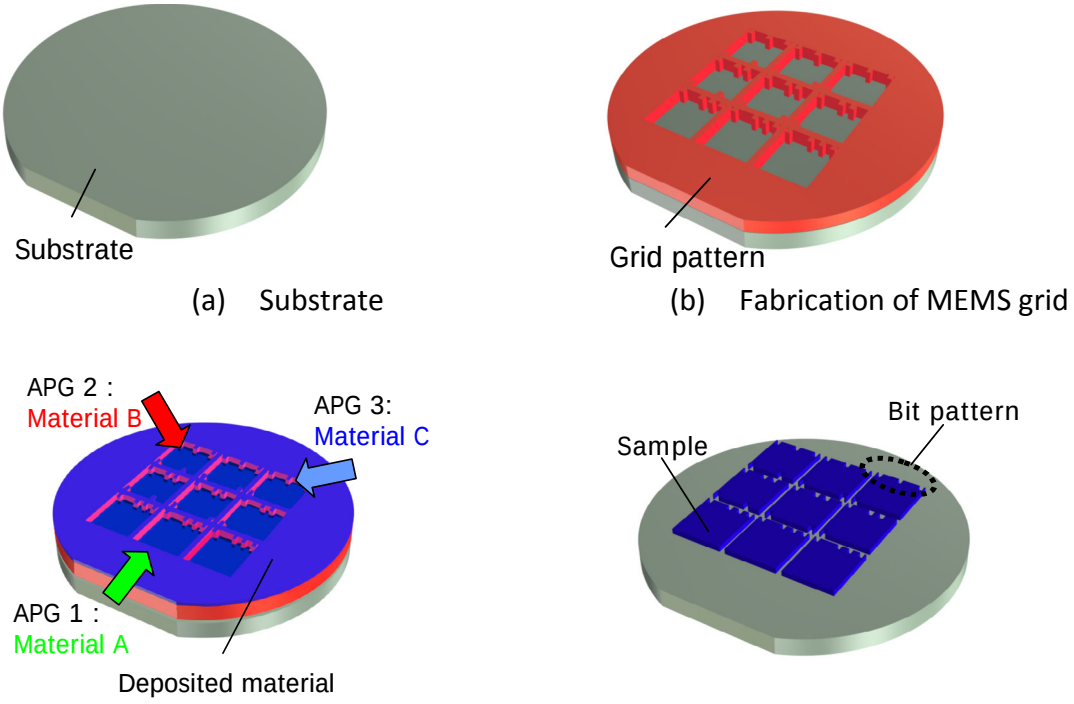

(a) Substrate (b) Fabrication of MEMS grid

(c) Deposition (d) Lift-off

Fig. 2.14 Fabrication process of thin film library

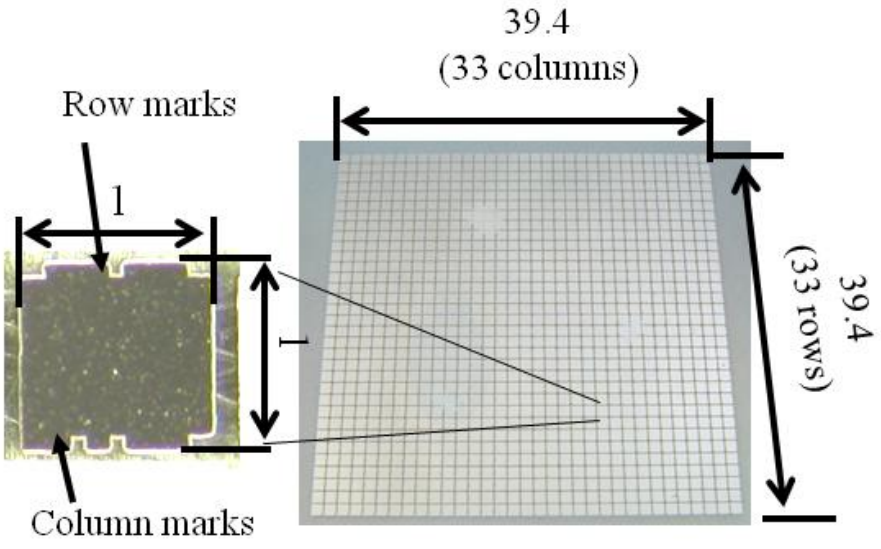

Fig. 2.15 Thin film library

2.3.2 Compositions and phases evaluation on Ni-Nb-Ti thin film libraries

Three Ni-Nb-Ti thin film libraries were deposited by CAPD, of which depositing condition is presented as Table 2.3. Moreover, compositions of these three thin film libraries were detected by Energy-dispersive X-ray spectroscopy (EDX). The results of these three thin film libraries are shown in Figure 2.16. Thin film libraries with a quite wide area of compositions can be obtained using this deposition method.

Table2.3 CAPD shot conditions for thin film libraries No.1~No.3

		Ni	Nb	Ti
No.1	Capacitance (μF)	8,800	8,800	4,400
	Shot cycle	[Ni - Nb - Ti]		
	Total cycle	10,000		
No.2	Capacitance (μF)	8,800	8,800	2,200
	Shot cycle	[Ni - Nb - Ti]		
	Total cycle	10,000		
No.3	Capacitance (μF)	8,800	8,800	6,600
	Shot cycle	[Ni x2 - Nb - Ti x2]		
	Total cycle	7,500		

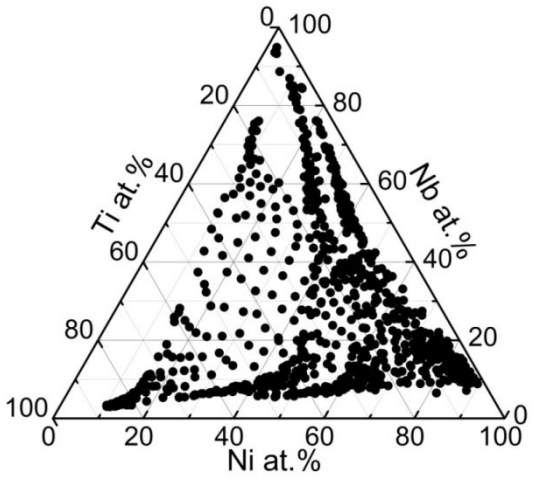

Fig. 2.16 Composition distribution of thin film libraries (No.1~No.3)

Since the research objective is search for amorphous alloy as mold material for glass lens, the reason of which was described in Chapter 1, the phase of deposited thin film libraries need to be confirmed at first, which was evaluated by X-ray diffraction (XRD). The results of those tree thin film libraries' phase are demonstrated as Figure 2.17, from which we make a conclusion that amorphous alloys with wide composition area can be achieved, Ni 18-87%,Nb 7-72%, Ti 4-78%.

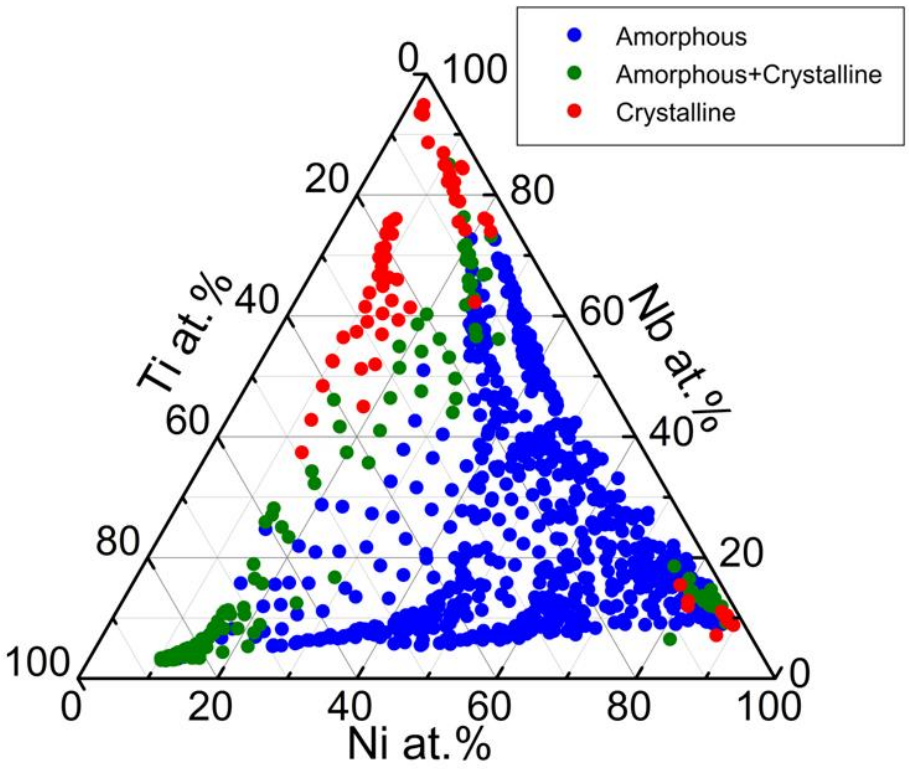

Fig. 2.17 Phase and composition distribution of thin film library (No.1~No.3) samples

2.3.3 Evaluation of thermal stability on Ni-Nb-Ti thin film library

Although amorphous alloys with wide composition area can be achieved, as glass lens mold material, the desired amorphous alloy needs to withstand high temperature during molding process. In order to evaluate this capability, thermal stability test was performed.

Thermal stability tests were carried out in a vacuuming furnace with gold IR reflector (MILA-300, Ulvac Technology). Samples were heated from room temperature (RT) to 723 K with a heating rate 20K/s. When

temperature reached to 723 K, samples were isothermally heated for 10h, 20 h, 50 h and 100 h, respectively. After that, X-ray diffraction (XRD; RINT2200, Rigaku) was employed to investigate the phases of those annealed samples.

Figure 2.18 manifests the results of thermal stability tests, (a) phase of thin film libraries before thermal stability, (b) phase of thin film libraries after 50h's heating, and (c) phase of thin film libraries after 100h's heating. Many amorphous alloys began to crystallize after long-time's heating. As presented in the Figure 3.8, an area of amorphous alloys with composition belonging to Ni 40-58 at.%, Nb 24-46 at.%, Ti 5-20 at.%, are endowed with high thermal stability which is able to endure high temperature for a long time.

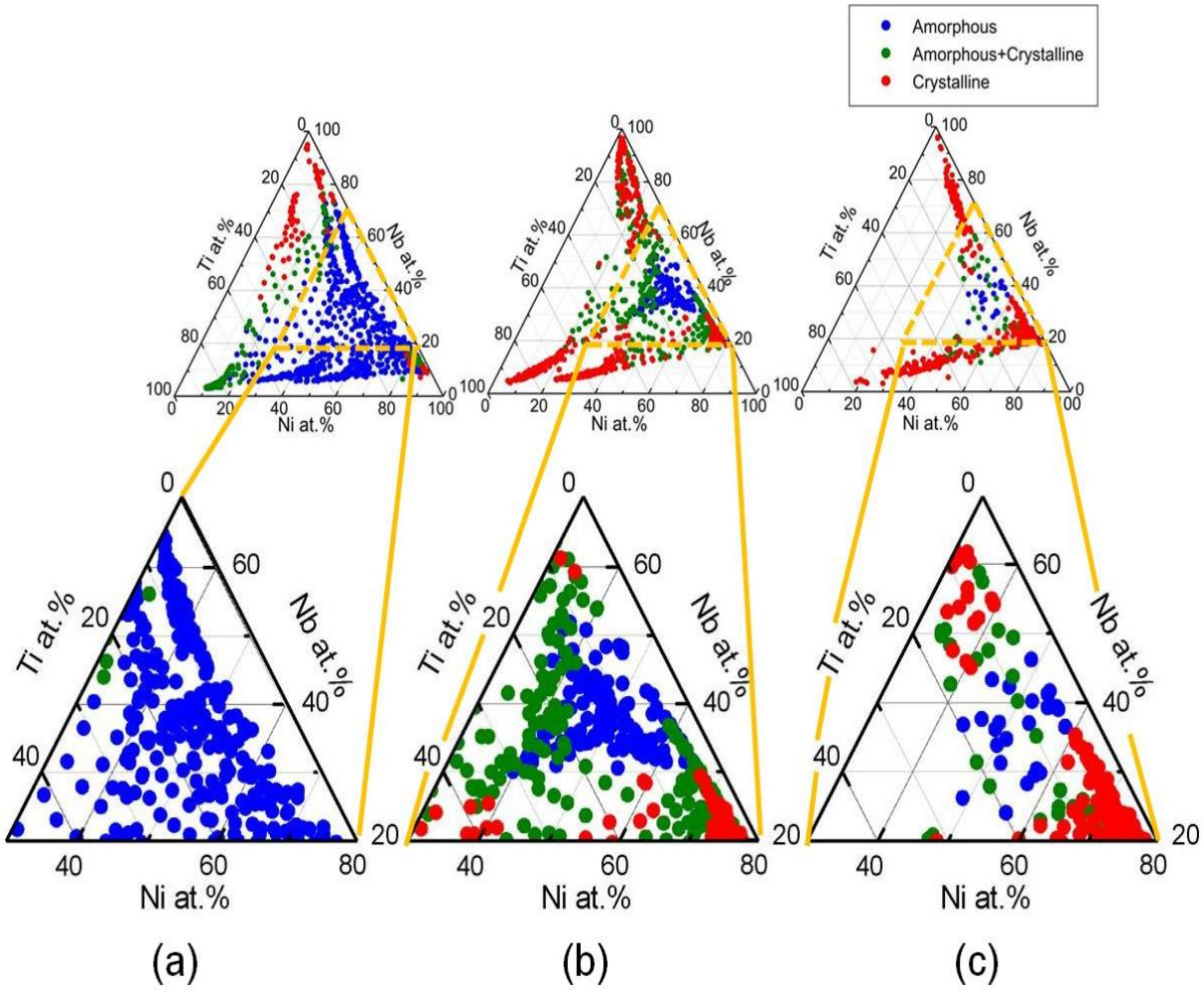

Fig. 2.18 (a) Phase of thin film libraries before thermal stability

(b) Phase of thin film libraries after 50h's heating

(c) Phase of thin film libraries after 100h's heating

2.4 Summary

Our research on Ni-Nb-Zr alloys has shown that one amorphous alloy composition ($Ni_{35}Nb_{40}Zr_{25}$ at.%) met almost all the requirements for glass lens mold materials. Unfortunately, when fabricating gratings on the mold, the immense wear on the bit, which may be caused by the high hardness of the alloy (more than 10GPa by the nano-indentation method), made it impossible to cut precise gratings. Consequently, the addition of a fourth element was considered to decrease the hardness. Al, Si and Ti were selected as candidate for the fourth element due to their low melting point and less valence electron. The experiment results showed that only the sample with Ti successfully attained our goal of reducing the hardness. Additionally, in the taper cutting tests, the samples containing Al and Si could not be cut at the start points. Therefore, our research was focused on the Ni-Nb-Zr-Ti system.

Three Ni-Nb-Zr-Ti thin film samples, $Ni_{30}Nb_{35}Zr_{25}Ti_{10}$ at.% , $Ni_{28}Nb_{32}Zr_{25}Ti_{15}$ at.% and $Ni_{25}Nb_{30}Zr_{25}Ti_{20}$ at.%, were fabricated to evaluate their properties, including their tensile strength, thermal stability, hardness, and machinability. The results demonstrated that adding Ti did decreased the hardness of the amorphous alloy thin films and made it possible for the samples to not only be taper cut but also micro-cut. Moreover the machinability of sample improved with increasing Ti content level. In order to maintain other properties such as tensile stress

and thermal stability, Ni-Nb-Ti was considered to be our research subject since higher Ti content can be achieved in this system.

A thin film library with different compositions can be obtained by combinatorial arc plasma deposition method in our laboratory. This thin film library made it possible to improve thermal stability test with high throughput. As a result, thermal stability test was carried out at first to narrow down the research area in the Ni-Nb-Ti alloy system. Three Ni-Nb-Ti thin film libraries were made for thermal stability test which almost covered the whole composition of Ni-Nb-Ti alloy system. From the results an area of amorphous alloys with composition belonging to Ni 40-58 at.%, Nb 24-46 at.%, Ti 5-20 at.%, presented high thermal stability which can endure high temperature for a long time. This area will be the main research area for the machinability test. However, the conventional research method for machinability is not suitable for our research. It will have a high cost and take a lot of time to evaluate the compositions in the target area one by one. A novel combinatorial method for evaluation of machinability will be proposed in our research.

Chapter 3 Introduction of novel combinatorial evaluation method for machinability

3.1 The concept of novel combinatorial evaluation method

Conventional evaluation method for machinability becomes time consuming and costly. As manifested as Figure 3.1, at first, a sample with only one composition was made. Next this sample was used for cutting test to cut the surface. Then the cutting depth and roughness (Ra) of cutting surface were measured to determine the machinability. If the result was not good, the same process would need to be repeated for many times until a material with satisfying machinability was found.

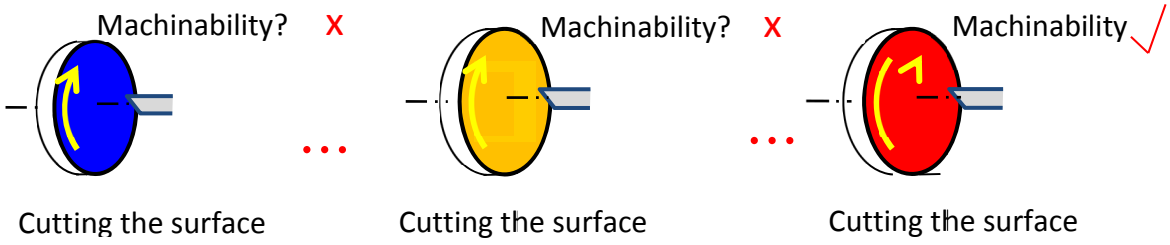

Fig.3.1 Conventional evaluation method for machinability

A novel combinatorial evaluation method for machinability is proposed in this chapter. The key point of this combinatorial method is to fabricate a sample with grading compositions which means that each position on the surface of sample represents a particular composition. Figure 3.2 displays one sample with grading compositions, of which in the center Ti content is rich and becomes gradually decreasing from center to

edge. The values of Ti content level on the concentric circle centered on the center of sample were almost same which can avoid bad impact of great composition difference on the cutting result. If using this sample for cutting test, roughness (Ra) of many compositions can be measured.

It is clearly to see this new method is more efficient than conventional method, which is able to measure a lot of compositions' machinability at one time with one sample.

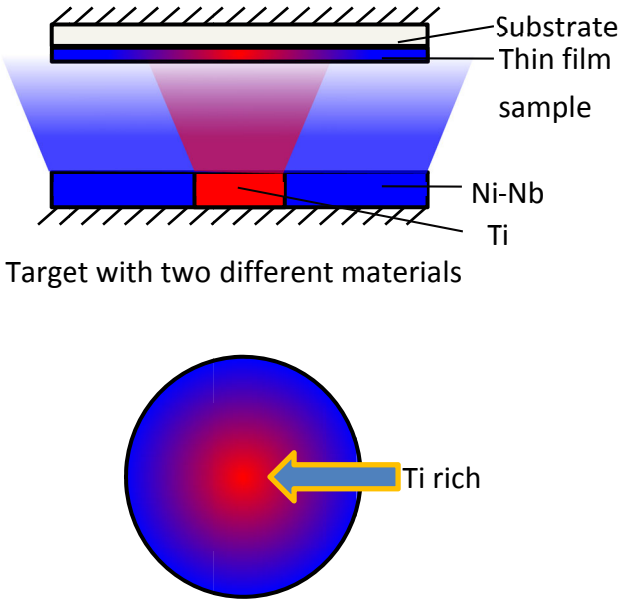

Fig. 3.2 Fabrication of the sample with grading compositions

3.2 Design of combinatorial targets

A conventional parallel-plate sputtering machine was adopted in this research to deposit thin film samples with grading compositions, for which special combinatorial targets were designed which have two parts, outer part made of Ni-Nb alloy and inner part made of pure Ti.

For the combinatorial targets, there is an important thing needing to determine, the size of inner part. As we known, in parallel-plate sputtering system, due to the effect of magnetic field, an area of target will have a high erosion rate, which was calculated and presented as Figure 3.3. According to this, three targets with different sizes of inner part, diameter 11mm, 23.5mm, 36mm respectively, were designed as displayed as Figure 3.4. Moreover, Zr and Al were utilized for trial experiments as outer part of target instead of Ni-Nb alloy because of the lower price and similar sputtering rate.

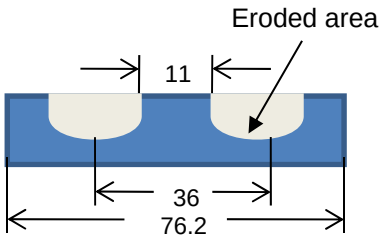

Fig. 3.3 Eroded target (unit:mm)

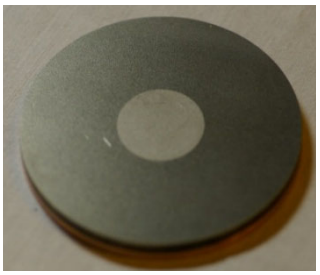

Fig.3.4 The target with inner part Ø 23.5mm

3.3 Trial experiments using Ti-Zr targets

3.3.1 Relationship among Ti content, size of inner part target and TS distance

Ti-Zr target and Ti-Al target were both fabricated at first. However, the thin film samples which were deposited using Ti-Al target were broken due to the high residual stress. Then the trial experiments were carried out only using Ti-Zr targets.

Based on the results from Chapter 2 that when Ti content belongs to 5-20%, thin film sample manifests high thermal stability, the desired area of Ti content was selected as 5-30%, which can also provide a possibility to research on machinability of samples with higher Ti content.

From Figure 3.2 it is clearly that at least there are two factors which can bring important impact on the grading condition of Ti content in the deposited samples, the size of inner part target, pure Ti, and the distance between target and substrate, marked as TS distance. The minimum and the maximum TS distance of the sputtering machine employed for trial experiments in this research is 53.5mm, 91mm, which were chosen as TS for trial experiments at first to determine the relationship between TS distance and grading condition of Ti content.

After determining the sizes of inner part targets and TS distance, trial experiments were performed under sputtering condition, plasma power 300W, sputtering time 30min, to fabricate thin film samples. Compositions of deposited thin film samples were detected by

Energy-dispersive X-ray spectroscopy (EDX), and the result is listed as Table 3.1. Ti content ranges of the samples deposited with a TS distance 53.5mm are more than twice that of the samples deposited with a TS distance 91mm. Ti content level of the thin film sample deposited by using the inner part target Ø11mm is less than 3% which is lower than the minimum requirement for the target area 5%. This target was then temporarily ceased for the trial experiments.

Table 3.1 Results for the TS 53.5mm and 91mm

	TS=53.5mm	TS=91mm
Ti size Ø23.5	Ti %: 14.1% to 17% Content range: 2.9%	Ti%: 11.1% to 12.3% Content range:1.2%
Ti size Ø36	Ti %: 47.3% to 53.8% Content range : 6.5%	Ti %: 41% to 44.2% Content range : 3.2%

The grading conditions of Ti content on the samples were measured by Origin software based on those results from EDX. And they were displayed as Figure 3.5 and Figure 3.6. The grading conditions of Ti on the samples deposited with a TS distance 53.5mm are better than those of samples deposited with a TS distance 91mm. From those results, we can make an assumption that Ti content range increases with decreasing TS distance, meanwhile the grading condition of Ti also improves.

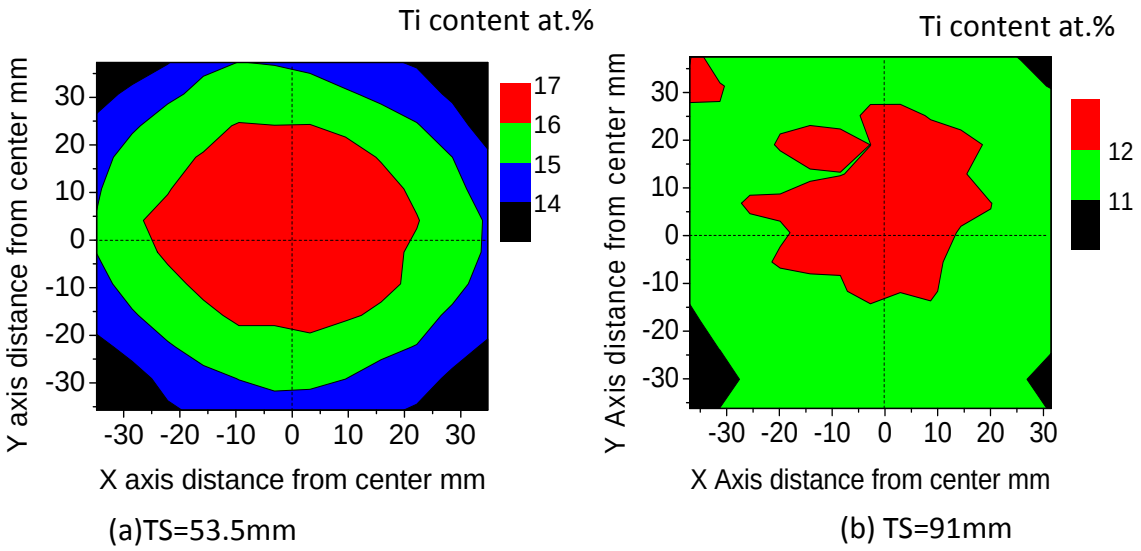

Figure 3.5 Grading condition, Ø Ti= 23.5mm

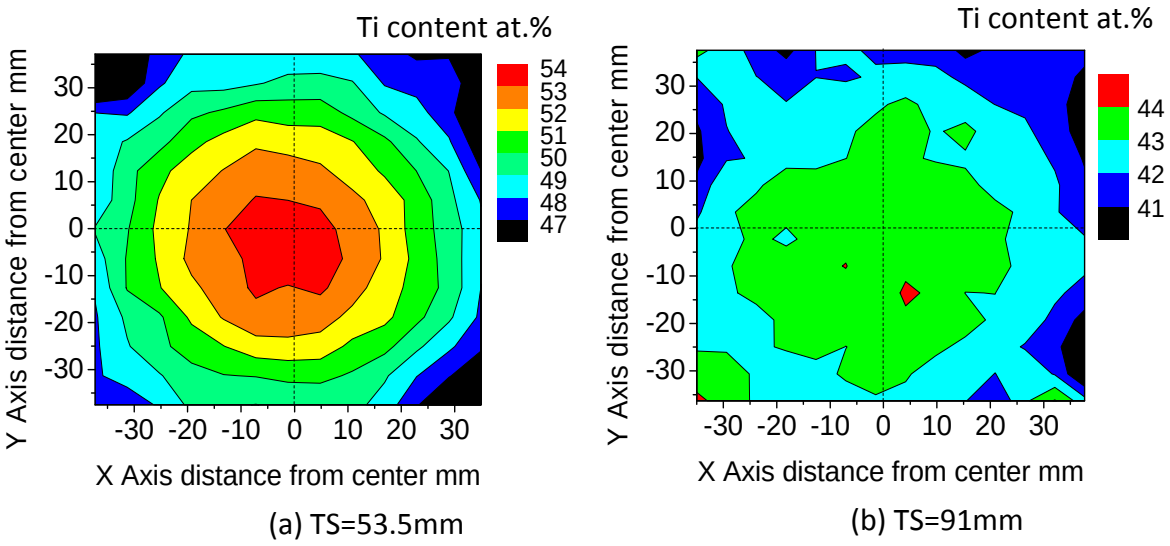

Fig. 3.6 Ti content grading condition (Ø Ti= 36mm)

In order to further decrease TS distance, new jigs with different thickness, presented as Figure 3.7 were designed to decrease TS distance to obtain a larger Ti content range.

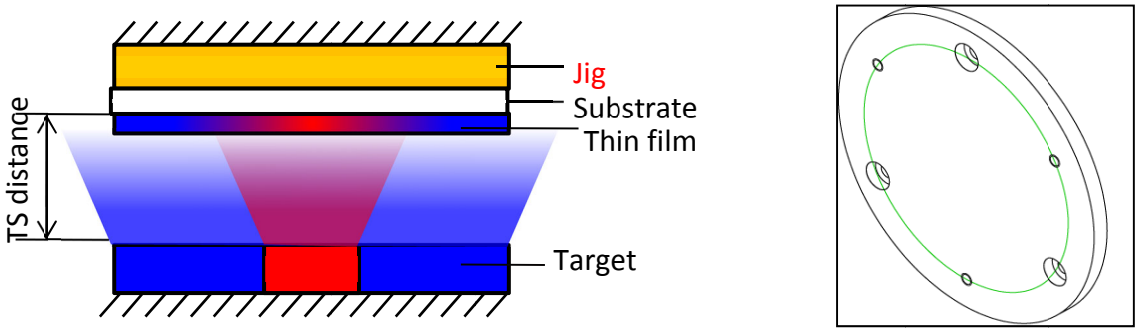

(a) The position of new jig (b) The schematic of new jig

Fig. 3.7 The new jig to decrease TS

Utilizing these jigs, new TS distances were decided as 41mm and 31mm to do the experiments. The composition analyzing results are listed as Table 3.2. Figure 3.8 and 3.9 demonstrate Ti content's grading conditions of the samples made by targets with inner parts Ø23.5mm and Ø36mm. Ti content range rapidly enlarges with decreasing TS distance.

Table 3.2 Results for the TS 31mm and 41mm

	TS=31mm	TS=41mm
Ti size Ø23.5	Ti%:13% to 23.4% Content range:10.4%	Ti%:13.1% to 17.1% Content range: 4%
Ti size Ø36	Ti%:44.1% to 61.5% Content range: 17.4%	Ti%:44.7% to 55% Content range:10.3%

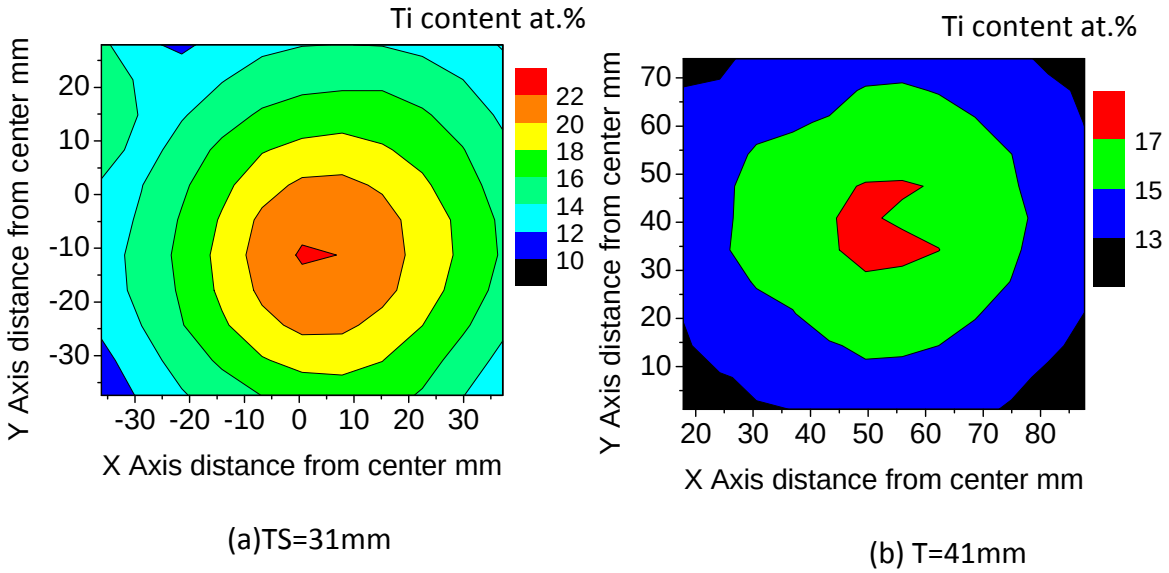

Figure 3.8 Grading condition, Ø Ti= 23.5mm

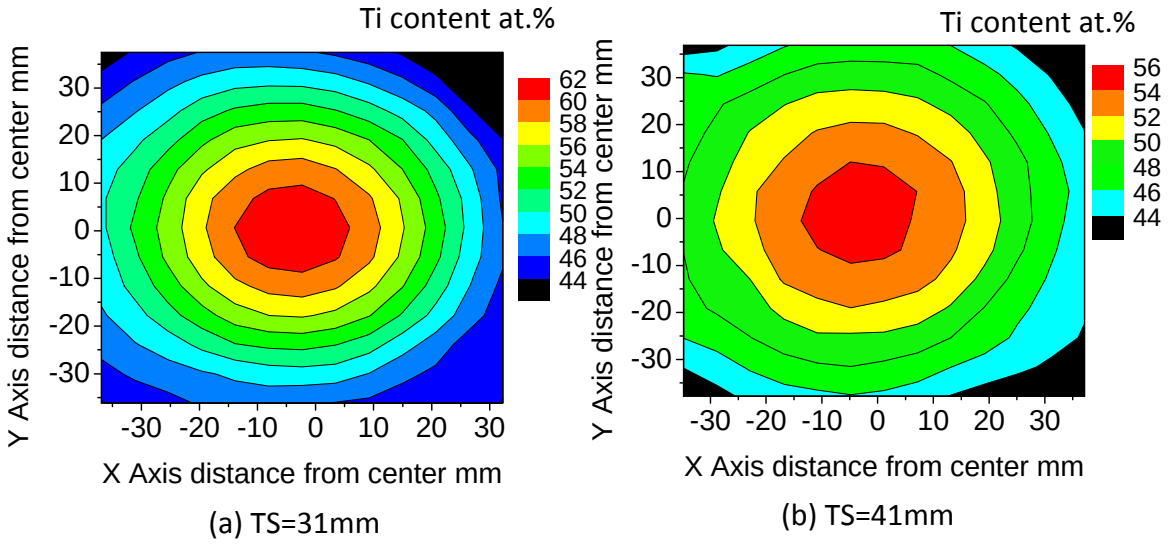

Fig. 3.9 Ti content grading condition (Ø Ti= 36mm)

From Table 3.2, it is clearly to see that the Ti content range of the sample which was deposited under conditions, size of inner target Ø36, TS distance 31mm, is relatively satisfying which is about 17.4%. Moreover, the grading condition of Ti content of this thin film sample as displayed as

Figure 3.9(a) is as wonderful as desired. However, Ti content level of this thin film sample from 44.1% to 61.5% is much higher than desired one from 5% to 30%. We figured out two ways which can decrease Ti content level of the sample. One way is to use an inner target with a smaller size than Ø36, and another way is to utilize Zr-Ti alloy inner target instead of pure Ti. These two methods were carried out at the same time.

Based on those results, one more thing was taken into consideration that the desired Ti content range from 5% to 30% is too large to be possibly obtained in one thin film sample. Besides even if it is possible, the Ti content of sample will change sharply within a small area. During cutting test, some compositions with certain Ti contents in the cutting area will be destroyed and unable to measure their machinability. Therefore, the desired Ti content range from 5% to 30% was considered to separate into three smaller ranges, 5% to 10%, 8% to 18%, 15% to 30%

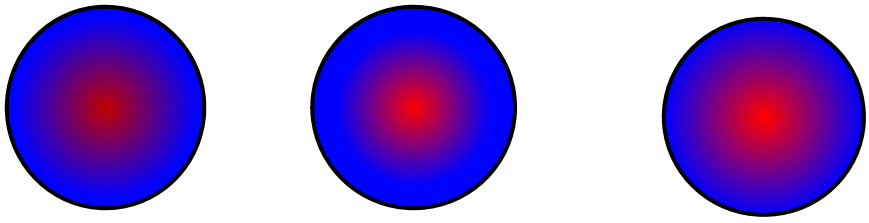

Ti content: 5% to 10% Ti content: 8% to 18% Ti content: 15% to 30%

Fig.3.10 Three samples with target Ti content

3.3.2 Design of new inner targets to decrease Ti content level

Two kinds of new inner targets were designed to decrease Ti content level to the desired area:

1. ZrTi alloy inner target with a size Ø36(at first $Zr_{50}Ti_{50}$ alloy)
2. Pure Ti inner targets with smaller sizes than Ø36

Based on the results in Table 3.2 a figure manifesting the relationship among Ti content, size of inner part target and TS distance can be drawn as shown as Figure 3.11. Pure Ti inner target Ø15 is supposed to lead to a thin film sample of which minimum Ti content level is 5%, meanwhile, Ø25.6 is supposed to result in a thin film sample of which maximum Ti content level is 30%. Given the consideration of degree of accuracy and the possibility to amend the size of inner target, finally the sizes of new pure Ti inner target were decided as Ø17 and Ø27.

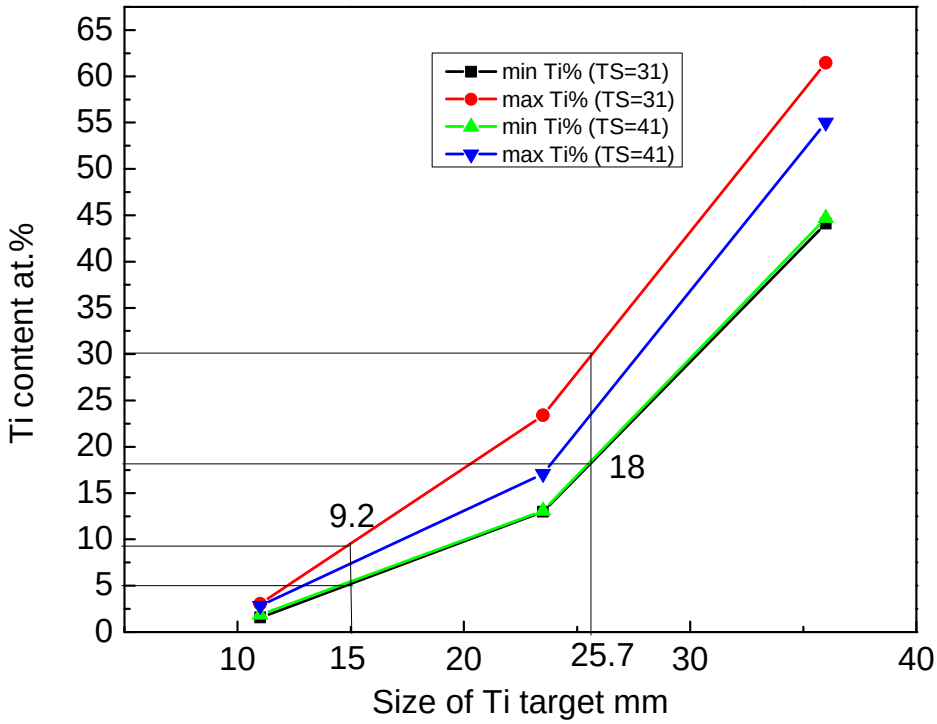

Fig. 3.11 Relationship among Ti content, size of inner part target and TS distance

These three new inner targets were employed to do the trial experiments and results were analyzed with same methods mentioned before. Ti content level in the thin film sample by using $Zr_{50}Ti_{50}$ alloy inner target with a size Ø36, under sputtering condition: plasma power 300W, TS distance 31mm, was from 17.9% to 29.6% which successfully decreased to the desired area. Although the Ti content range also decreased from 17.4% to 11.7%, it was enough to match the third desired range from 18% to 30% described in Figure 3.10. As shown in Figure 3.12, the grading condition of Ti content in this thin film sample is acceptable except for the offset between the center of sample and the center of grading, which is induced by the offset between the centers of substrate and target. In

order to solve this problem, a jig presented as Figure 3.13 was designed on which substrate can slide to adjust the position.

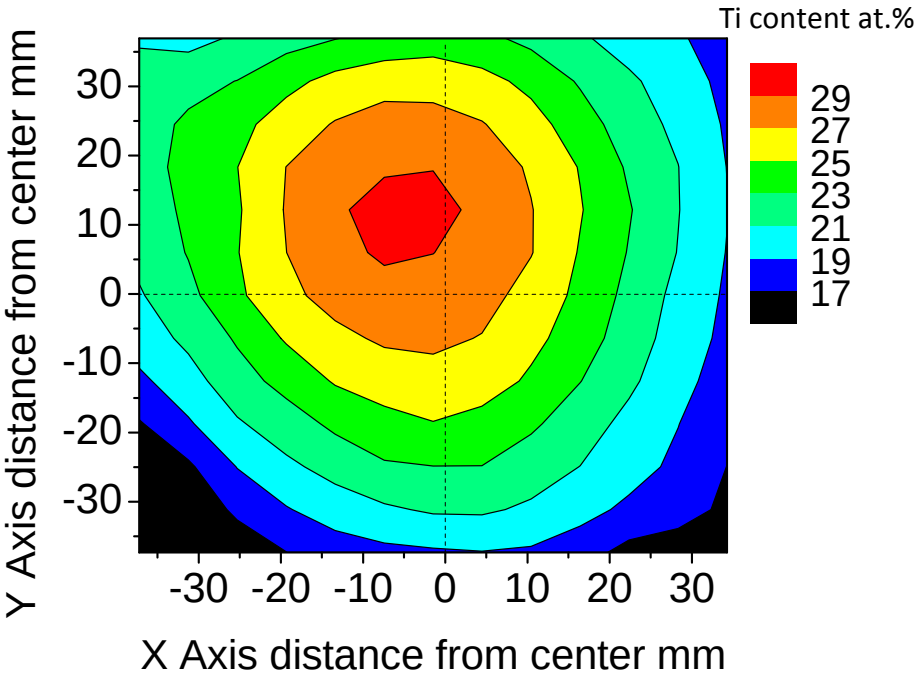

Fig.3.12 Ti content grading condition (Ø $Zr_{50}Ti_{50}$= 36mm, TS=31mm)

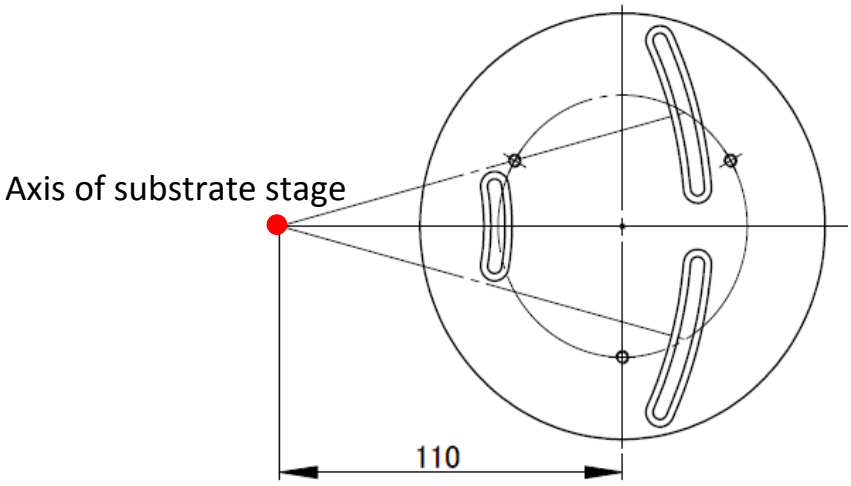

Fig.3.13 Schematic of new jig

Ti content level in the samples by using pure Ti inner targets with sizes of Ø17 and Ø27, under sputtering condition plasma power 300W, TS distance 31mm, were 5.05% to 8.88% and 18% to 28.9% respectively, which are almost the same as expected results based on Figure 3.11

As a result, both these two methods can decrease Ti content level to the desired area. However, if using pure Ti inner targets, three desired Ti content ranges means it needs to make three sets of inner part targets and outer part targets with different sizes of inner targets. On the contrary, in the case of alloy inner target, only by adjusting the composition of inner alloy target, thin film samples with different Ti content level can be achieved. Besides, all the outer targets can be shared due to the same size of inner part. Consequently, for the experiment adopting Ni-Nb-Ti target, inner part target was determined to be Ni-Nb-Ti alloy instead of pure Ti with a size of Ø36.

3.4 Trial experiments using Ni-Nb-Ti alloy inner targets

Ni-Nb-Ti alloy inner targets were fabricated in an arc furnace (ACM-S01T, Diavac Limited). Based on the results of previous experiments using Zr-Ti targets, three inner part targets and outer part targets were made at first with compositions as: inner parts, $Ni_{28}Nb_{50}Ti_{22}$, $Ni_{21}Nb_{35}Ti_{44}$, $Ni_{15}Nb_{20}Ti_{65}$, and outer parts, $Ni_{35}Nb_{65}$, $Ni_{40}Nb_{60}$, $Ni_{50}Nb_{50}$.

By using those targets, thin film samples with grading compositions were fabricated under the sputtering condition described in Table 3.3.The compositions and the Ti grading condition of those thin film samples were examined by EDX and the results are displayed as Figure 3.14, Figure 3.15 and Figure 3.16.

Table 3.3 Parameters for fabrication of thin film samples

RF power	Sputtering pressure	Sputtering time	TS distance
300 W	1 Pa	30 min	31 mm

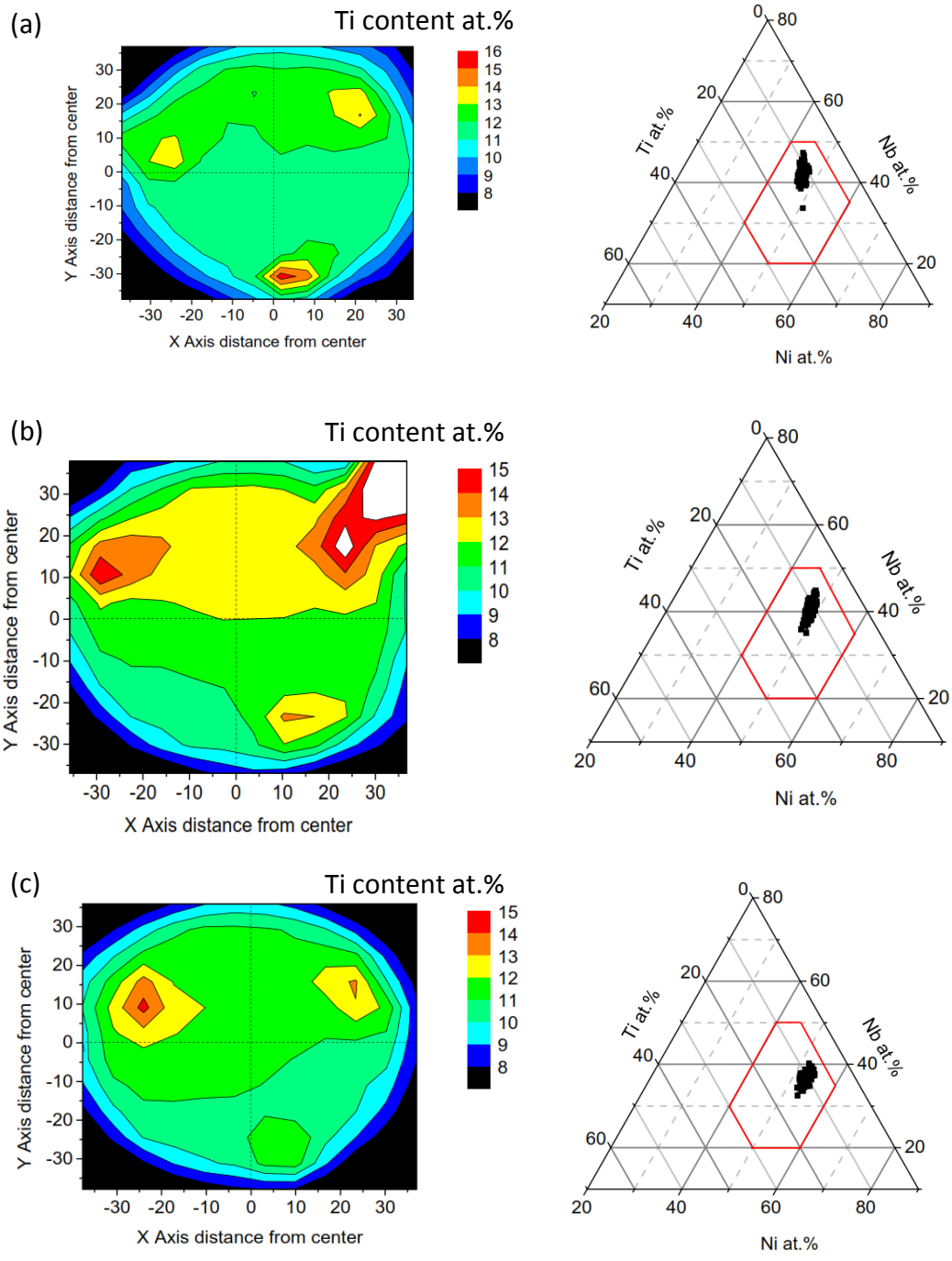

Fig. 3.14 Results for inner part target $Ni_{28}Nb_{50}Ti_{22}$ outer part targets: (a) $Ni_{35}Nb_{65}$, (b) $Ni_{40}Nb_{60}$ and (c) $Ni_{50}Nb_{50}$

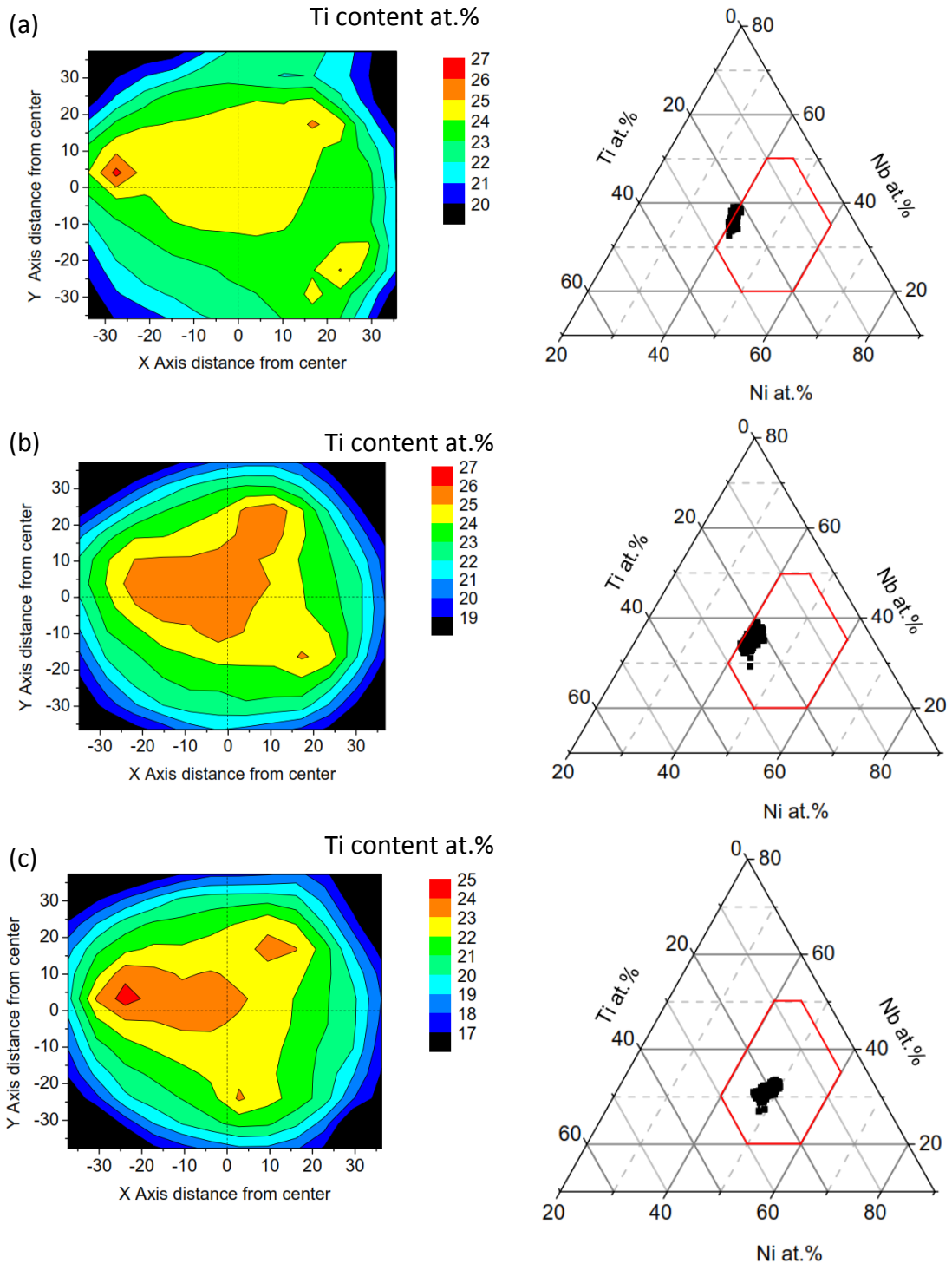

Fig. 3.15 Results for inner part target $Ni_{21}Nb_{35}Ti_{44}$ outer part targets: (a) $Ni_{35}Nb_{65}$, (b) $Ni_{40}Nb_{60}$ and (c) $Ni_{50}Nb_{50}$

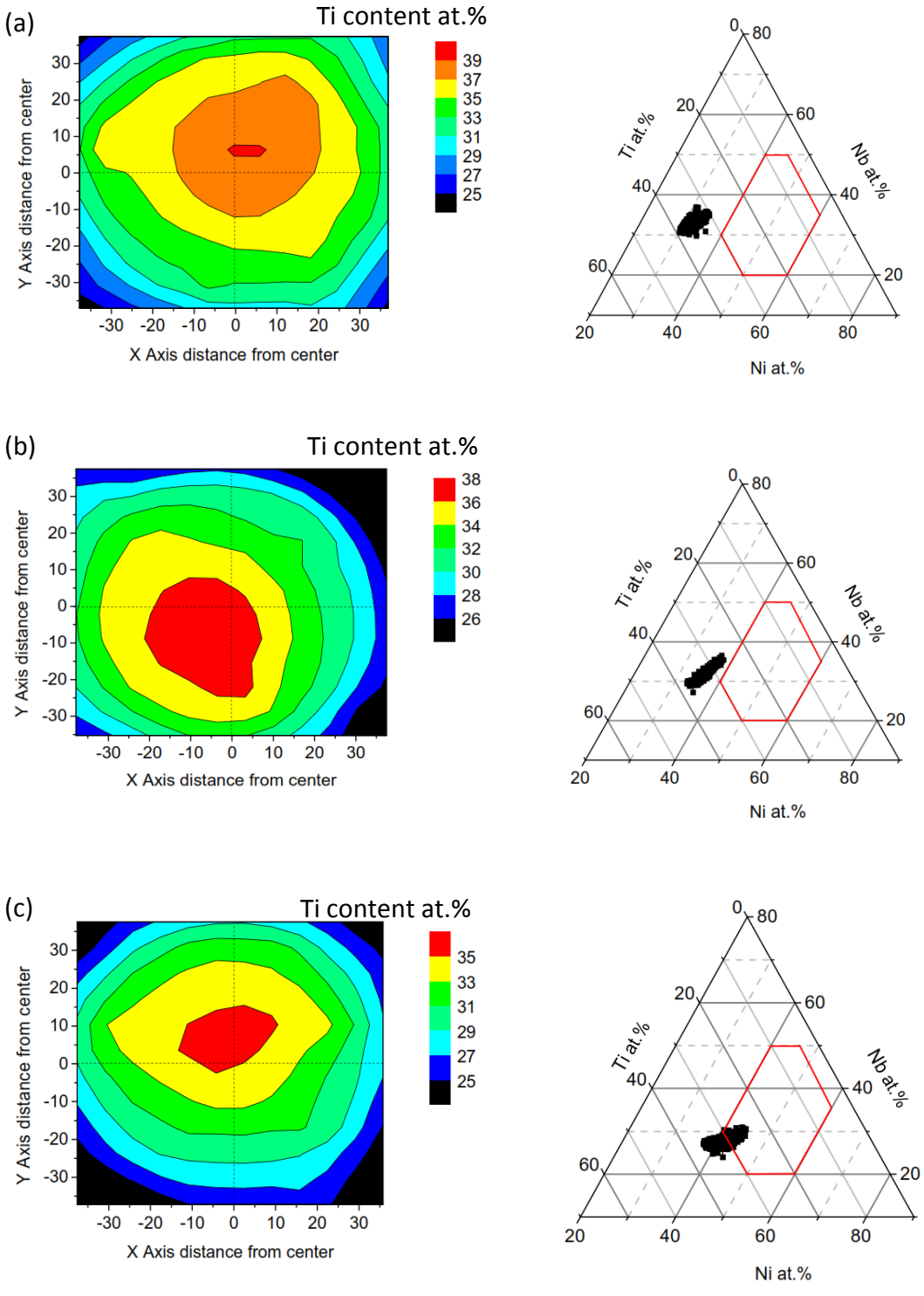

Fig. 3.16 Results for inner part target $Ni_{15}Nb_{20}Ti_{65}$, outer part targets: (a) $Ni_{35}Nb_{65}$, (b) $Ni_{40}Nb_{60}$ and (c) $Ni_{50}Nb_{50}$

It is clear that the grading condition of Ti content in those thin film samples were not as good as trial experiments. Sputtering process for three elements is more complicated than that for two elements. But from these three figures, an assumption can be made that there is a tendency that Ti content grading condition of thin film samples made by using inner target $Ni_{15}Nb_{20}Ti_{65}$ with less Ni content becomes a little better than that of samples made by using other two inner targets. However compositions of thin film samples are beyond the desired area with less Ni content as shown in Figure 3.16.

In order to further improve the Ti grading condition, Ni content in inner targets was decided to reduce to zero. As a result, the inner targets become to be two elements Nb-Ti alloy without Ni element, which is expected to obtain thin film samples with good Ti grading condition as trail experiments using Zr-Ti alloy inner targets. Meanwhile the outer targets are decided to become Ni-Nb alloy with higher Ni content level to make sure the compositions of samples are within the desired area. Based on the results of trial experiments, the compositions of Nb-Ti inner targets were calculated to be: $Nb_{50}Ti_{50}$, $Nb_{66}Ti_{34}$ and $Nb_{83}Ti_{17}$, while Ni-Nb outer targets to be $Ni_{60}Nb_{40}$, $Ni_{70}Nb_{30}$, $Ni_{80}Nb_{20}$ and $Ni_{90}Nb_{10}$. Those targets will be used to fabricate thin film samples for machinability test.

Before that there is one thing need to be confirmed, the feasibility of the novel combinatorial method of machinability. As shown in Figure 3.16 thin film sample made by the target with inner part $Ni_{15}Nb_{20}Ti_{65}$ and

outer part $Ni_{50}Nb_{50}$ has best Ti grading condition even though some compositions is with Ni content less than desired area. Outer part $Ni_{60}b_{40}$ with little higher Ni content was used to made sample for trial experiment of cutting test of confirm the feasibility of combinatorial method of machinability.

3.5 Trial experiment of cutting test using sample made by inner target $Ni_{15}Nb_{20}Ti_{65}$ and outer target $Ni_{60}Nb_{40}$

Thin film sample was deposited on the cutting substrate as shown as Figure 3.17 for cutting test by using the target with inner part $Ni_{15}Nb_{20}Ti_{65}$ and outer part $Ni_{60}Nb_{40}$ under sputtering condition as TS distance 31mm, plasma power 300W, sputtering time 13h.

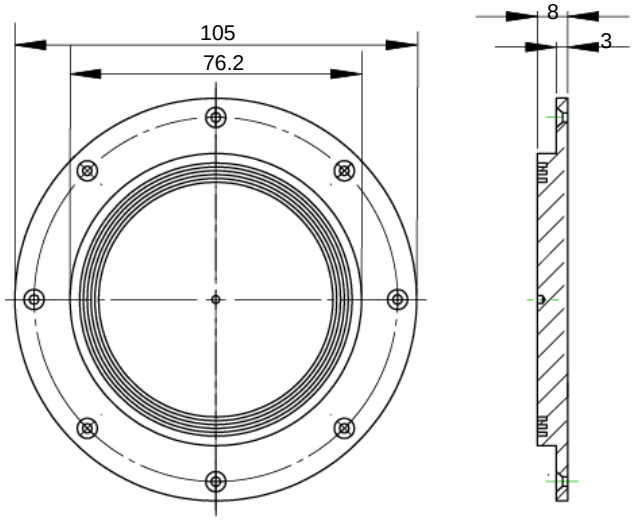

Fig. 3.17 Schematic of cutting substrate

In order to avoid the appearance of crystallization of thin film sample which might be induced by the long-time sputtering and high temperature, a cooling jig was design to place under cutting substrate, presented as Figure 3.18. Composition result of the cutting sample was measured and shown in Figure 3.19.

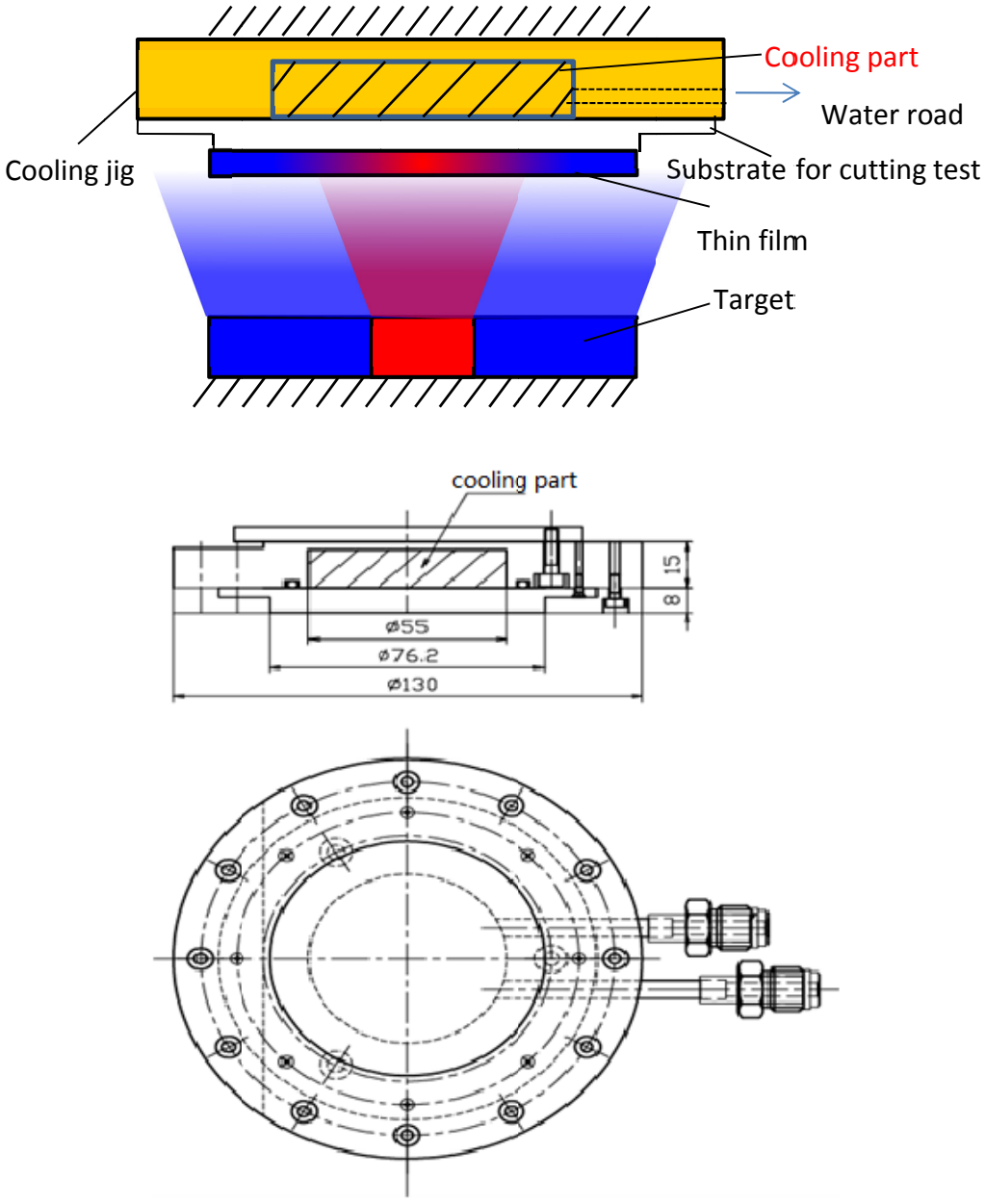

Fig.3.18 Schematic of cooling jig

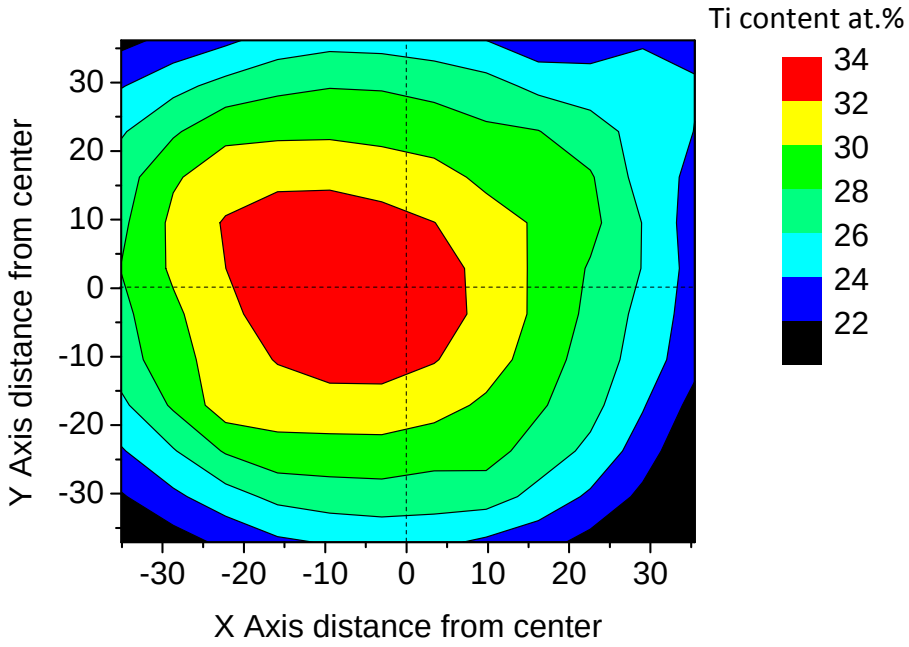

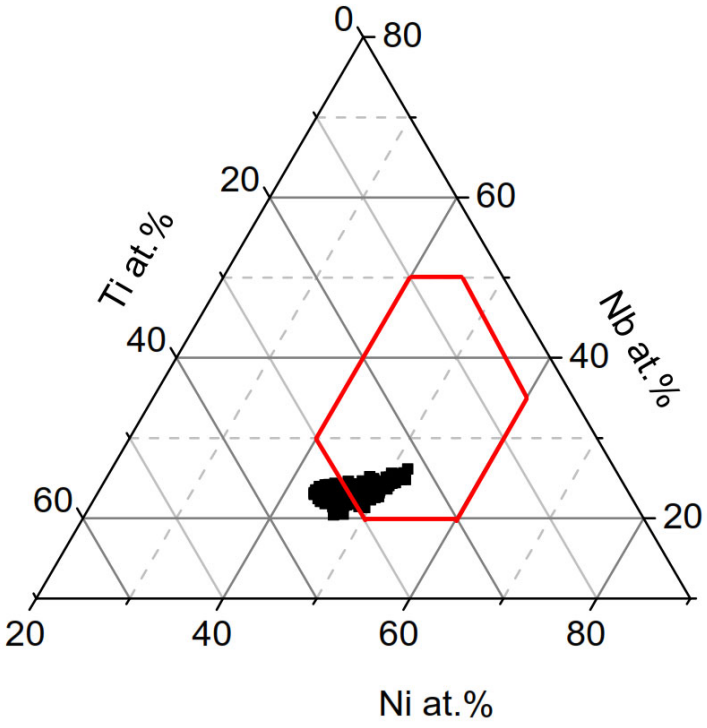

Fig. 3.19 Results of target with inner part $Ni_{15}Nb_{20}Ti_{65}$ and outer part $Ni_{60}Nb_{40}$

An ultra-precision diamond machining system (Nano-100) was adopted for cutting tests to measure the machinability of thin film sample. The sample was cut by a cutting tool with single crystal diamond radius bit (R=0.5 mm) with a constant cutting speed 4mm /s, a radial feeding rate 1μm /rev, a constant axial feeding distance 0.1 μm and feed direction from the center to the outer. The rotation speed of main spindle was controlled to make the cutting speed constant. The same cutting process was repeated for 50 times to obtain a cutting depth 5 μm. As we known, the surface of thin film sample fabricated by conventional parallel-plate sputtering system is arc-shaped. So the cutting sample was ground into flat before cutting test. The sample after cutting test is shown in Figure 3.20. Some part around center peeled off which was assumed to be the result of lack of sticking force between sample and cutting substrate. The roughness (Ra) of cut surface was measured along X Axis drawn in Figure 3.20 and the result is displayed as Figure 3.21.

The area marked A is with a relatively less roughness (Ra) 18nm which does not reach the requirement of glass lens mold material. Within this thin film sample with grading composition, we have not found out a composition qualified for glass lens mold material with high requirement on machinability. However, the result demonstrates the advantage of this novel combinatorial method for evaluation of machinability that it is able to measure the machinability of plenty of compositions at one time using one sample.

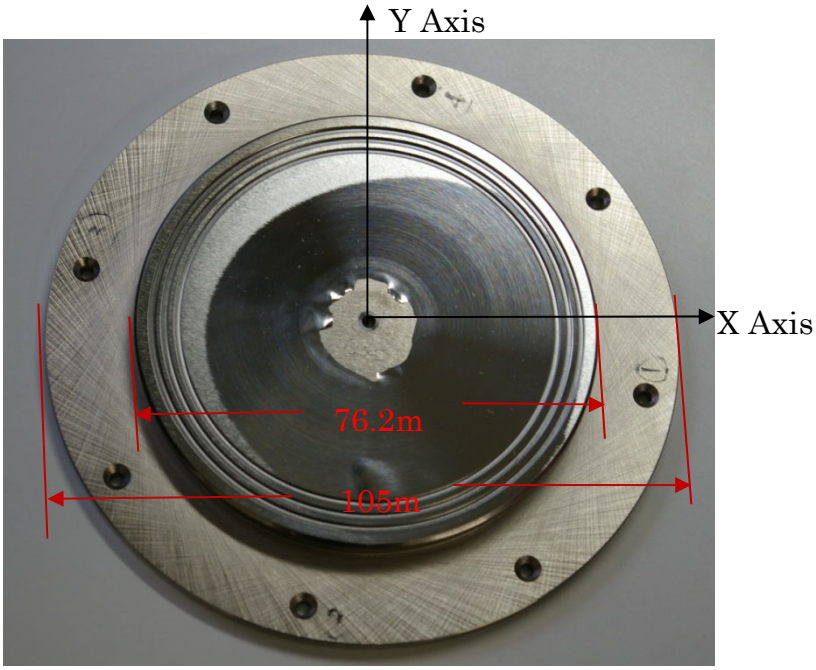

Fig. 3.20 Sample after cutting

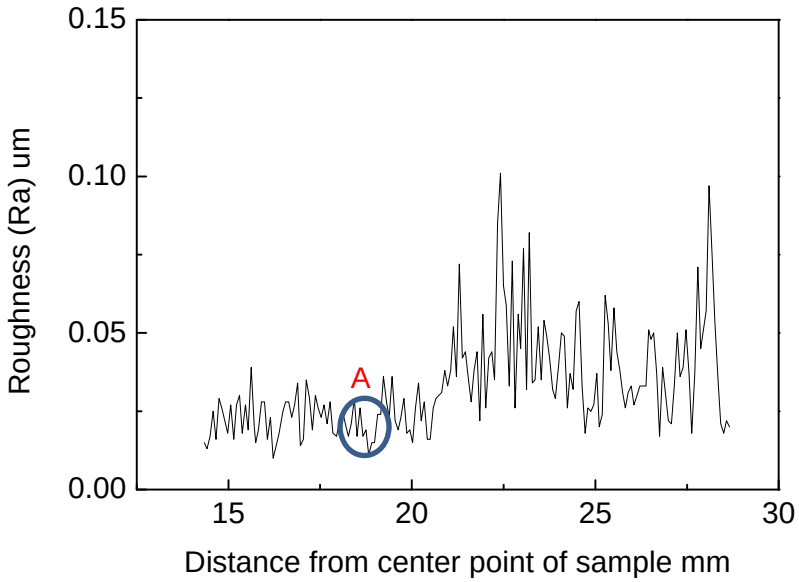

Fig. 3.21 Result of roughness (Ra) measurement

3.6 Summary

Since the conventional method for machinability test is time-consuming and has a high cost, a novel combinatorial evaluation method for machinability was proposed in this chapter. The feasibility of this novel method relies on whether a thin film sample with grading composition can be fabricated or not.

At first trial experiments were carried out to determine the influence of two factors: the size of inner target and the distance from target to substrate, on the grading condition of Ti of the thin film samples. Zr was applied for trial experiment, instead of Ni-Nb, due to the nearly same sputtering rate and lower price. The results are displayed in Table 3.1 and 3.2.

The thin film samples deposited under conditions: size of inner target Ø36, TS distance 31mm, were found out to have satisfying results, good Ti content range and grading condition. As a result, the size of inner target and TS distance were decided to be Ø36 and 31mm for fabrication of thin film samples with grading compositions. However, under this condition Ti content level was higher than the desired one. Then Ti alloy inner targets were adopted instead of pure Ti to decrease Ti content level on the samples.

Three inner part targets were designed at first, $Ni_{28}Nb_{50}Ti_{22}$, $Ni_{21}Nb_{35}Ti_{44}$, $Ni_{15}Nb_{20}Ti_{65}$. The results of those targets shows that

increasing Ni's content level in outer part or decreasing Ni's content level in inner part, Ti content grading condition becomes a little better. As a result, the inner targets are decided to become Nb-Ti alloy without Ni element to fabricate thin film samples for machinability test by combinatorial method.

Before the experiments using Nb-Ti alloy inner targets, the feasibility of novel combinatorial method on machinability has to be confirmed. As shown in Figure 3.16 thin film sample made by the target with inner part $Ni_{15}Nb_{20}Ti_{65}$ and outer part $Ni_{50}Nb_{50}$ has best Ti grading condition even though some compositions is with Ni content less than desired area. Outer part $Ni_{60}b_{40}$ with little higher Ni content was used to made sample for trial experiment of cutting test.

The roughness of cut surface had been measured. Although the best value of roughness is 21nm which is larger than the requirement for glass lens mold material 5nm, the result had proved the feasibility of the novel combinatorial method on machinability introduced in this research.

Chapter 4 Evaluation of machinability for Ni-Nb-Ti alloys using the novel combinatorial method

4.1 Experiments using Nb-Ti inner targets

As mentioned in chapter 3, inner part targets were decided to be Nb-Ti alloy with Ni element in order to improve Ti grading conditions of thin film samples which were finally designed as $Nb_{50}Ti_{50}$, $Nb_{66}Ti_{34}$, $Nb_{83}Ti_{17}$ with diameter 36mm. While outer part targets were decided to be Ni-Nb alloy with higher Ni content level to make sure Ni content within desired area which were finally designed as $Ni_{90}Nb_{10}$, $Ni_{80}Nb_{20}$, $Ni_{70}Nb_{30}$ and $Ni_{60}Nb_{40}$. 12 groups of targets can be obtained by combining those outer targets with three inner targets mentioned above. Those targets were assembled to a conventional parallel-plate sputtering system respectively to make twelve thin film samples under the following conditions: Sputtering pressure 1Pa, RF power 300W, Sputtering time 30 min, TS distance 31mm.

The compositions of fabricated thin film samples were examined by EDX. Based on EDX data, the composition and Ti grading condition of each sample was analyzed and shown from Figure 4.1.to Figure 4.3

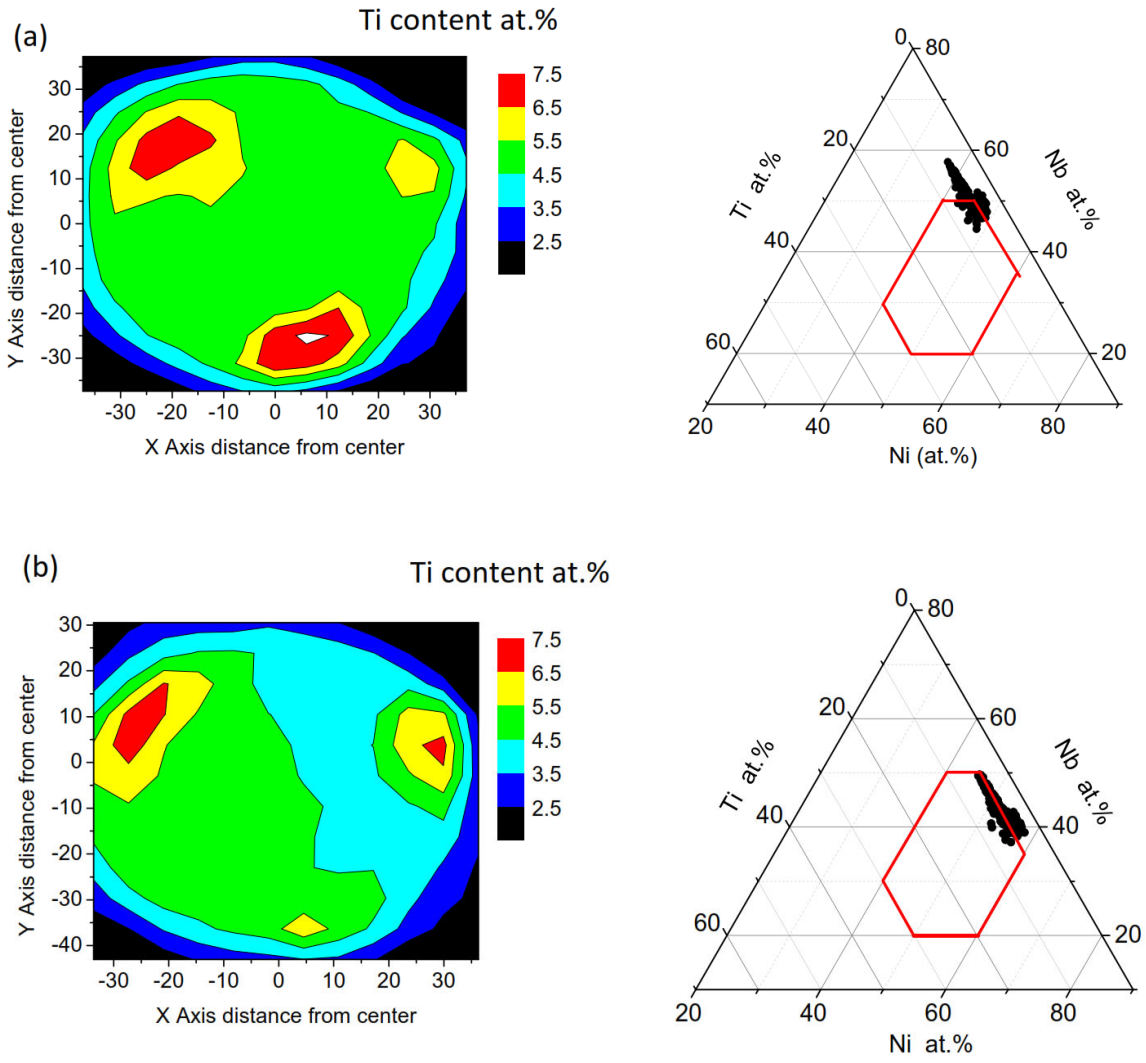

Fig. 4.1 Results for inner part target $Nb_{83}Ti_{17}$, outer part targets: (a) $Ni_{60}Nb_{40}$, (b) $Ni_{70}Nb_{30}$, (c) $Ni_{80}Nb_{20}$ and (d) $Ni_{90}Nb_{10}$

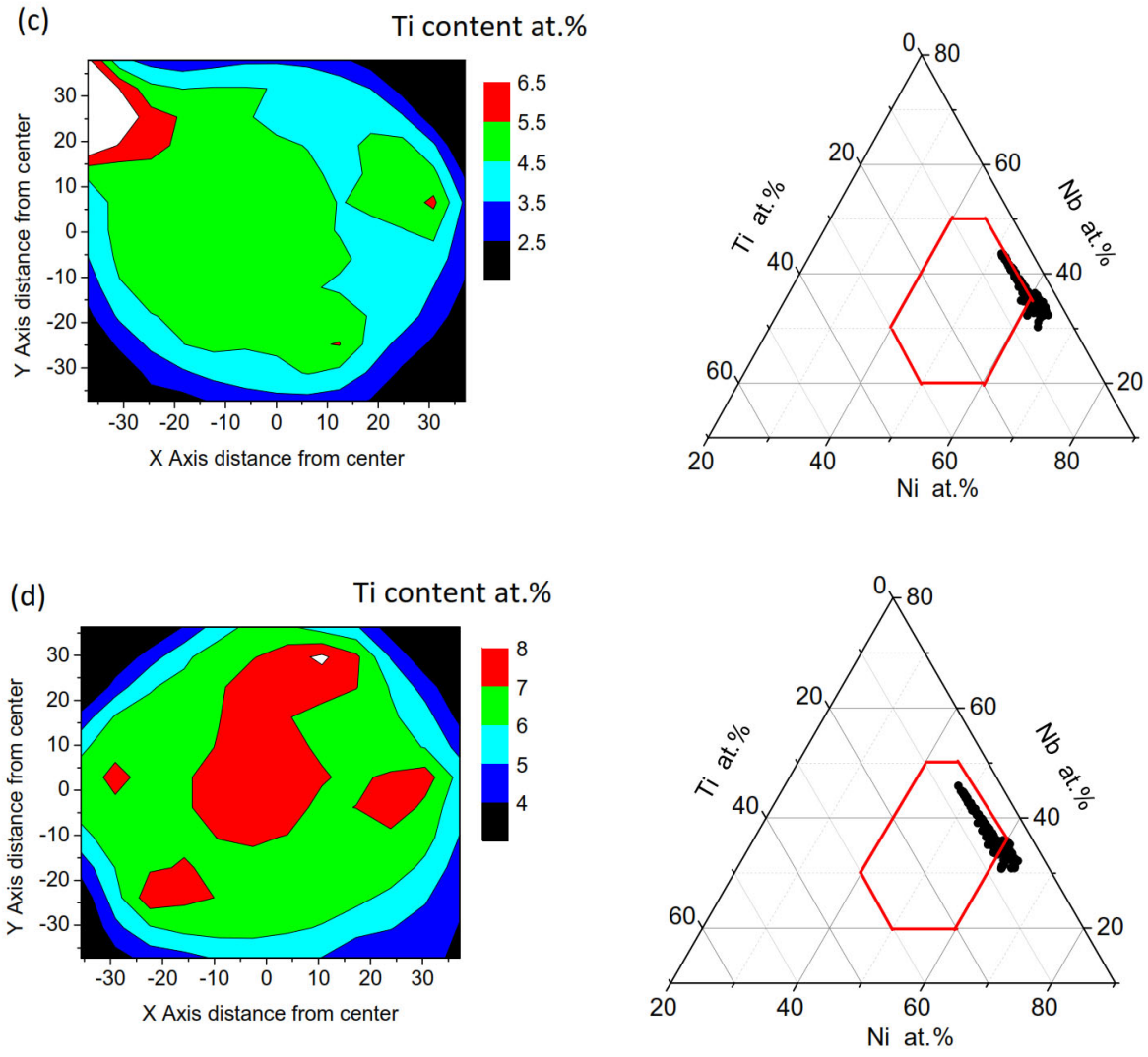

Fig. 4.1 Results for inner part target $Nb_{83}Ti_{17}$, outer part targets: (a) $Ni_{60}Nb_{40}$, (b) $Ni_{70}Nb_{30}$, (c) $Ni_{80}Nb_{20}$ and (d) $Ni_{90}Nb_{10}$

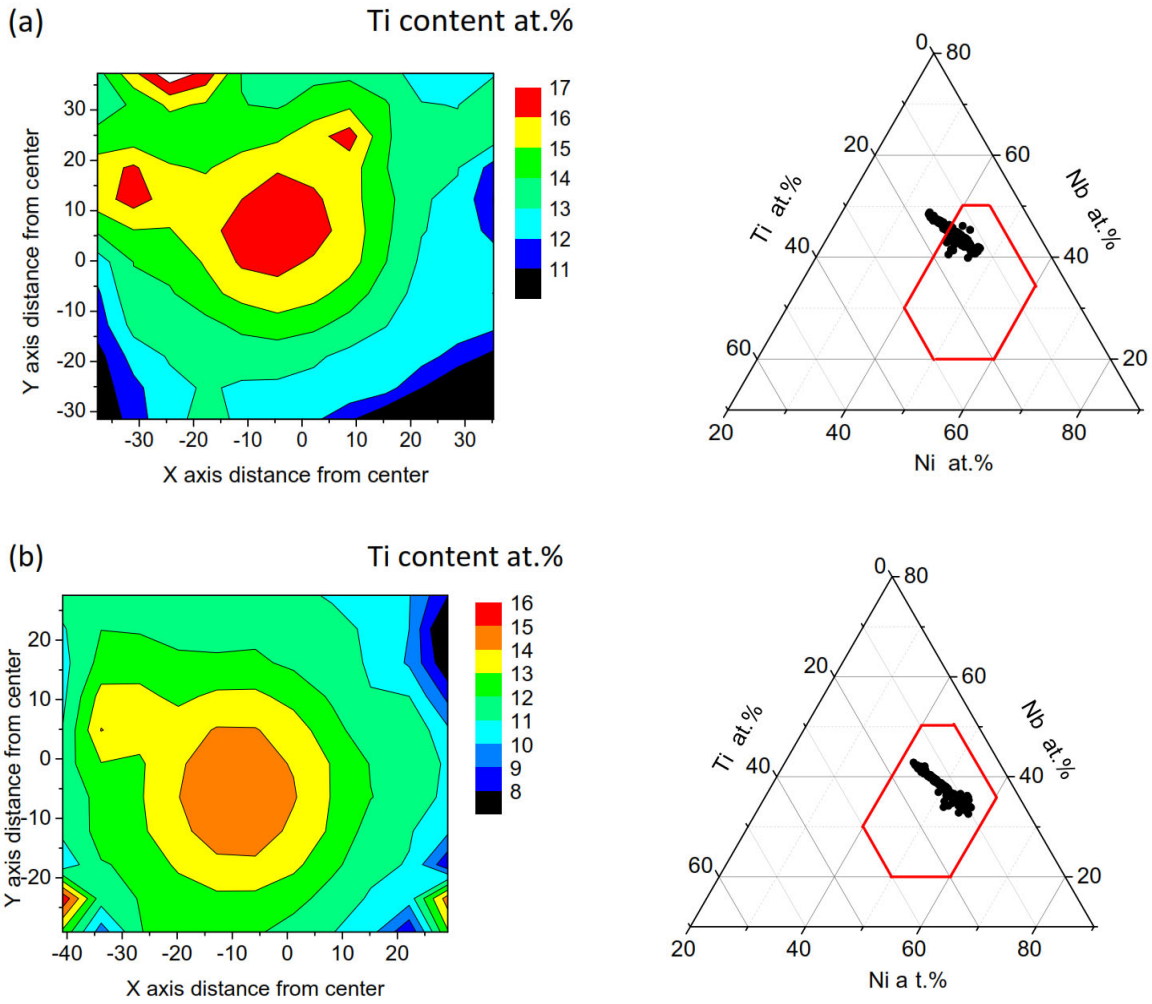

Fig. 4.2 Results for inner part target $Nb_{66}Ti_{34}$, outer part targets: (a) $Ni_{60}Nb_{40}$, (b) $Ni_{70}Nb_{30}$, (c) $Ni_{80}Nb_{20}$ and (d) $Ni_{90}Nb_{10}$

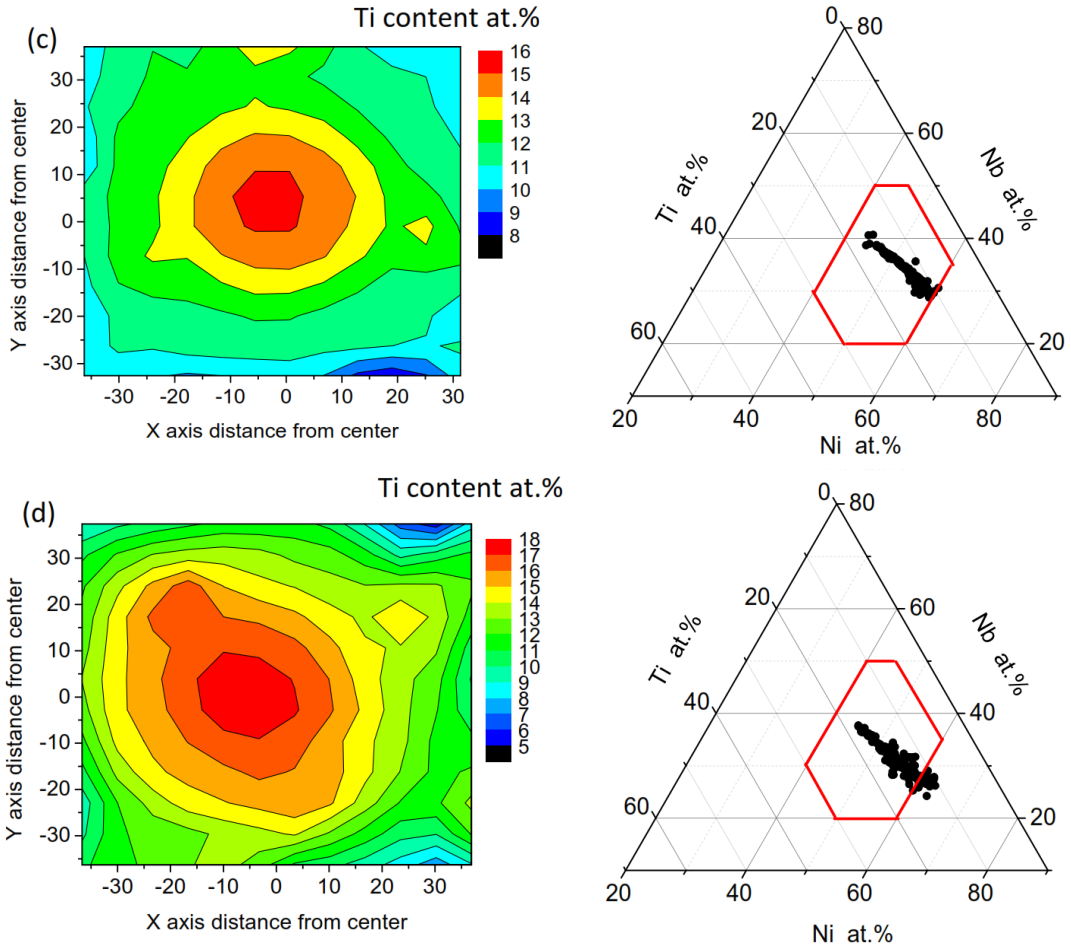

Fig. 4.2 Results for inner part target $Nb_{66}Ti_{34}$, outer part targets: (a) $Ni_{60}Nb_{40}$, (b) $Ni_{70}Nb_{30}$, (c) $Ni_{80}Nb_{20}$ and (d) $Ni_{90}Nb_{10}$

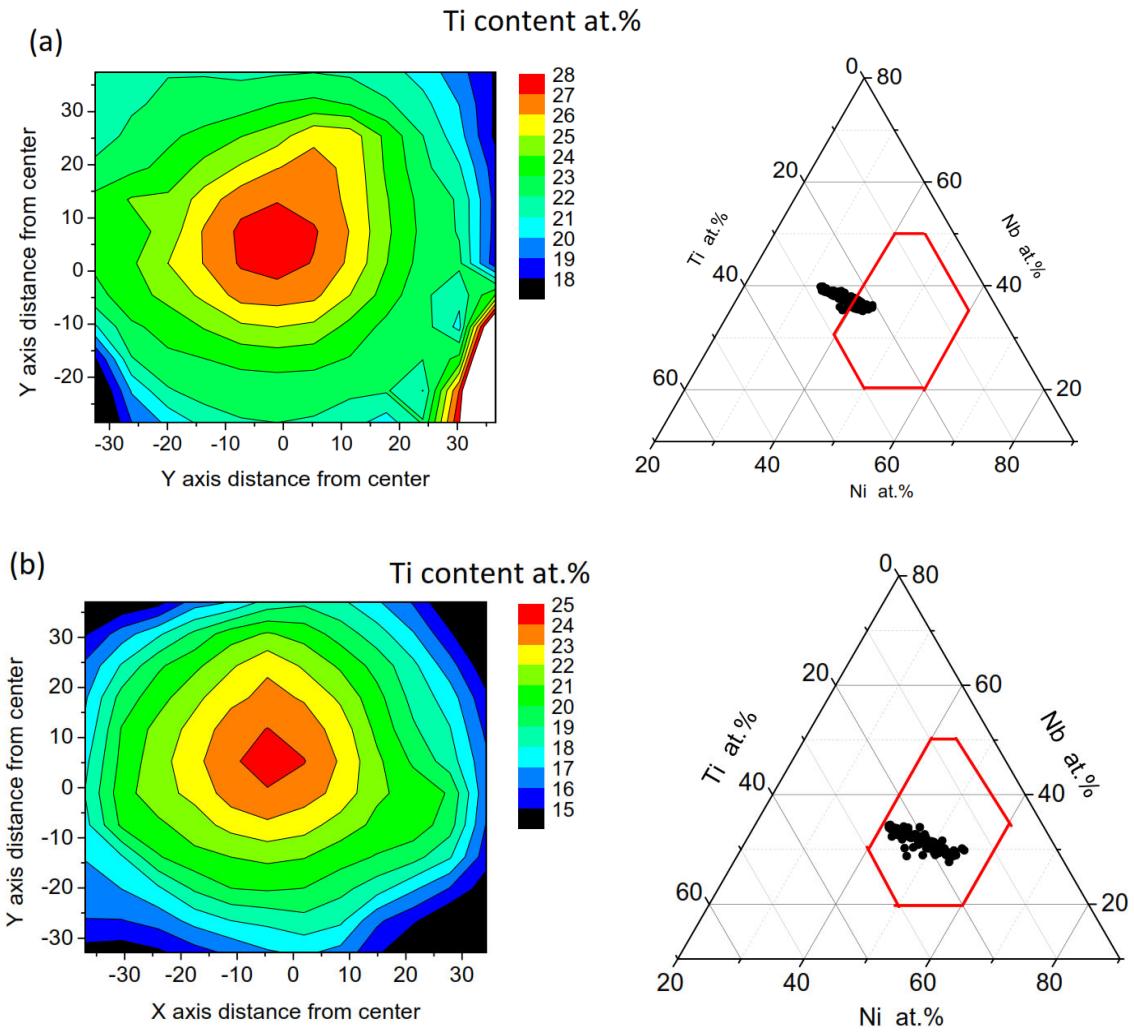

Fig. 4.3 Results for inner part target $Nb_{50}Ti_{50}$, outer part targets: (a) $Ni_{60}Nb_{40}$, (b) $Ni_{70}Nb_{30}$, (c) $Ni_{80}Nb_{20}$ and (d) $Ni_{90}Nb_{10}$

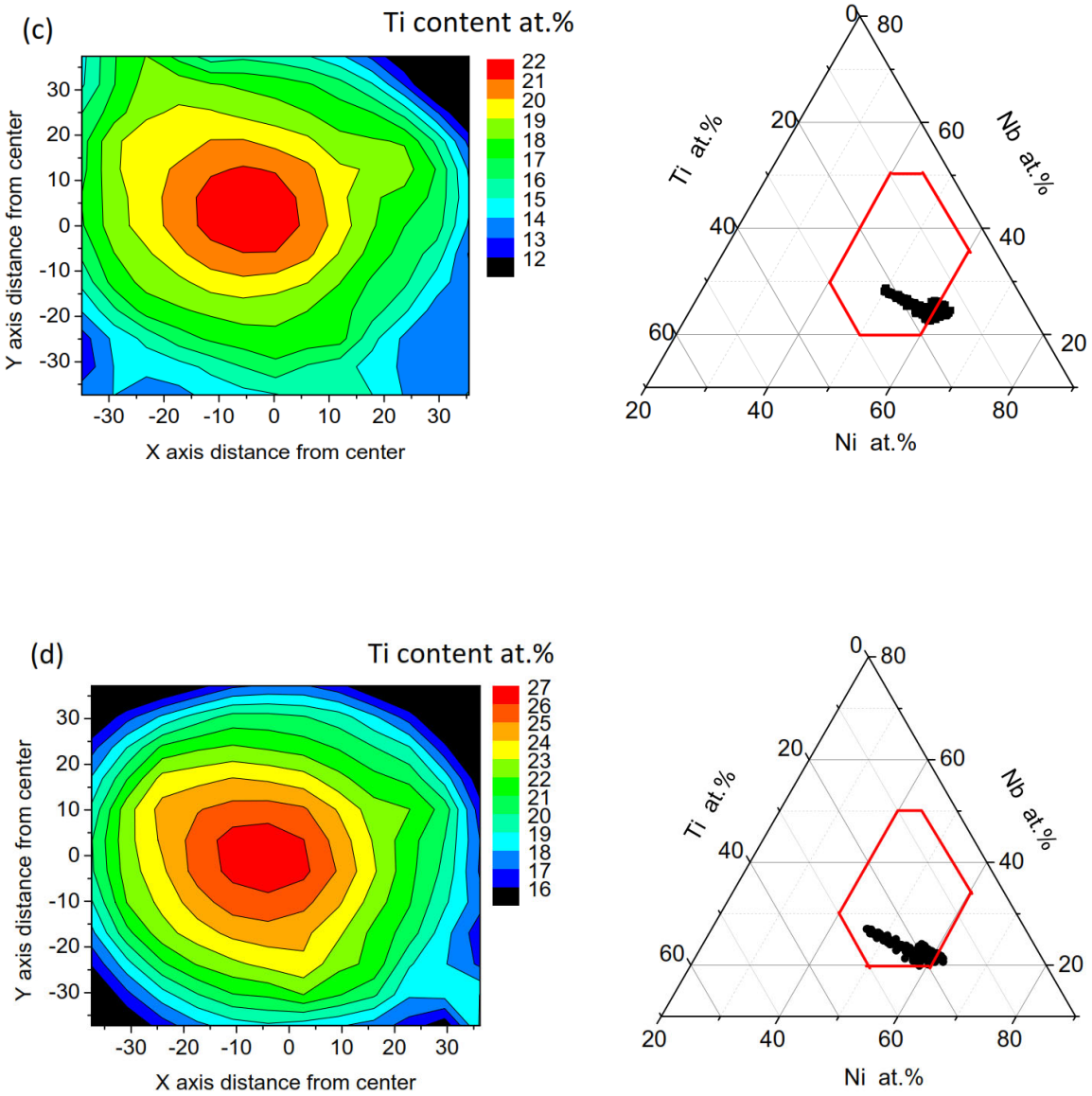

Fig. 4.3 Results for inner part target $Nb_{50}Ti_{50}$, outer part targets: (a) $Ni_{60}Nb_{40}$, (b) $Ni_{70}Nb_{30}$, (c) $Ni_{80}Nb_{20}$ and (d) $Ni_{90}Nb_{10}$

Ti content level and range of each thin film sample have been summarized in Table 4.1, which reveals that the higher Ti content level is in inner target, the larger is Ti content range in the thin film sample. Four thin film samples made by using inner target $Nb_{50}Ti_{50}$ have larger Ti

content range than that of thin film samples made by using other two inner targets with lower Ti content level. The thin film sample 1 deposited by inner target $Nb_{50}Ti_{50}$, outer target $Ni_{70}Nb_{30}$ has the largest Ti content range about 10.5%. In addition, Ti grading conditions of those thin film samples shown in Figure 4.3 are better than that of the thin film samples made by other inner targets.

According to the data from EDX presented in Table 4.1, Figure 4.4 can be drawn to demonstrate composition results of those twelve thin film samples. The area marked by red line in Figure 4.4 is the desired area which has high thermal stability acquired from previous research's result in our laboratory. These twelve samples' compositions can cover most part of the desired area. However, there is still some blank area uncovered. New inner targets are going to be designed to cover the blank area.

Table4. 1 The Ti content level and range results of thin film samples

Outer / Inner	$Ni_{90}Nb_{10}$	$Ni_{80}Nb_{20}$	$Ni_{70}Nb_{30}$	$Ni_{60}Nb_{40}$
$Nb_{50}Ti_{50}$	Ti : 16.8% to 26.8% Range: 10% (1)	Ti :13% to 21.9% Range: 9.1% (2)	Ti : 15.5% to 26% Range:10.5% (3)	Ti: 20% to 28% Range:8% (4)
$Nb_{66}Ti_{34}$	Ti : 10% to 17.7% Range: 7.7% (5)	Ti:9.2% to 16.7% Range: 7.5% (6)	Ti : 8% to 15% Range : 7% (7)	Ti :11% to 17% Range :6% (8)
$Nb_{83}Ti_{17}$	Ti:4% to 8% Range: 4% (9)	Ti:2.5% to 6.5% Range: 4% (10)	Ti:2.7% to 7.7% Range: 5% (11)	Ti:2.6% to 7.6% Range: 5% (12)

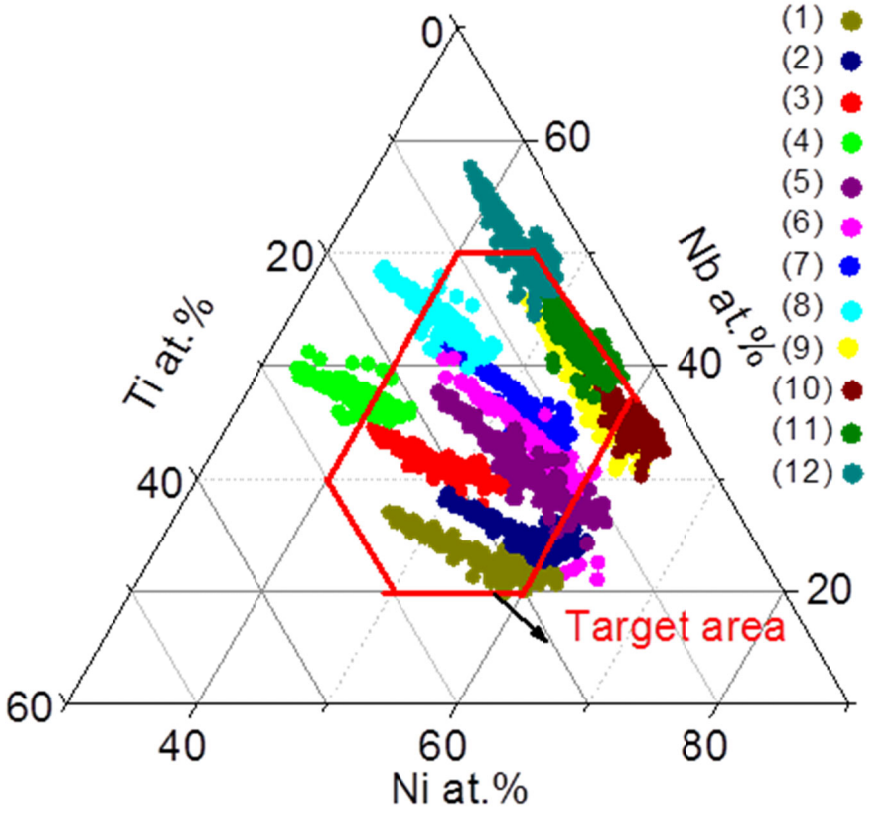

Fig.4.4 The composition results of thin film samples

The compositions of thin film sample 3 are entirely within the desired area. Besides that, it has largest Ti content range among those twelve thin film samples as presented in Table 4.1. As shown in Figure 4.3(b), thin film sample 3 also owns great grading condition of Ti. According to those, thin film sample 3 was considered to be first sample for cutting test.

4.2 Cutting test result for the sample made by inner target $Nb_{50}Ti_{50}$

Due to the largest Ti content range and good Ti grading condition, thin film sample 1 deposited by inner target $Nb_{50}Ti_{50}$ and outer target $Ni_{70}Nb_{30}$, was decided to be the first sample for cutting test. In this case, sputtering time was extended to around 5 hours to make a cutting sample with a thickness about 20μm.

Figure 4.5 displays the composition result of this cutting sample. The compositions of entire sample are within the desired area marked by red line in the Figure 4.5. Ti content level of the sample is from 15.6% to 24.4%. Although it has a deviation about 1.7%, it is assumed that long-time sputtering does not have a serious impact on the condition distribution. Ti's grading condition of this cutting sample is shown as Figure 4.6. There is a deviation about 5mm between the centers of Ti grading and substrate. However, on the concentric circles centered on the center hole of substrate, there is only less than 1% change of Ti content level. So this deviation is assumed to have little impact on cutting test.

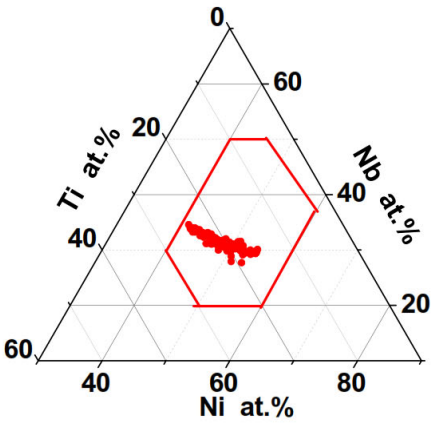

Fig.4.5 Composition of cutting sample

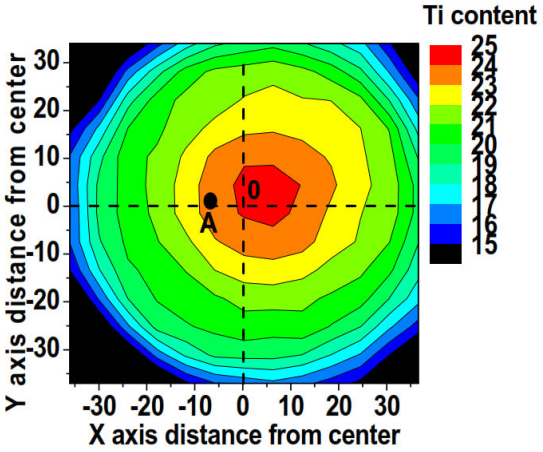

Fig.4.6 Ti grading condition of cutting sample

An ultra-precision diamond machining system (Nano-100) was adopted for cutting tests to measure the machinability of thin film samples. The sample was cut by a cutting tool with single crystal diamond radius bit(R=0.5 mm) with a peripheral speed 4 mm /s, a radial feeding rate 1 μm /rev, a constant axial feeding distance 0.1 μm. The same cutting process was repeated for 50 times to obtain a cutting depth 5 μm. As we known, the surface of thin film sample fabricated by conventional parallel-plate sputtering system is arc-shaped. So the cutting sample was ground into flat before cutting test.

As demonstrated in Figure 4.6, Ti grading condition is round and symmetric, which leads to that every diameter line can contain whole Ti content range of the entire cutting sample. In other words, it only needs to measure the roughness of a diameter line instead of entire surface to acquire machinability of whole sample. Subsequently, surface condition of

the sample after cutting test was evaluated along X axis as displayed in Figure 4.7 by an optical metrology instrument.

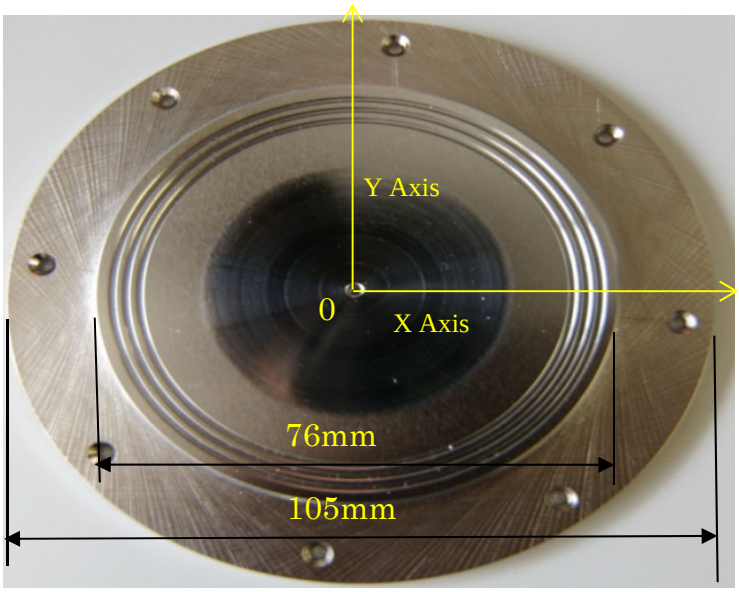

Fig.4.7 The sample after cutting test

The result of roughness measurement is demonstrated in Figure 4.8. Ra of a sampling length 0.07mm is recorded as roughness value of center point of this sampling area. In Figure 4.8, the area marked A has relatively better surface condition with an average roughness 21nm, and the average composition of this area measured by EDX is to be $Ni_{37.7}Nb_{38.5}Ti_{23.8}$. Although the smallest value of roughness on the surface of this cutting sample is higher than 5nm which is required as mold material for glass lens with diffractive gratings, the results of this cutting test successfully confirm the feasibility of the novel combinatorial method on machinability proposed in our research.

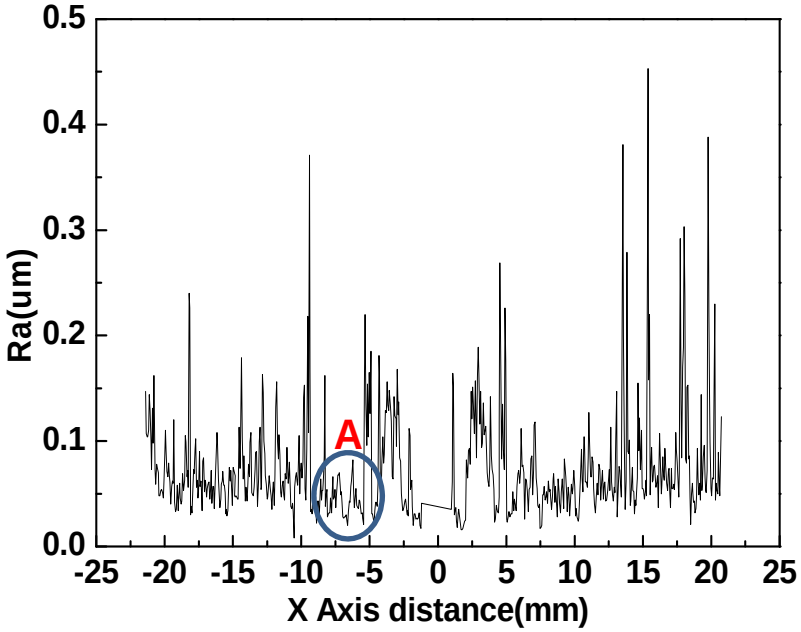

Fig.4.8 The roughness results of the cutting sample

4.3 Experiment using new additional Nb-Ti inner targets

As shown in Figure 4.4, there is still some blank area uncovered by using exist inner targets. Therefore, new inner targets $Nb_{40}Ti_{60}$, $Nb_{75}Ti_{25}$, were designed to cover it. Using these two inner targets, new thin film samples were made under the following conditions: Sputtering pressure 1Pa, RF power 300W, Sputtering time 30 min, TS distance 31mm.

The composition of each sample was examined by EDX and the results of Ti content level and range were summarized in Table 4.2. The results also confirm the conclusion made before that the higher Ti content

level is in the inner target, the larger is the Ti content range of thin film samples.

Table 4.2 The Ti content level and range results of new thin film samples

Outer / Inner	$Ni_{90}Nb_{10}$	$Ni_{80}Nb_{20}$	$Ni_{70}Nb_{30}$	$Ni_{60}Nb_{40}$
$Nb_{40}Ti_{60}$	Ti : 18.7% to 33.6% (1) Range:14.9%	Ti : 18.4% to 29.1% (2) Range: 10.7%	Ti : 15.7% to 27.2% (3) Range:11.5%	Ti : 17.8% to 30.1% (4) Range:12.4%
$Nb_{75}Ti_{25}$	Ti : 6% to 12.3% Range:6.3% (8)	Ti : 5.2% to 11.3% Range: 6.1% (7)	Ti : 4% to 10.5% Range:6.5% (6)	Ti : 4.1% to 10.7% Range:6.6% (5)

Figure 4.9 and Figure 4.10 present the composition results of thin film samples made by inner target $Nb_{40}Ti_{60}$ and $Nb_{75}Ti_{25}$ respectively. In the Figure 4.9 and Figure 4.10, the gray area is the composition results of thin film sample made by previous three inner targets $Nb_{50}Ti_{50}$, $Nb_{66}Ti_{34}$, $Nb_{83}Ti_{17}$, same as in Figure 4.4. As we can see, by using the two new inner targets, it can fabricate thin film samples to cover the blank area in Figure 4.4.

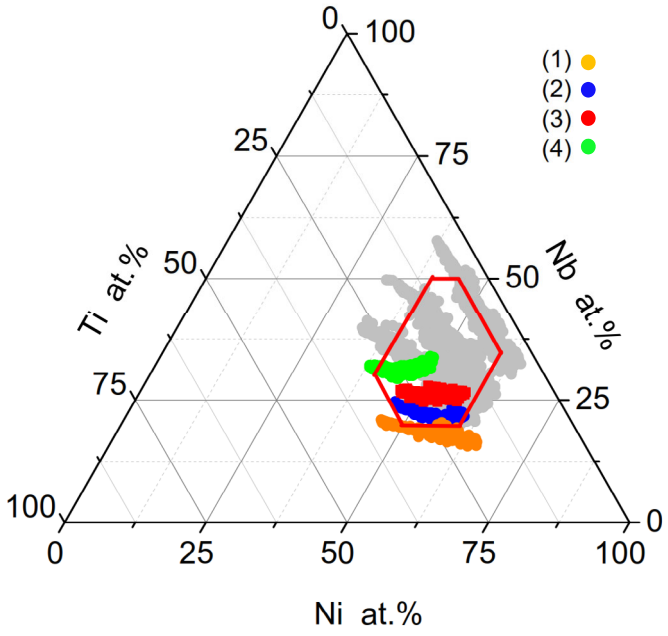

Fig.4.9 Composition results for the samples made by inner targets $Nb_{40}Ti_{60}$

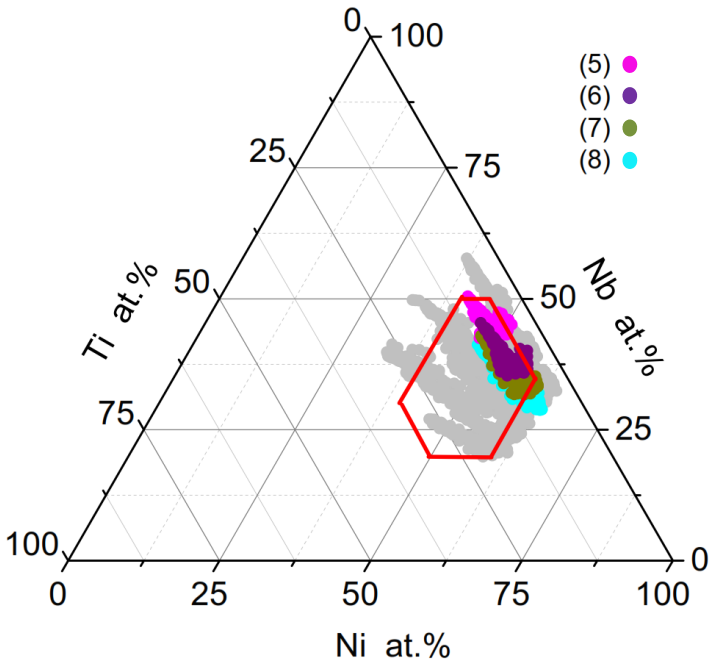

Fig.4.10 Composition results for the samples made by inner targets $Nb_{75}Ti_{25}$

The grading conditions of Ti content for the thin film samples made by inner target $Nb_{40}Ti_{60}$ and $Nb_{75}Ti_{25}$ are shown in Figure 4.11 and Figure 4.12. Since the composition of the thin film sample 1 fabricated by using inner target $Nb_{40}Ti_{60}$ and outer target $Ni_{90}Nb_{10}$ is almost out of the desired area as shown in Figure 4.11(d), and the composition result of thin film sample 7 fabricated by using inner target $Nb_{75}Ti_{25}$ and outer target $Ni_{80}Nb_{20}$ coincides with that of other samples as shown in Figure 4.10, these two thin film samples are no need to fabricate for cutting test. Moreover, thin film samples made by inner target $Nb_{75}Ti_{25}$ contain the useful part of composition in thin film samples made by inner target $Nb_{83}Ti_{17}$ as shown in Figure 4.10. Thus inner target $Nb_{83}Ti_{17}$ will be useless for the following experiments. Only four inner targets $Nb_{75}Ti_{25}$, $Nb_{66}Ti_{34}$, $Nb_{50}Ti_{50}$, and $Nb_{40}Ti_{60}$, will be used to make thin film samples for cutting test.

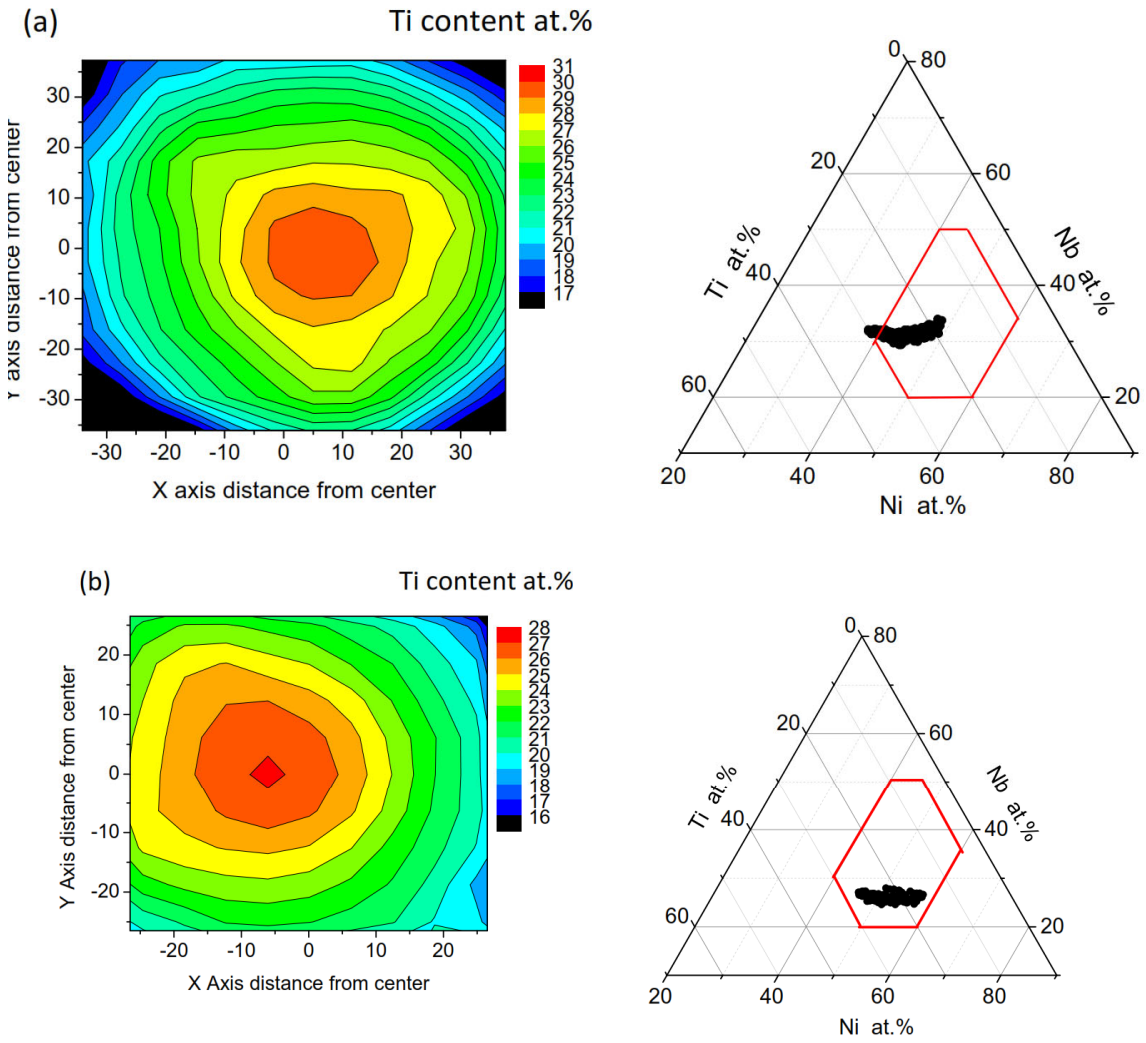

Fig. 4.11 Results for inner part target $Nb_{40}Ti_{60}$, outer part targets: (a) $Ni_{60}Nb_{40}$, (b) $Ni_{70}Nb_{30}$, (c) $Ni_{80}Nb_{20}$ and (d) $Ni_{90}Nb_{10}$

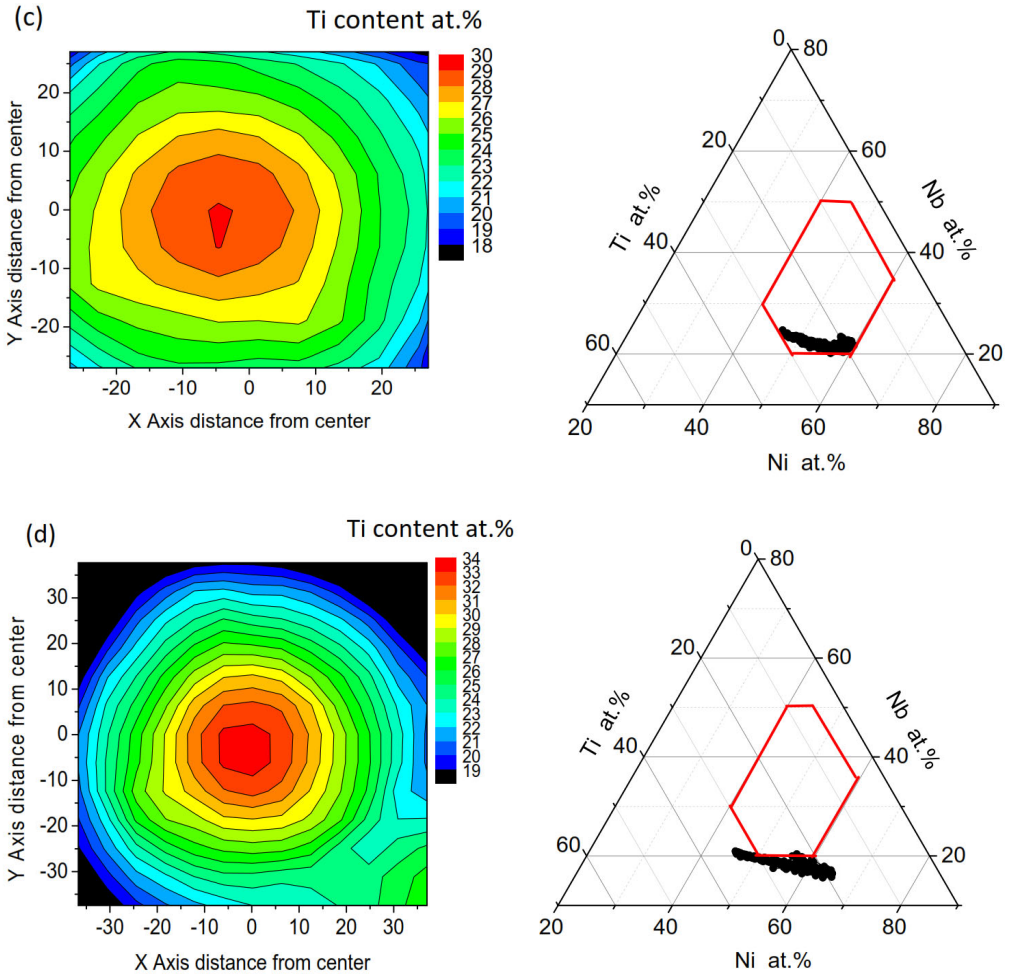

Fig. 4.11 Results for inner part target $Nb_{40}Ti_{60}$, outer part targets: (a) $Ni_{60}Nb_{40}$, (b) $Ni_{70}Nb_{30}$, (c) $Ni_{80}Nb_{20}$ and (d) $Ni_{90}Nb_{10}$

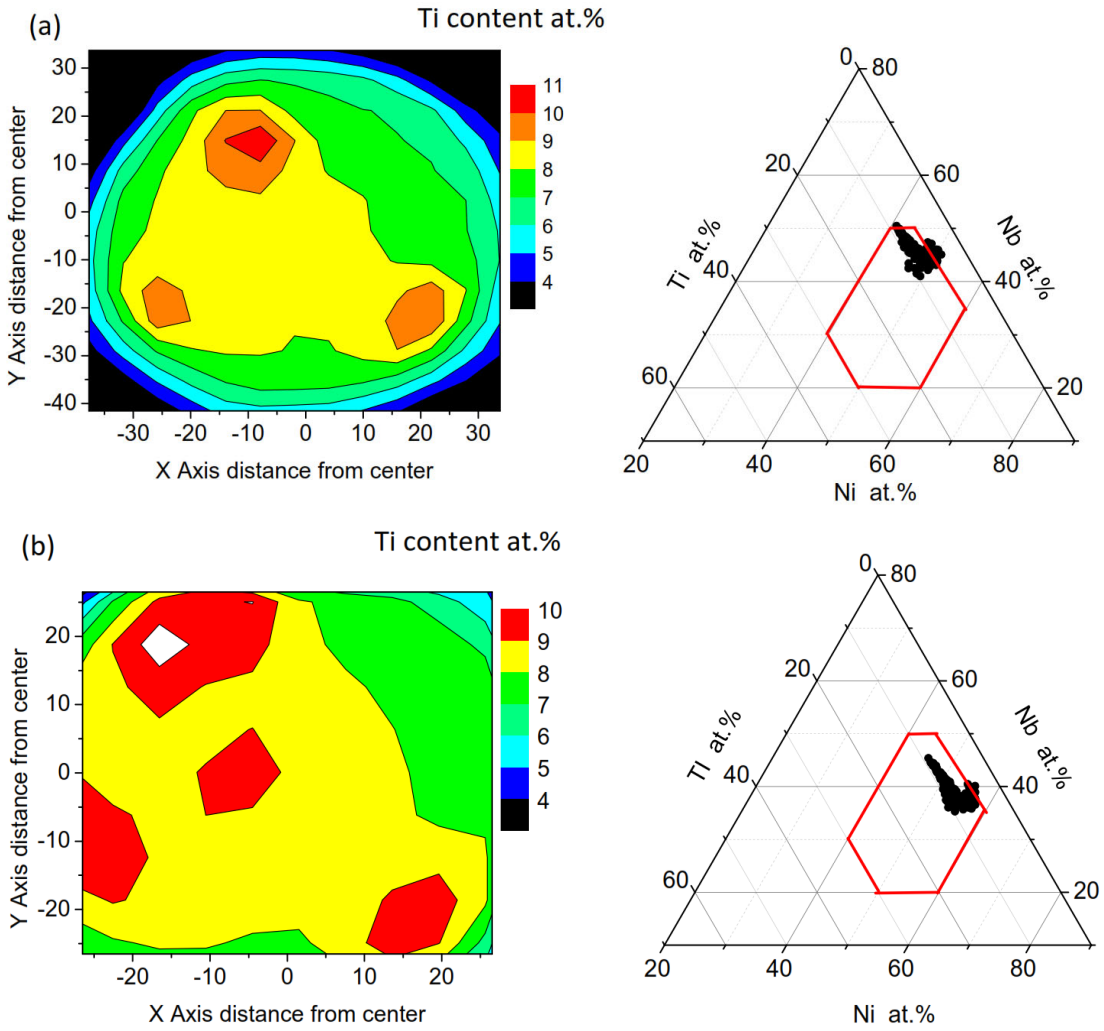

Fig. 4.12 Results for inner part target $Nb_{75}Ti_{25}$, outer part targets: (a) $Ni_{60}Nb_{40}$, (b) $Ni_{70}Nb_{30}$, (c) $Ni_{80}Nb_{20}$ and (d) $Ni_{90}Nb_{10}$

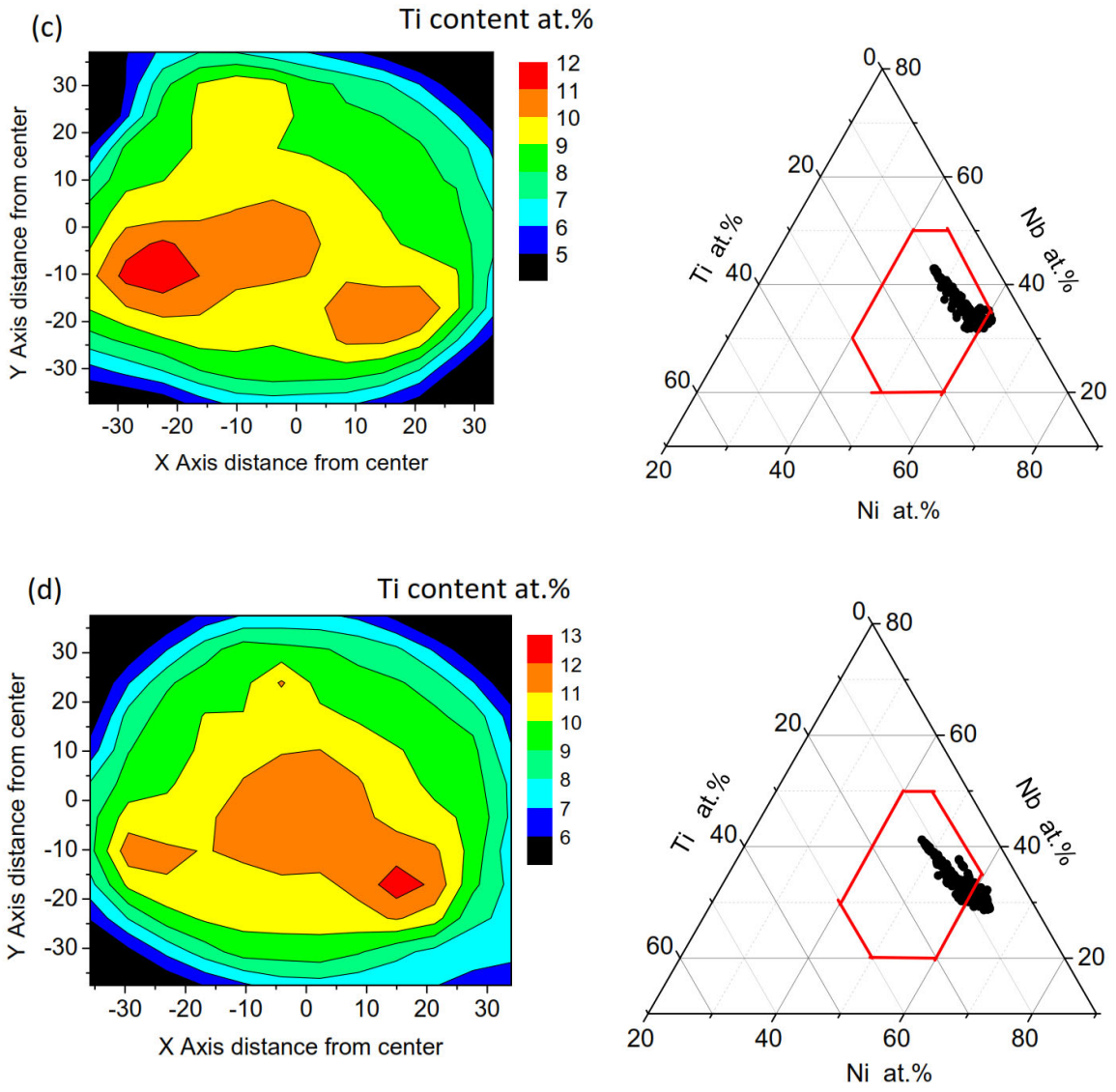

Fig. 4.12 Results for inner part target $Nb_{75}Ti_{25}$, outer part targets: (a) $Ni_{60}Nb_{40}$, (b) $Ni_{70}Nb_{30}$, (c) $Ni_{80}Nb_{20}$ and (d) $Ni_{90}Nb_{10}$

4.4 Experiments using a cover mask

4.4.1 Design of a cover mask

As mentioned above, Ti grading condition of the thin film sample made by combinatorial targets is symmetrical. During the measurement of surface roughness of cutting sample, it is only need to examine the surface roughness along one diameter which can contain the entire Ti content level of the whole sample. As a result, a cover mask was designed to deposit cutting sample on two perpendicular diameters of substrate. Meanwhile other cutting samples can be deposited on the blank area of the same substrate.

By using a cover mask, three samples can be deposited onto one substrate displayed as Figure 4.13. First, a cover mask with four slits is used to cover the substrate. Then sample 1 is sputtered on the substrate by target 1. Next, the cover mask is rotated and sample 2 is sputtered on the substrate by target 2. The same process will be repeated until a library with 3 samples has been sputtered on the substrate. Consequently machinability evaluation of three samples can be done by just one cutting test, which will further reduce experiment times and cut down the cost.

According to the dimension of the substrate and jigs, the cover mask was designed as in Figure 4.14. Grooves with the depth 0.5mm were designed in order to avoid destroying deposited samples on the substrate while new samples were being sputtered by the other target.

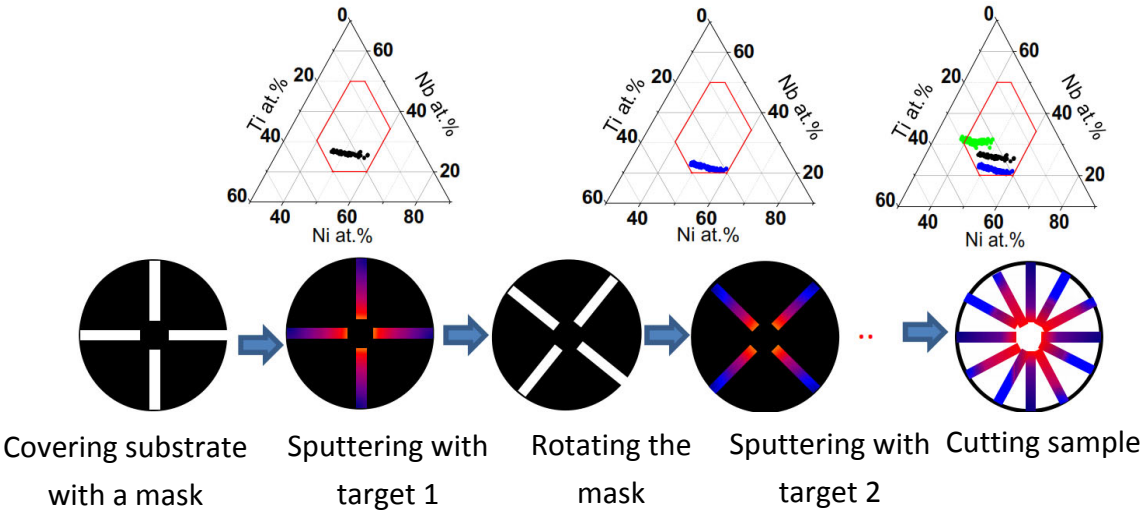

Fig.4.13 Fabrication of a cutting sample using a cover mask

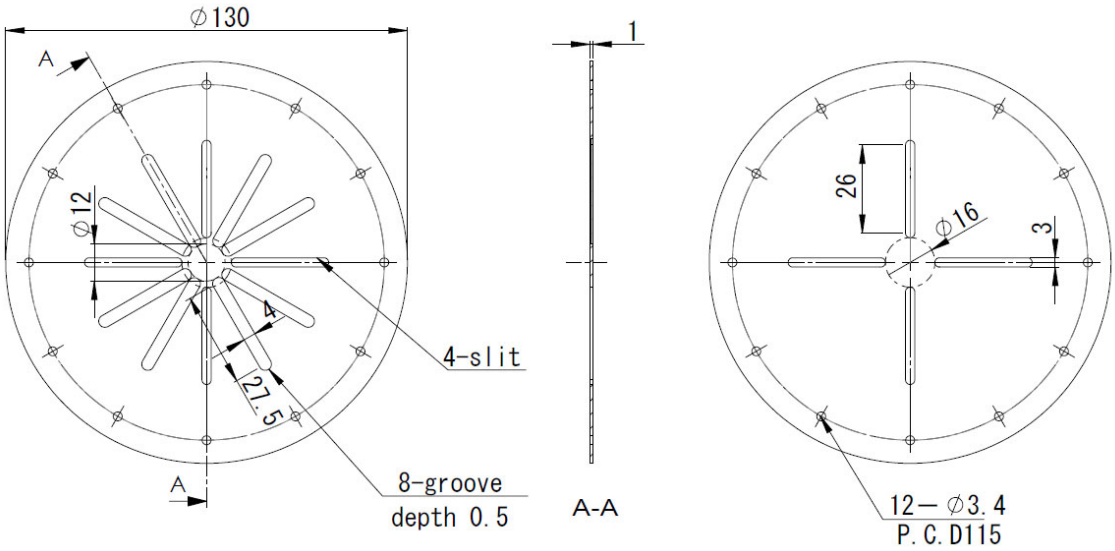

Fig.4.14 Schematic of the cover mask

4.4.2 Composition results of thin film library samples made by using a cover mask

As mentioned in last section, cover mask was designed to further improve the combinatorial method of machinability which is able to combine three samples onto one substrate. The slits on cover mask were designed with a length 26mm, width 3mm. Since these dimensions are relatively small, the thickness of cover mask cannot be too large or it will have a great impact on the deposition of thin film samples. However, cover mask is too thin to contact the substrate firmly, which makes deposited sample shown in Figure 4.15 not as expected that some part of thin film samples are overlapping.

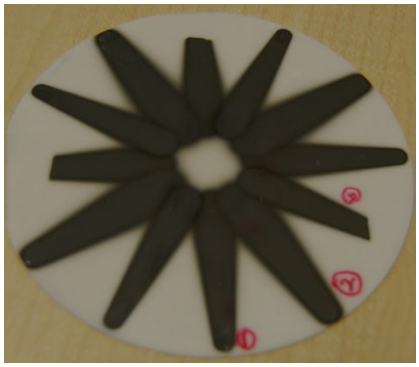

Fig. 4.15 Sample by using only cover mask without support jig

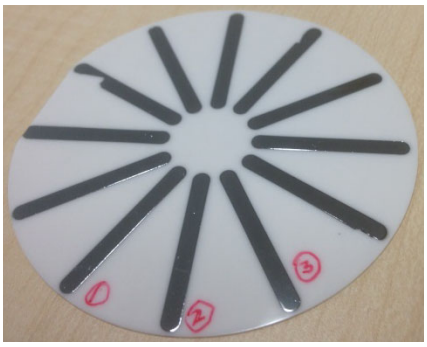

Fig.4.16 sample by using cover mask and support jig

As a result, a support jig was designed to make the cover mask firmly in contact with substrate. In order not to bring bad impact on the deposition of thin film samples, the width of slits on support jig is almost three times that on the cover mask. Using this support make it to fabricate

thin film sample as expected shown in Figure 4.16. The specific dimensions of the support jig are explained in Figure 4.17.

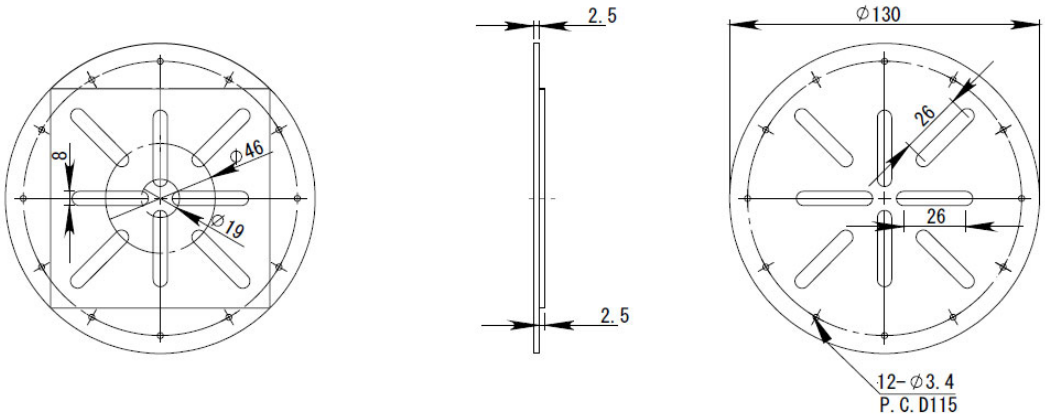

Fig.4.17 Schematic of the support jig

Thin film samples were fabricated by using cover mask and the support jig, composition of which were evaluated to check the impact induced by the use of cover mask. Based on the results explained in previous sections, inner target $Nb_{40}Ti_{60}$ with less Nb element was combined with outer targets with high Nb element, $Ni_{80}Nb_{20}$, $Ni_{70}Nb_{30}$and $Ni_{60}Nb_{40}$ to make thin film library. Meanwhile the rest inner targets were combined with $Ni_{90}Nb_{10}$ $Ni_{80}Nb_{20}$ and $Ni_{70}Nb_{30}$ to make thin film libraries. The composition distribution of those thin film libraries were measured and displayed in following figure from Figure 4.18 to Figure 4.22.

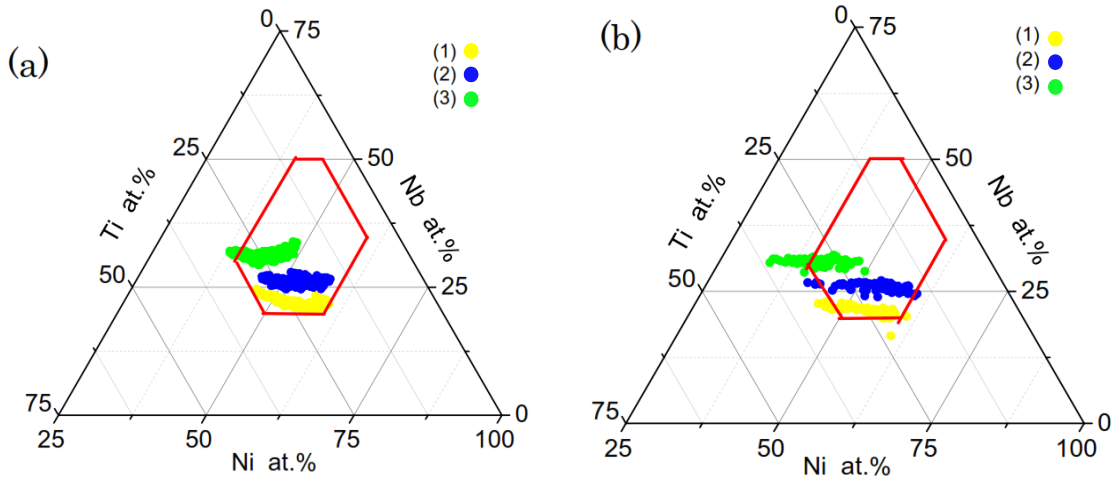

Fig.4.18 Results for inner part target $Nb_{40}Ti_{60}$, outer part targets: (1) $Ni_{60}Nb_{40}$, (2) $Ni_{70}Nb_{30}$, (3) $Ni_{80}Nb_{20}$; (a) without using cover mask (b) using cover mask

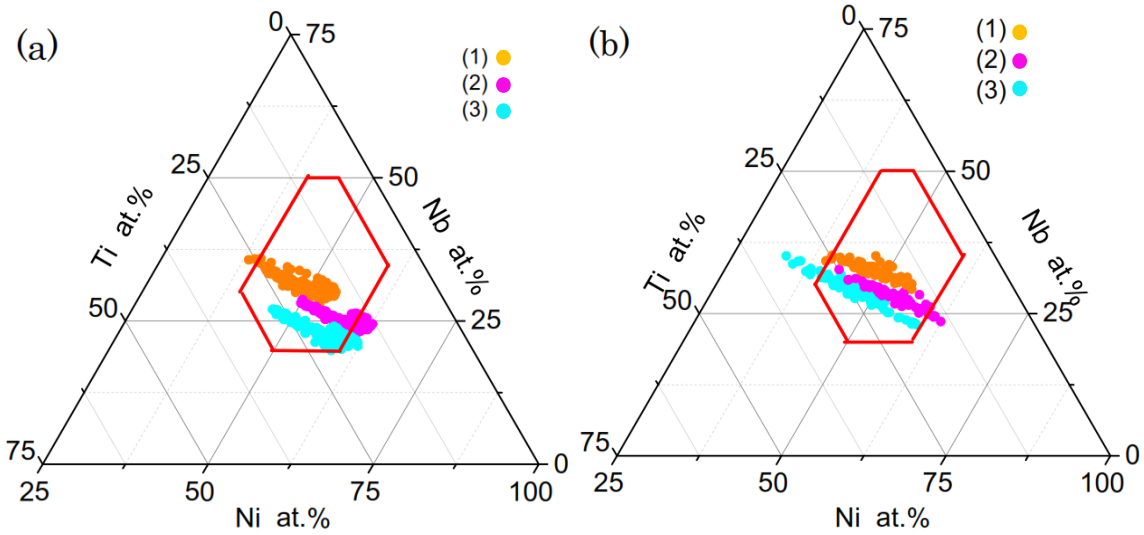

Fig.4.19 Results for inner part target $Nb_{50}Ti_{50}$, outer part targets: (1) $Ni_{70}Nb_{30}$, (2) $Ni_{80}Nb_{20}$ and (3) $Ni_{90}Nb_{10}$; (a) without using cover mask (b) using cover mask

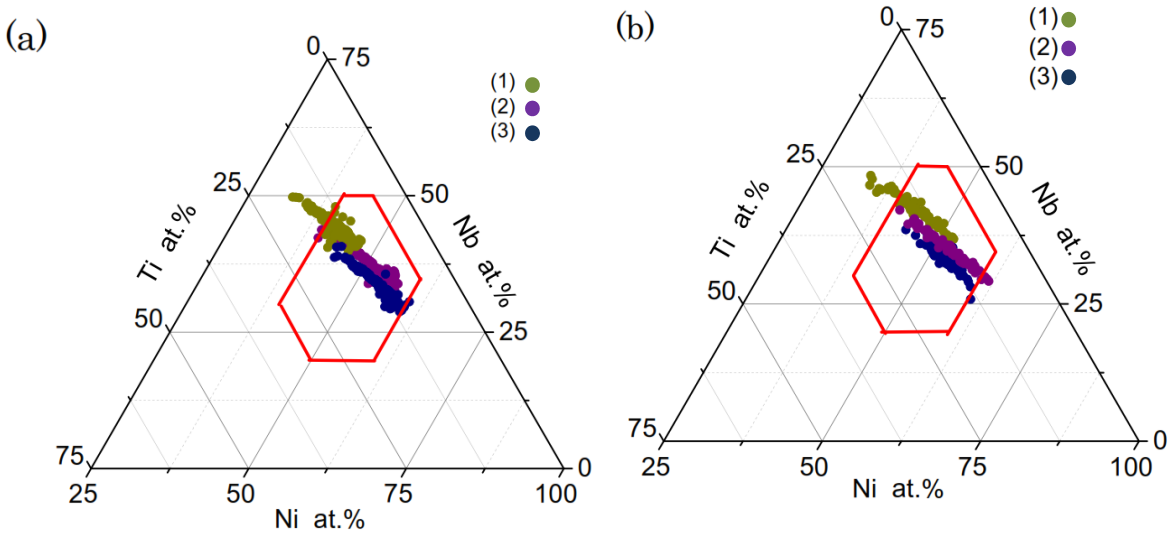

Fig.4.20 Results for inner part target $Nb_{66}Ti_{34}$, outer part targets: (1) $Ni_{70}Nb_{30}$, (2) $Ni_{80}Nb_{20}$ and (3) $Ni_{90}Nb_{10}$; (a) without using cover mask (b) using cover mask

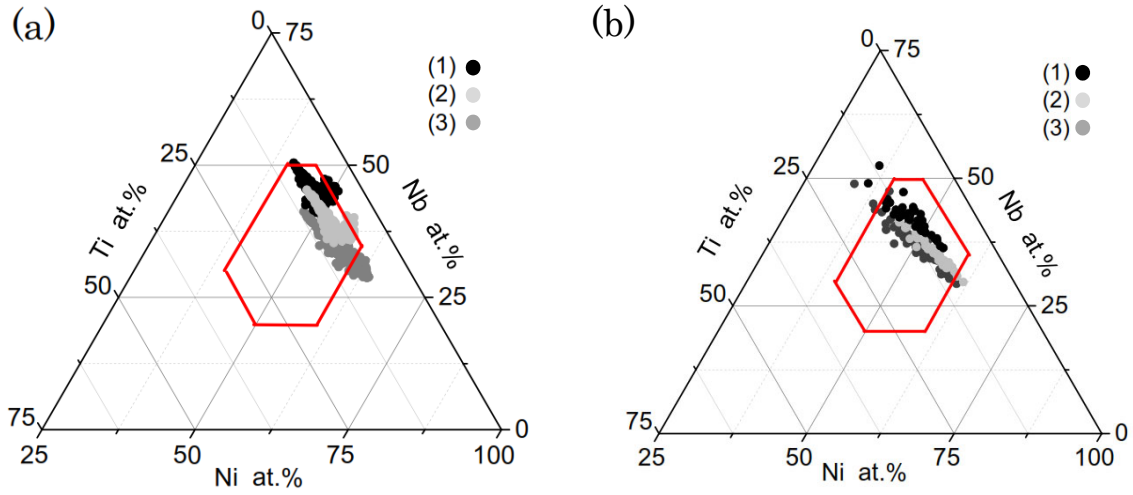

Fig.4.21 Results for inner part target $Nb_{75}Ti_{25}$, outer part targets: (1) $Ni_{70}Nb_{30}$, (2) $Ni_{80}Nb_{20}$ and (3) $Ni_{90}Nb_{10}$; (a) without using cover mask (b) using cover mask

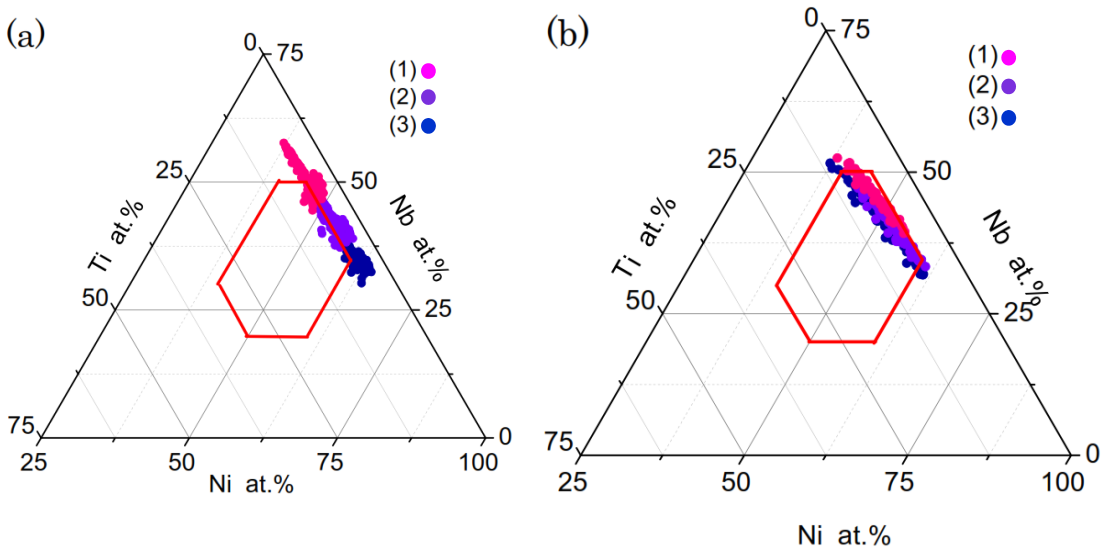

Fig.4.22 Results for inner part target $Nb_{83}Ti_{17}$, outer part targets: (1) $Ni_{70}Nb_{30}$, (2) $Ni_{80}Nb_{20}$ and (3) $Ni_{90}Nb_{10}$; (a) without using cover mask (b) using cover mask

Composition range of thin film samples made by using cover mask is, as expected, smaller than that of thin film samples made without cover mask. However, the compositions of thin film libraries made by cover mask are within desired area and the difference of composition caused by the use of cover mask is acceptable.

As shown in Figure 4.20 (b) and Figure 4.21 (b), composition area of thin film library made by inner target $Nb_{75}Ti_{25}$ almost coincide with that of thin film library made by inner target $Nb_{66}Ti_{34}$. As a result, this inner target is useless for the following experiments. Four thin film libraries made by other four inner targets can almost cover the entire desired area as shown in Figure 4.23. The results of Ti content level and range of these four thin film libraries are displayed in Table 4.3.

Due to the application of cover mask, it needs only four times cutting test to evaluate the machinability of entire target area. Among those thin film libraries, library 2 and library 3 are decided to be the first two cutting samples for machinability test.

Table 4.3 The Ti content level and range results of four thin film libraries

	$Ni_{90}Nb_{10}$	$Ni_{80}Nb_{20}$	$Ni_{70}Nb_{30}$	$Ni_{60}Ti_{40}$
$Nb_{40}Ti_{60}$ （1）		Ti : 15.1% to 31.9% Range: 16.8%	Ti : 19% to 32.2% Range:13.2%	Ti : 20.1% to 36.2% Range:16.1%
$Nb_{50}Ti_{50}$ （2）	Ti : 19.6% to 36.3% Range: 16.7%	Ti : 15.7% to 27.1% Range: 11.4%	Ti : 17.7% to 28.8% Range:11.1%	
$Nb_{66}Ti_{34}$ （3）	Ti : 11.7% to 17.5% Range: 5.8%	Ti : 9.1% to 16.7% Range: 7.6%	Ti : 10.8% to 19.2% Range:8.4%	
$Nb_{83}Ti_{17}$ （4）	Ti : 6.6% to 11.2% Range: 4.6%	Ti : 5.6% to 9.2% Range: 3.6%	Ti : 5.4% to 9.5% Range:4.1%	

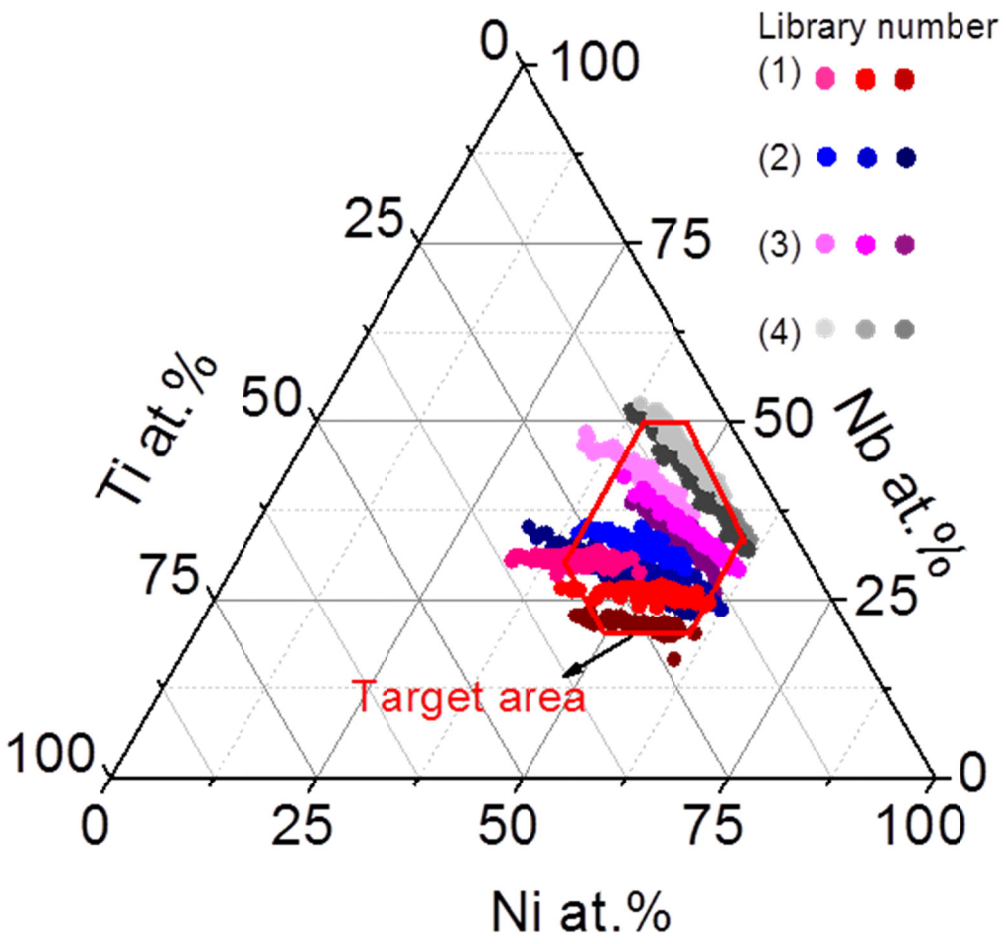

Fig.4.23 Composition results of four thin film libraries

4.5 The result of cutting test for thin film library

As mentioned in the last section, library 2 and 3 shown in Figure 4.23 were chosen to be the first two samples for cutting test. The cutting sample shown in Figure 4.24 (a) was fabricated by using inner target $Nb_{50}Ti_{50}$, outer targets $Ni_{90}Nb_{10}$; $Ni_{80}Nb_{20}$ and $Ni_{70}Nb_{30}$. Each strip of cutting sample is with a width 3mm which is too thin and easy to be broken during cutting process. Before applied to cutting test, fabricated cutting sample was electroplated a layer of Ni to fill the gap between the strips of cutting sample and ground into a flat. Since Ni is with good machinability, the filling of Ni in our case was considered not to have serious influence on the cutting result of sample.

An ultra-precision diamond machining system (Nano-100) was adopted for cutting tests to measure the machinability of thin film sample. The sample was cut by a cutting tool with single crystal diamond radius bit (R=0.5 mm) with a constant cutting speed 4mm /s, a radial feeding rate 1μm /rev, a constant axial feeding distance 0.1 μm and feed direction from the center to the outer. The rotation speed of main spindle was controlled to make the cutting speed constant. The same cutting process was repeated for 50 times to obtain a cutting depth 5 μm.

Figure 4.24 (b) displays the cutting sample after cutting test. It is clearly to note that sample 1 was completely peeled off and so did some part of sample 2 and 3. The occurrence of this problem was regarded as the lack of adhesion between cutting sample and substrate. In order to

solve this problem, an adhesive layer of Cr was considered to be deposited between cutting sample and substrate during the fabrication of subsequent cutting samples.

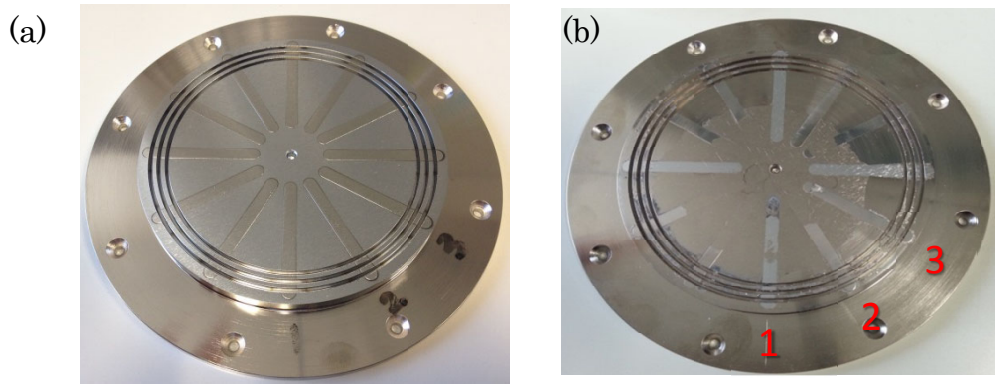

Fig.4.24 Cutting sample made inner target $Nb_{50}Ti_{50}$: (a) before cutting test; (b) after cutting test

Figure 4.25 (a) shows the cutting sample fabricated by using inner target $Nb_{66}Ti_{34}$, outer targets $Ni_{90}Nb_{10}$; $Ni_{80}Nb_{20}$ and $Ni_{70}Nb_{30}$. As shown in Figure 4.2, Ti content in this cutting sample changes sharply in the edge area of sample, which make the edge part more valuable since it contains a large range of Ti content. As a result, the grooves in the cutting substrate were removed in order to obtain more results of machinability test. The cutting sample was cut under same cutting condition described before. As shown in Figure 4.25 (b), the peeling off problem has been improved. Only two strips of sample 3 have been broken.

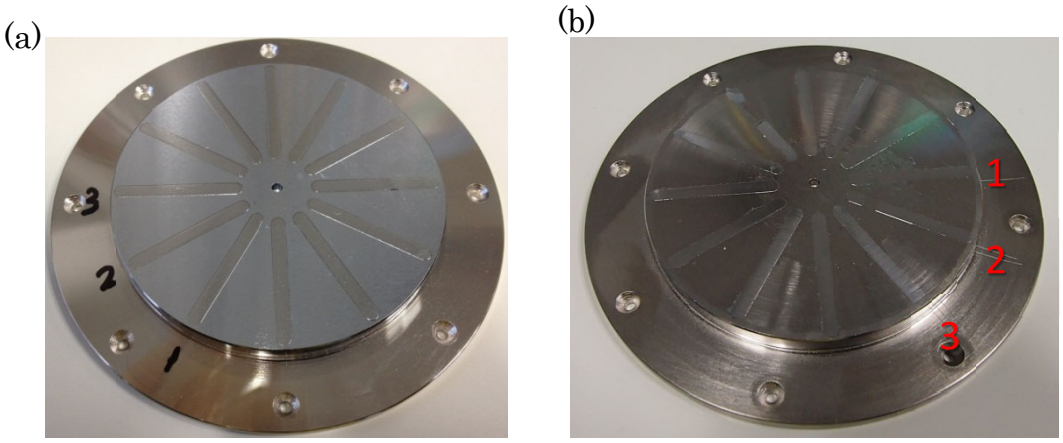

Fig.4.25 Cutting sample made inner target $Nb_{66}Ti_{34}$: (a) before cutting test; (b) after cutting test

After the cutting test, roughness of the surface of these two cutting samples was measured and the result is demonstrated in Figure 4.26. Roughness of each composition is distinguished by color. Red one represents that the roughness is less than 5nm which is the requirement for glass lens mold material. The specific result roughness is presented in Figure 4.27. Finally, the average composition of those with good machinability was measured to be $Ni_{51}Nb_{33}Ti_{16}$. The compositions with good machinability locate around the edge area of the cutting sample where the condition of bit was supposed to be worse than the beginning. It makes roughness result of this composition more reliable.

It is successful to find the amorphous alloy with good machinability for glass lens mold material by the novel combinatorial method proposed in this paper. However, as mold material for glass lens, there is another important requirement which needs to meet, thermal stability. In the next chapter, thermal stability of this composition will be evaluated to confirm whether it qualifys for mold material for glass lens.

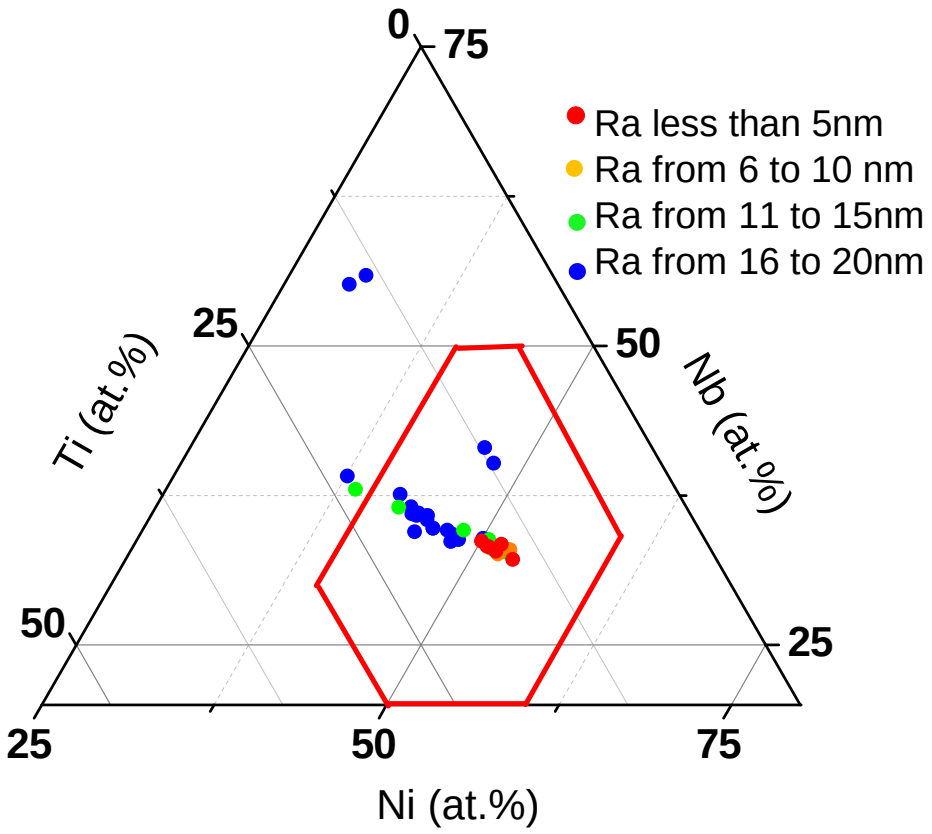

Fig.4.26 The roughness results for the cutting sample

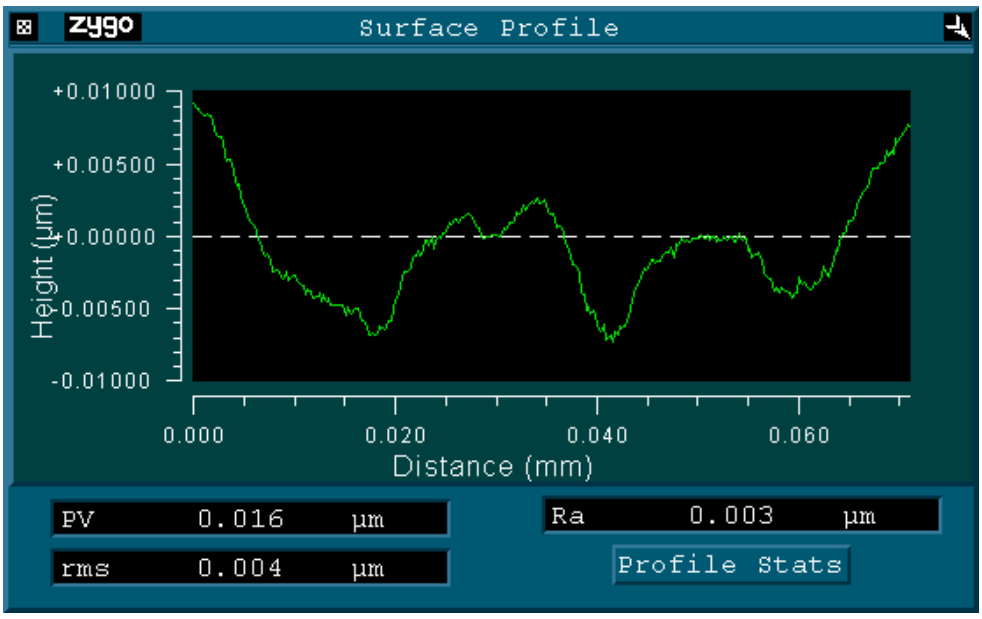

Fig.4.27 specific result of roughness

4.6 Evaluation of mechanical properties of $Ni_{51}Nb_{33}Ti_{16}$

4.6.1 Evaluation of tensile strength

In order to measure the tensile strength, alloy samples were sputterred on Cu foils, which were dissolved in HNO2+H2O (1:1). Left samples were cut into 1mm x 7mm shape by a diamond wire saw (Musashino Electron) for tensile tests which were performed using a thermal mechanical analyzer (TMA; TMA-60, Shimadzu) with a strain rate of 1.42x10-4/s.

From tensile test's results, stress-strain curve was drawn as Figure 4.28. The samples fractured during the tests and the fracture stresses is 2.24 GPa higher than desired one (1.0 GPa) for glass lens mold materials.

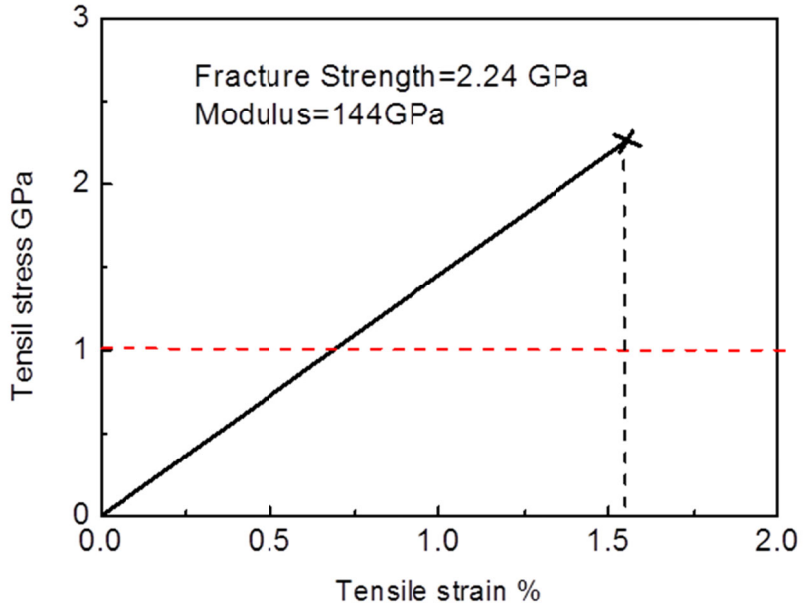

Fig.4.28 Stress-strain curve of $Ni_{51}Nb_{33}Ti_{16}$

4.6.2 Evaluation of hardness

For hardness test, the nano-indentation method was applied using the equipment with atomic force microscope (SPI-3000, Seiko Instruments) and a nonoindenter (Triboscope, Hysitron).

Figure 4.29 displays the result of hardness test. The hardness of $Ni_{51}Nb_{33}Ti_{16}$ is lower than $Ni_{35}Nb_{40}Zr_{25}$ as predicted in Chapter 2. It becomes apparent that hardness of the sample is higher than desired one (7.0GPa) for glass lens mold materials.

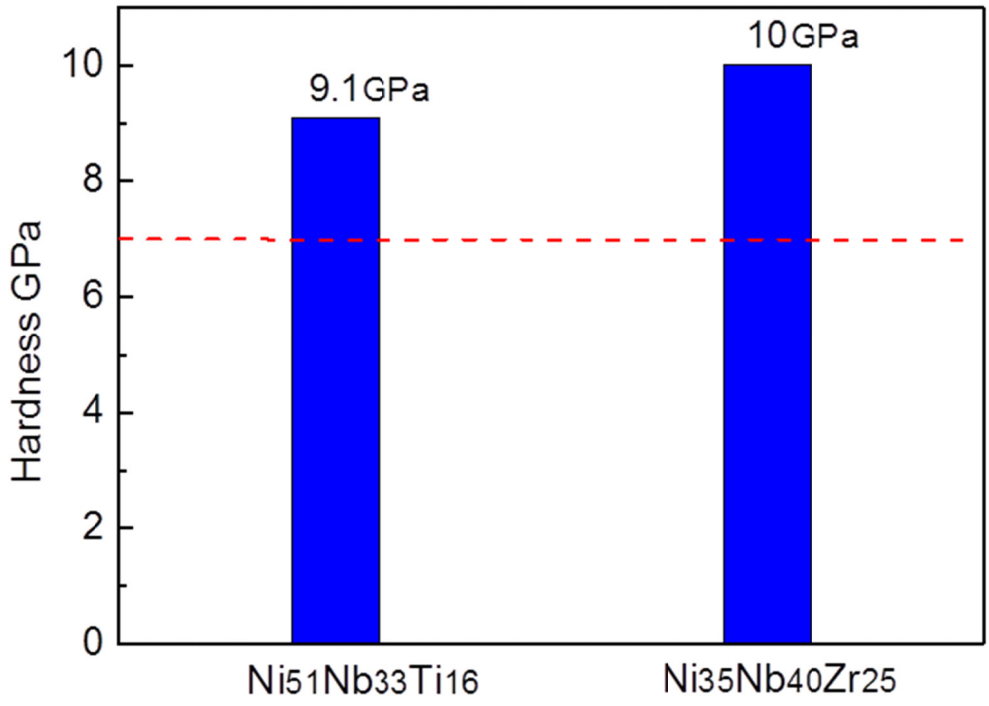

Fig.4.29 Hardness result of $Ni_{51}Nb_{33}Ti_{16}$

4.7 Summary

In this chapter, Nb-Ti alloy inner targets were designed to do the experiments. Based on the results in last chapter, the composition of inner targets were decided to be $Nb_{50}Ti_{50}$, $Nb_{66}Ti_{34}$ and $Nb_{83}Ti_{17}$, which were combined with outer targets $Ni_{90}Nb_{10}$, $Ni_{80}Nb_{20}$, $Ni_{70}Nb_{30}$ and $Ni_{60}Nb_{40}$ to fabricate thin film samples. These twelve samples can almost cover the desired composition area with high thermal stability. The composition result of these samples manifest a tendency that the higher Ti content level is in inner target, the larger is Ti content range in the thin film sample. The thin film sample deposited by inner target $Nb_{50}Ti_{50}$, outer target $Ni_{70}Nb_{30}$ has the largest Ti content range and a good grading condition of Ti, which was decided to be the first cutting sample.

The composition result of cutting sample confirmed that long- time sputtering does not have a serious impact on the condition distribution. Roughness of the sample was measured to be larger than the requirement for glass lens mold material 5nm. Although the composition with good machinability has not been found, it confirmed the feasibility of the novel combinatorial method for evaluation of machinability proposed in this thesis.

Ti grading condition of the thin film sample made by combinatorial targets is symmetrical which means that only a few parts of sample can cover the Ti content range of the entire sample. This makes it possible to further improve the combinatorial method by a cover mask. By using a

cover mask, three samples can be deposited onto one substrate. The composition results of thin film libraries confirmed that the application of cover mask did not have serious influence on the composition distribution of samples.

Two cutting samples were fabricated for cutting test, by using inner target $Nb_{50}Ti_{50}$ and $Nb_{66}Ti_{34}$, combined with outer targets $Ni_{90}Nb_{10}$; $Ni_{80}Nb_{20}$ and $Ni_{70}Nb_{30}$. After cutting test, surface roughness of cutting samples was examined. Finally, a composition $Ni_{51}Nb_{33}Ti_{16}$ was found to be with roughness less than 5nm which is the requirement for glass lens mold material. Moreover, the mechanical properties of $Ni_{51}Nb_{33}Ti_{16}$ are measured to meet the requirements for glass lens mold material. Thermal stability of this composition will be evaluated in the next chapter to confirm whether it qualifys for mold material for glass lens.

Chapter 5 High-throughput evaluation of crystallization properties

5.1 Measurement of crystallization temperature

In the chapter 4, amorphous alloy $Ni_{51}Nb_{33}Ti_{16}$ was found to be with good machinability. However, as mold material for glass lens with microstructures, there are many requirements other than machinability, the important one of which is thermal stability. Since the mold will be heated up to the melt temperature of glass, it requires that amorphous alloy as mold material can withstand the high temperature during glass lens fabrication process.

As we known, amorphous materials, when heated up to the temperature over T_x (crystallization temperature), will turn into crystalline materials. As mold material for glass lens, T_x of $Ni_{51}Nb_{33}Ti_{16}$ is demanded to be higher than melt temperature of glass. In this research, BK7(Schott AG) with melt temperature 723K is chosen as glass lens material, which is widely used as lens material.

Along with the crystallization, several optical properties of amorphous material are changed. One of that is emissivity which is applied to the measurement of T_x. All matter with a temperature greater than absolute zore emits thermal radiation. The emissivity of a material ε is the relative ability of its surface to emit energy by radiation. The amount of radiation emitted by an object increases with temperature. The

relationship among radiation energy W, temperature T and emissivity ε is demonstrated as Function 5.1 according to Stefan-Boltzman law. σ is Stefan-Boltzman constant.

$$W = \varepsilon\sigma T^4 \qquad (5.1)$$

According to Stefan-Boltzman law, the thermography is used to make a temperature measurement of an object by setting an emissivity. Since it can be difficult to determine the appropriate emissivity for a subject, the temperature obtained by the set emissivity ε', is called apparent temperature T_a which is not the real temperature of the object. The principle of the measurement is simply described as Figure 5.1.

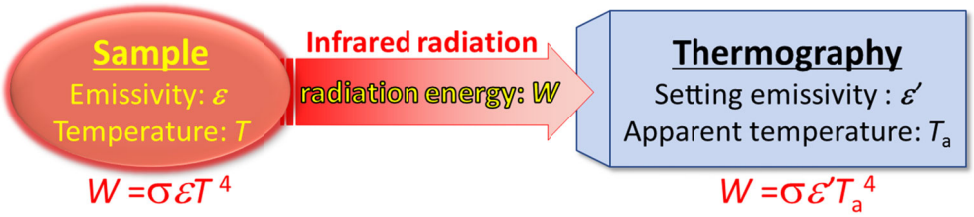

Fig.5.1 Principle of thermography

However, thermography actually can detect only the infrared radiation with a certain wavelength area not the entire one. This problem is considered and corrected in the software. According to the principle demonstrated in Figure 5.1, Function 5.2 can be deduced.

$$\frac{T}{Ta} = \left(\frac{\varepsilon'}{\varepsilon}\right)^{1/4} \qquad (5.2)$$

As it mentioned before, when amorphous materials crystallize, the emissivity ε will change. Based on Function 5.2, the change of emissivity ε can be detected on T- Ta curves as shown in Figure 5.2. The temperature of change point is defined as crystallization temperature Tx. As a result, Tx

of amorphous materials can be measured by T- Ta data.

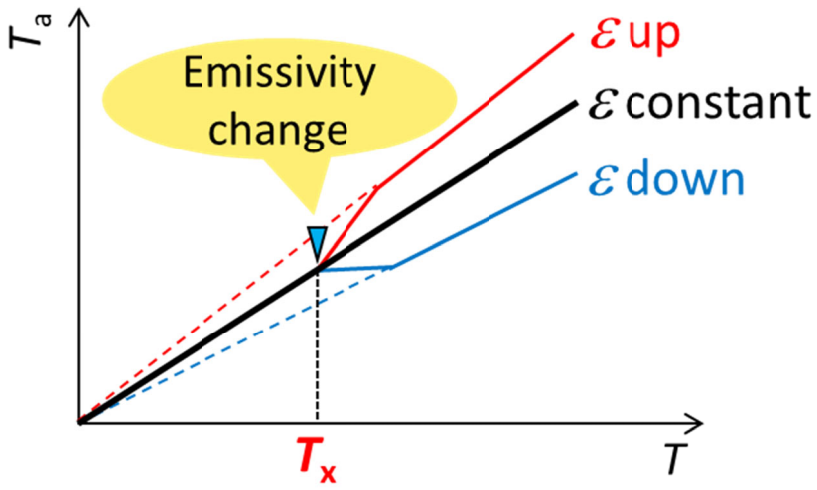

Fig.5.2 Change of emissivity on T-T_a curves

The crystallization temperature of $Ni_{51}Nb_{33}Ti_{16}$ which has good machinability explained in Chapter 4 was evaluated by the same method. $Ni_{51}Nb_{33}Ti_{16}$ thin film sample was deposited on Alumina substrate. This sample was heated in a vacuum chamber up to 1023K at heating speed 12K/min. The real temperature of sample was measured by thermocouple while the apparent temperature of sample was measured by thermography.

Based on the temperature data, the T-T_a curve was drawn as Figure 5.3. It shows a clear change of emissivity when temperature reaches to 881K. The crystallization temperature of $Ni_{51}Nb_{33}Ti_{16}$ is 881K which is higher the molding temperature of glass lens 723K.

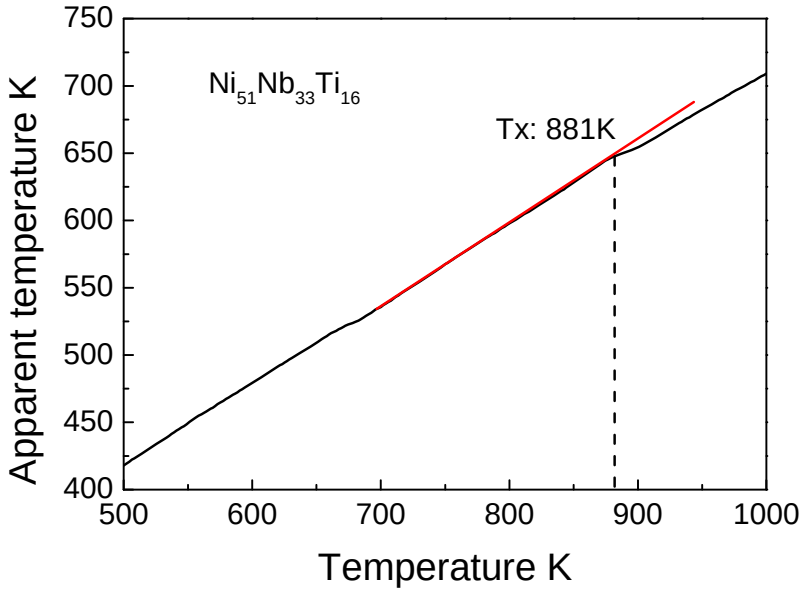

Fig. 5.3 T-T_a curve of $Ni_{51}Nb_{33}Ti_{16}$ thin film amorphous alloy

5.2 Principle of TTT test and results

As shown in section 5.1, the crystallization temperature of $Ni_{51}Nb_{33}Ti_{16}$ is measured to be 881K which is higher than the molding temperature of glass lens. However, even at lower temperature, crystallization can also happen as long as the heating time is long enough. Time is a very important factor other than temperature for the evaluation of thermal stability.

For the TTT (time-temperature-transformation) test, a setup as displayed in Figure 5.4 was used. Since a heater is set at one end of sample while a cooling system at the other end, there is a grading distribution of temperature on the sample. As a result, it can obtain Time-T_a results of different temperature by one sample which is explained

in Figure 5.5. As shown in Figure 5.5 (b), the crystallization is displayed by the change of apparent temperature measured by thermography since the real temperature is constant. The real temperature of each position can evaluate by the reference. Finally the TTT diagram can be made as shown in Figure 5.5(c)[32].

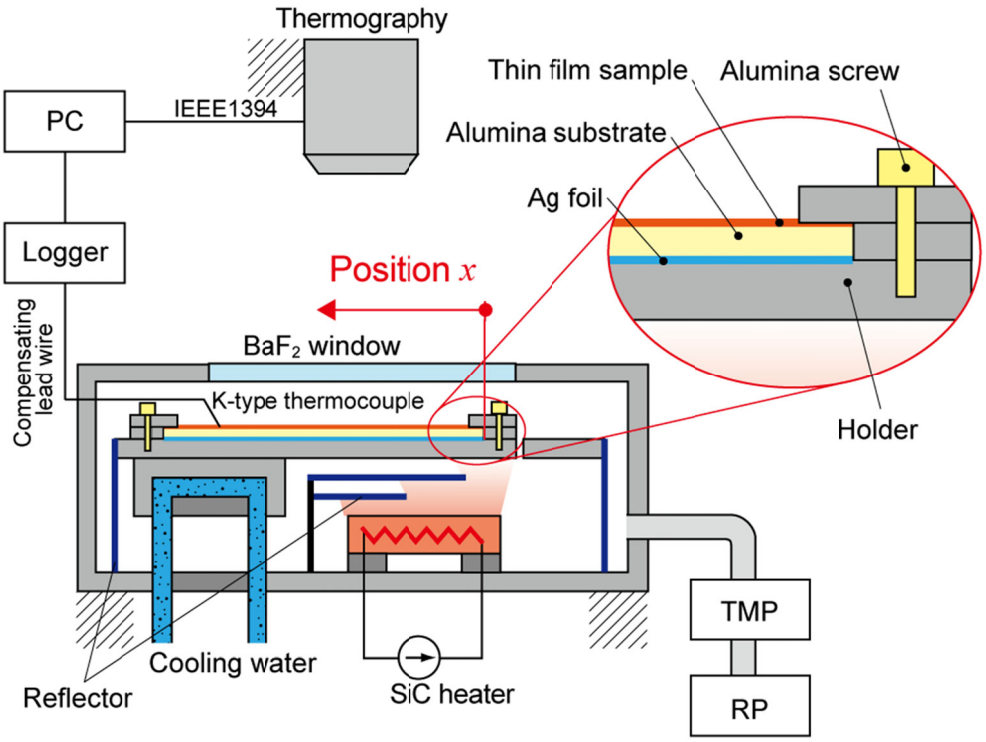

Fig.5.4 Schematic of experiment setup of TTT test

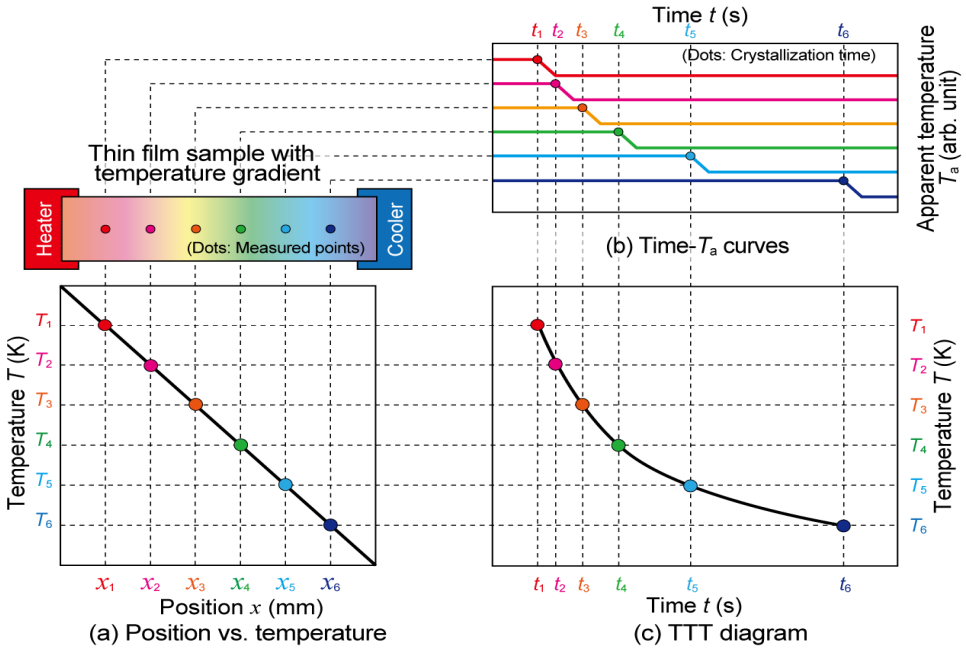

Fig.5.5 The principle of TTT test

The real temperature distribution of substrate was measured when the controller's temperature increased to 773K, 873K, 973K, 1023K and 1123K. The controller's temperature is the surface temperature on the end of sample near heater which is measured by thermocouple. As a result, the controller's temperature can be considered as the highest temperature of sample. The temperature distribution result is shown in Figure 5.6. The temperature distribution on the sample is linear no matter in the case of low temperature or high temperature which meets the requirement for TTT test. Other than that, it is clearly to see that the temperature range of sample increases with the controller's temperature which makes it quite efficient in the case of high temperature test.

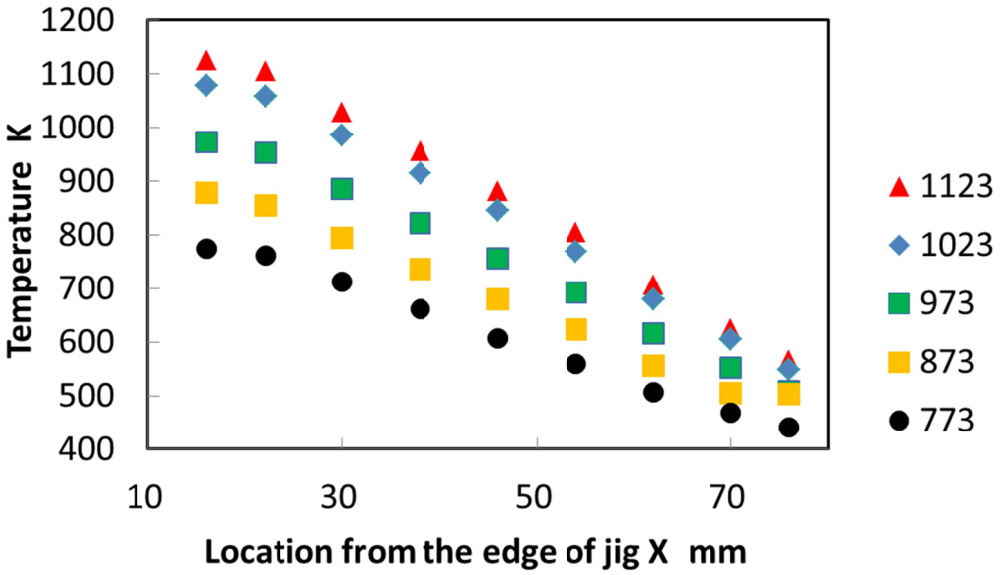

Fig.5.6 Temperature distribution on the sample

The thin film sample for TTT test is shown in Figure 5.7. $Ni_{51}Nb_{33}Ti_{16}$ alloy was sputtered on Alumina substrate with grooves. Those grooves are cut to avoid extension of crystallization which will have a bad impact on the TTT result. The phase of thin film sample was measured by XRD and the result displayed in Figure 5.8 shows that the sample made for TTT is amorphous before heating. This thin film sample was set in the vacuum chamber and heated at a speed around 12K/min until the controller's temperature increased up to 1023K and then maintain at this temperature for 2 hours.

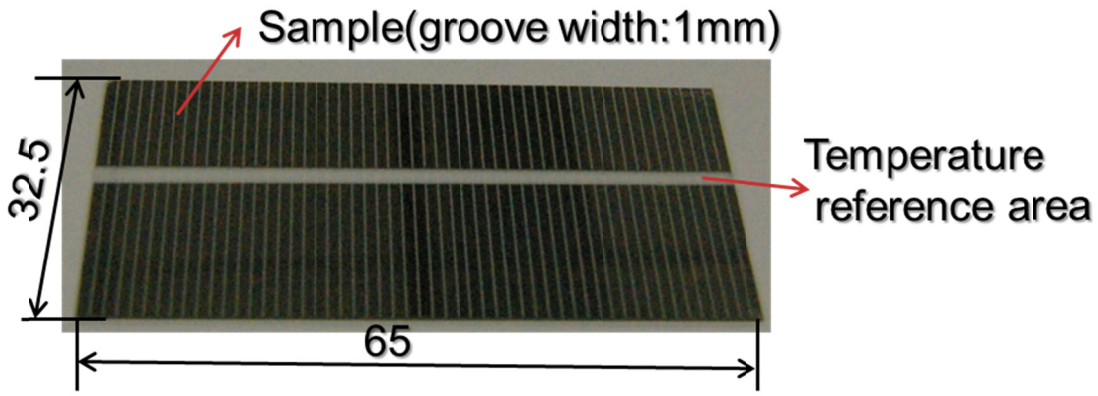

Fig.5.7 Thin film sample for TTT test

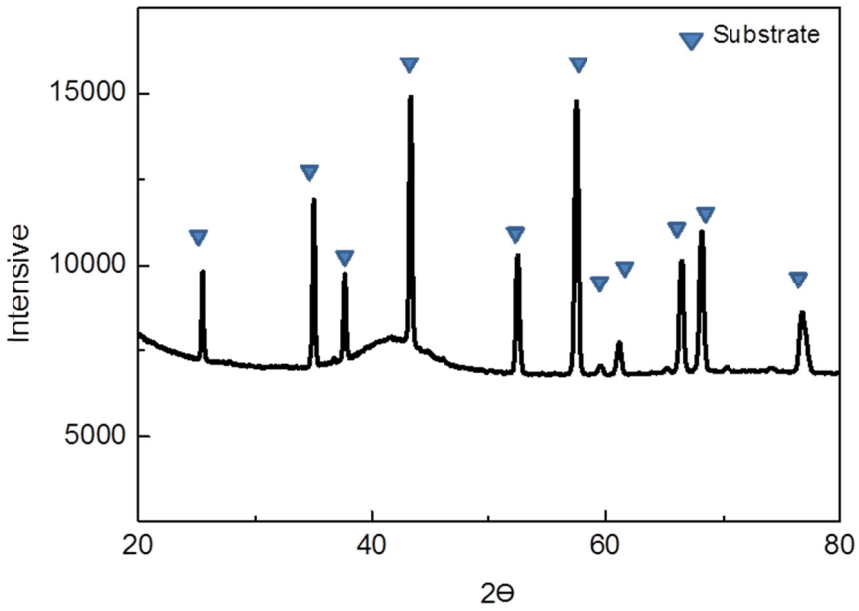

Fig.5.8 XRD profile of $Ni_{51}Nb_{33}Ti_{16}$

The temperature of controller was measured by thermocouple and demonstrated in Figure 5.9. It took around 4200s to increase to the set temperature 1023K. The apparent temperature of thin film sample was

recorded by thermography.

Figure 5.10 demonstrates the apparent temperature results of several points on the thin film sample with real temperature over than crystallization temperature 881K. The change of apparent temperature increasing rate shows that the sample crystallized in the heating process as expected. Figure 5.11 demonstrates the apparent temperature results of several points on the thin film sample with real temperature lower than crystallization temperature 881K. Even the real temperature of these points were lower than T_x, the change of apparent temperature marked by the black dash lines shows the occurrence of crystallization. From the results shown in Figure 5.11, the TTT diagram can be drawn as in Figure 5.12.

The fitted time-temperature curve indicates that the lower the temperature is, the more time is needed for crystallization. The thermal stability of $Ni_{51}Nb_{33}Ti_{16}$ is satisfying as mold material for glass lens.

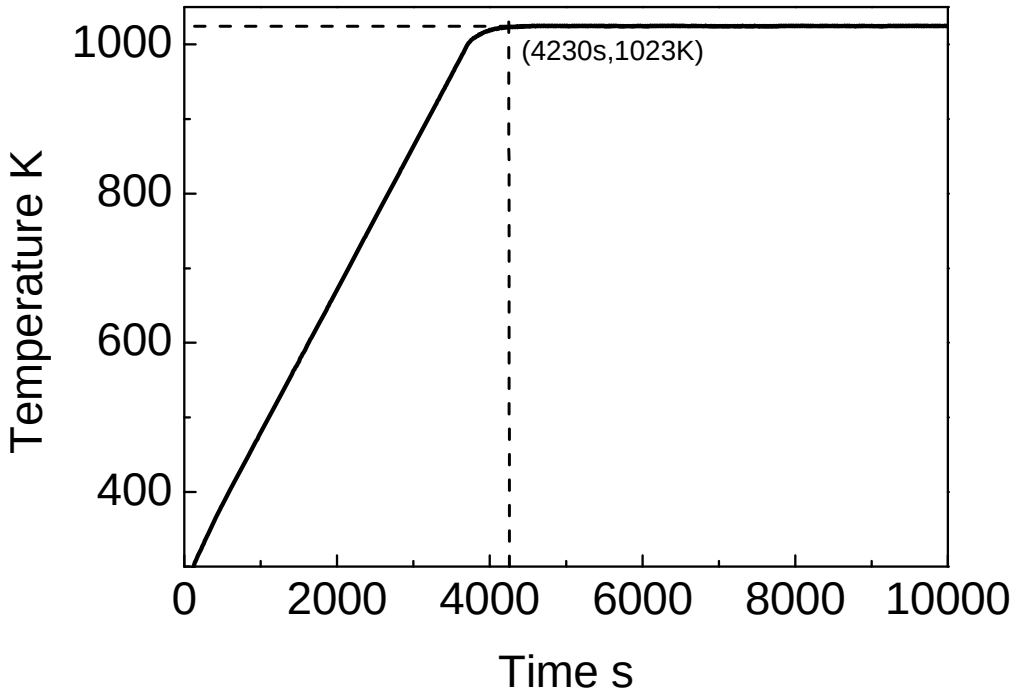

Fig 5.9 Temperature of controller measured by thermocouple

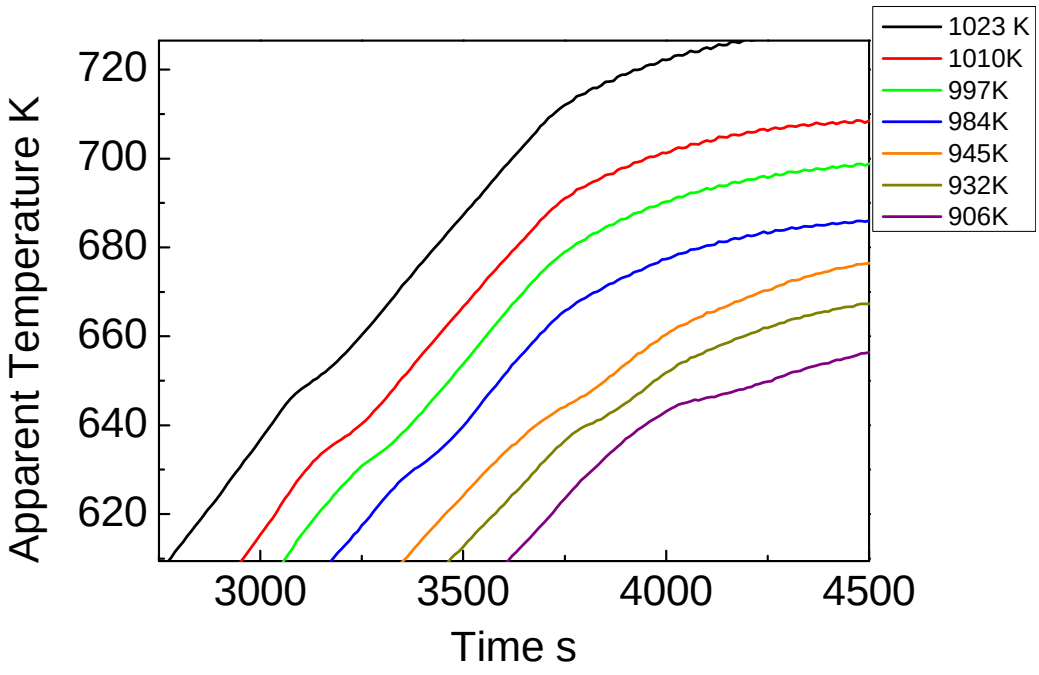

Fig 5.10 Time-Apparent temperature curves

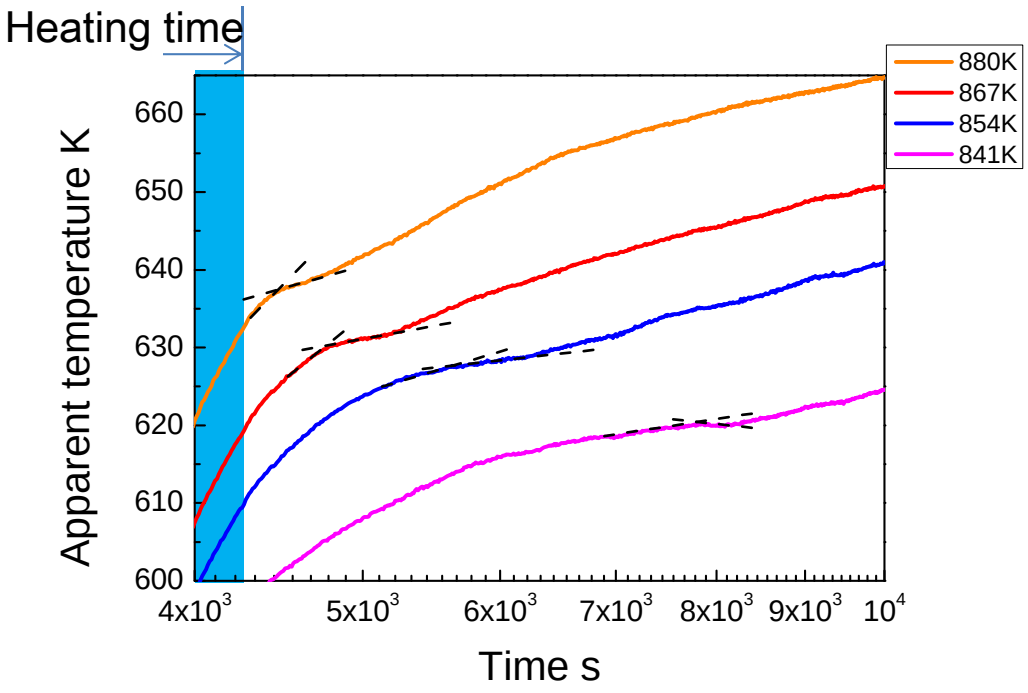

Fig 5.11 Time-Apparent temperature curves

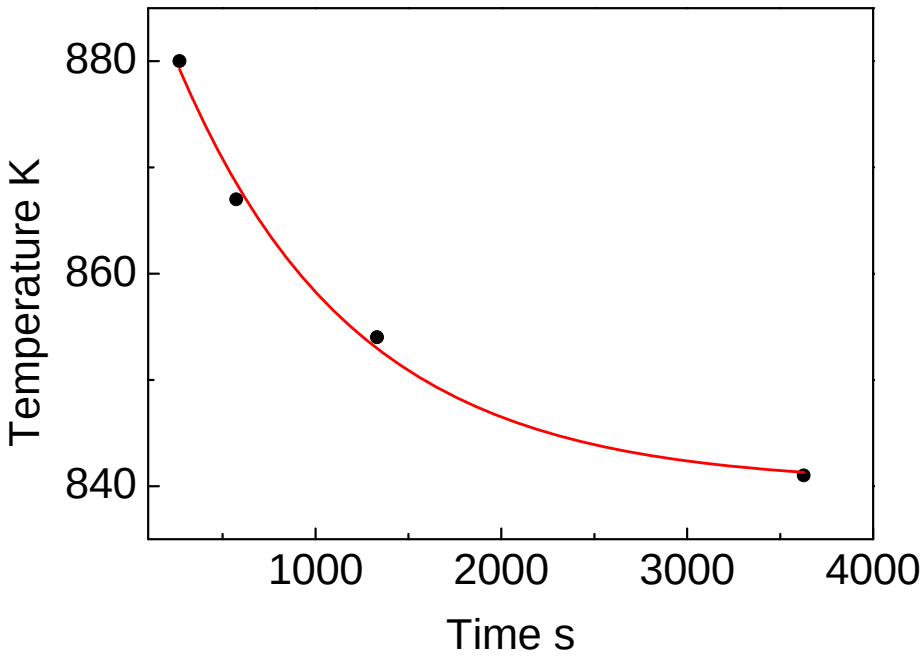

Fig 5.12 TTT curve of $Ni_{51}Nb_{33}Ti_{16}$ thin film sample

5.3 Experiments of oxidation resistance and adherence to glass

5.3.1 Experiment of oxidation resistance

In the production of glass lens, the molding process is operated in the air that requires mold material has high oxidation resistance. In our research, oxidation resistance experiment was carried out at temperature 723K in the air. The $Ni_{51}Nb_{33}Ti_{16}$ alloy sample was heated to 723 K and the temperature was maintained for 20h and 40h. After that, XRD was using to measure the occurrence of oxidation.

The result of $Ni_{51}Nb_{33}Ti_{16}$ was shown in Figure 5.13. The peak around 2Θ=26° is believed to be caused by oxidation product TiO_2. However, the oxidation condition does not enhance even when the heating time increase from 20h to 40h. It is considered that the formation of oxidation product TiO_2 provides a protective layer to prevent further oxidation. As a result, this peak is not a problem for our research.

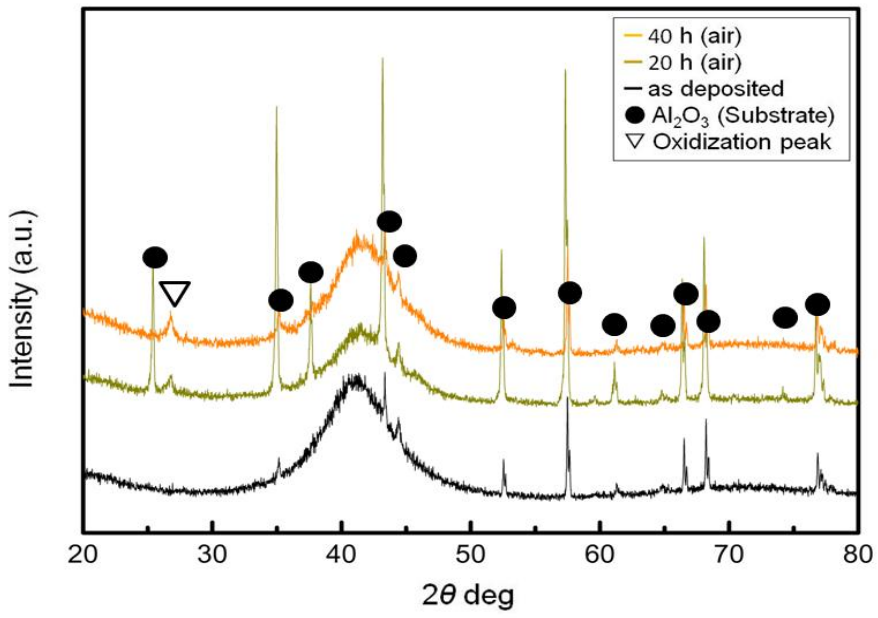

Fig.5.13 XRD pattern for $Ni_{51}Nb_{33}Ti_{16}$ sample

5.3.2 Experiment of adherence to glass

The mold material for glass lens is required not to react with glass products. The adherence of $Ni_{51}Nb_{33}Ti_{16}$ to glass was evaluated by the following experiment. A layer of $Ni_{51}Nb_{33}Ti_{16}$ amorphous alloy was deposited on the surface of mold with a thickness around 10μm. At first, a piece of glass material (K-PSFn3) was placed on the surface. Next, the mold was heated up to temperature 723K and the temperature was kept at 723K. After that, the glass material was pressed at pressure 0.82MPa for 600s. Finally, the glass product was removed from the mold. The same experiment was repeated for ten times. The glass product and mold after ten times molding are shown in Figure 5.14 and 5.15. There is no occurrence of discoloration or peeling off which proves that no reaction happens between glass and $Ni_{51}Nb_{33}Ti_{16}$ amorphous alloy.

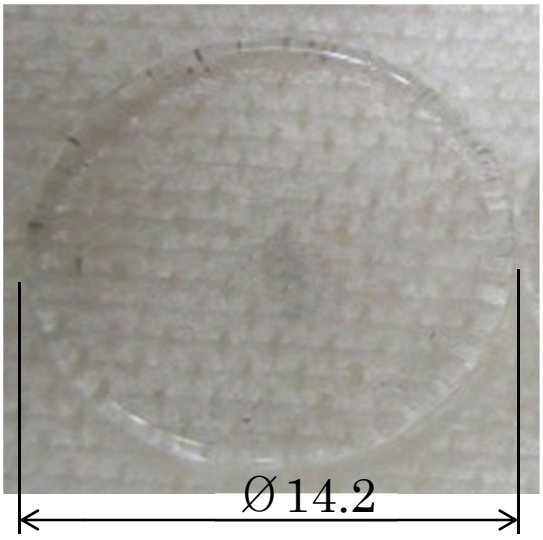

Fig.5.14 Molded glass

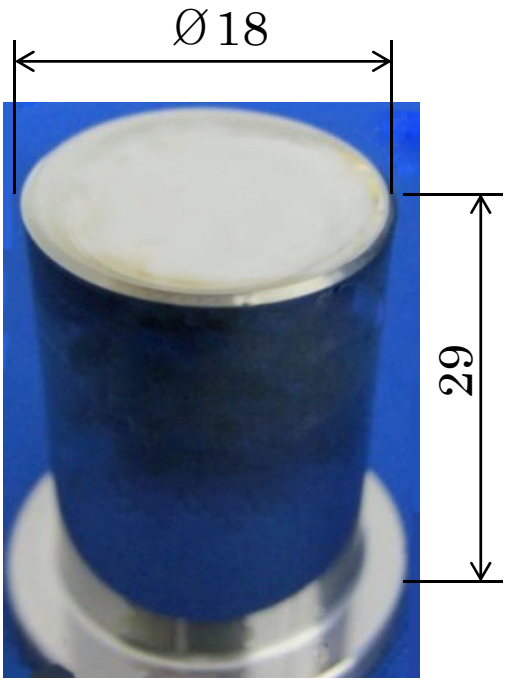

Fig.5.15 Mold after ten times molding test

5.4 Summary

The thermal property of $Ni_{51}Nb_{33}Ti_{16}$ with good machinability was evaluated. $Ni_{51}Nb_{33}Ti_{16}$ thin film sample was deposited on Alumina substrate. This sample was heated in a vacuum chamber up to 1023K at heating speed 12K/min. The real temperature of sample was measured by thermocouple while the apparent temperature of sample was measured by thermography.

The crystallization temperature of $Ni_{51}Nb_{33}Ti_{16}$ was measure to be 881K which is higher the molding temperature of glass lens 723K. However, even at lower temperature, crystallization can also happen as long as the heating time is long enough. Time is a very important factor other than

temperature for the evaluation of thermal stability. For TTT test, the temperature distribution of sample makes it possible to obtain TTT data with high throughput. The TTT curve of $Ni_{51}Nb_{33}Ti_{16}$ thin film sample explains that this material is with satisfying thermal stability.

The oxidation resistance experiment was carried out at temperature 723K for 20h in air. Moreover, another experiment was also carried out to measure adherence of $Ni_{51}Nb_{33}Ti_{16}$ to glass. The good results of those two experiments show that $Ni_{51}Nb_{33}Ti_{16}$ is qualified as glass lens mold material.

Chapter 6 Conclusions and future works

6.1 Conclusions

The objective of this research was to develop a combinatorial evaluation method to find out an amorphous alloy suitable for the mold material of glass lens which has diffraction gratings on the surface. The requirements of mold materials for glass lenses with diffraction gratings are listed as following: tensile strength over 1GPa which can prevent mold from breaking during cooling process, hardness over 7GPa which can make sure that the mold is able to withstand high compressing force during molding process, high thermal stability to endure to be heated for 100 h at temperature 723K which can guarantee no appearance of crystallization of mold material, excellent machinability which can provide the possibility to process gratings with high accuracy. Among those requirements, machinability and thermal stability are very difficult to meet. As a result, in this research, a novel combinatorial evaluation method of machinability was proposed and applied in the search for suitable glass lens mold material.

The experiments which were carried out using proposed combinatorial evaluation method to search for the glass lens mold material are described in this thesis. The specific content and results of each chapter are explained as following:

Based on the results of previous research on Ni-Nb-Zr, a fourth element was decided to add in order to reduce hardness and improve machinability. As explained in Chapter 2, the addition of Ti did succeed to reduce the hardness. Three Ni-Nb-Zr-Ti thin film samples, $Ni_{30}Nb_{35}Zr_{25}Ti_{10}$ at.% , $Ni_{28}Nb_{32}Zr_{25}Ti_{15}$ at.% and $Ni_{25}Nb_{30}Zr_{25}Ti_{20}$ at.%, were fabricated to evaluate their properties, including their tensile strength, thermal stability, hardness, and machinability. The results demonstrated that adding Ti did decreased the hardness of the amorphous alloy thin films and made it possible to not only be taper cut but also micro-cut. Moreover the machinability of sample improved with increasing Ti content level. In order to maintain other properties such as tensile stress and thermal stability, Ni-Nb-Ti was considered to be our research subject since higher Ti content can be achieved in this system.

Ni-Nb-Ti thin film libraries were obtained by combinatorial arc plasma deposition method for thermal stability test which was carried out at first to narrow down the research area in the Ni-Nb-Ti alloy system. Three Ni-Nb-Ti thin film libraries were made for thermal stability test which almost covered the whole composition of Ni-Nb-Ti alloy system. From the results an area of amorphous alloys with composition belonging to Ni 40-58 at.%, Nb 24-46 at.%, Ti 5-20 at.%, presented high thermal stability which can endure high temperature for a long time. This area will be the main research area for the machinability test.

Since conventional evaluation method for machinability becomes time-consuming and costly, novel evaluation method with high throughput was proposed in Chapter 3. A combinatorial target composed of two parts was designed to deposit a thin film sample with grading compositions of which in the center Ti content is rich and becomes gradually decreasing from center to edge. After cutting test, the roughness (Ra) of cutting surfaces will be measured. It is clearly to see this new method is more efficient than conventional method, which is able to measure a lot of compositions' machinability at one time with one sample.

In the trial experiment, two factors, the size of inner target and TS distance, which have great influence on the grading condition of Ti content in the thin film sample, were finally decided to be Ø36 and 31mm. But Ti content level was 44% to 62% higher than desired one 5%-30%. As a result, Ni-Nb-Ti alloy was made as inner part target instead of pure Ti. Although, at first, Ti content grading condition were not as good as trial experiment, there was a tendency that when increasing Ni's content level in outer part or decreasing Ni's content level in inner part, Ti content grading condition becomes a little better. New inner part targets $Nb_{50}Ti_{50}$, $Nb_{66}Ti_{34}$, $Nb_{83}Ti_{17}$ and outer part targets $Ni_{60}Nb_{40}$, $Ni_{70}Nb_{30}$, $Ni_{80}Nb_{20}$, $Ni_{90}Nb_{10}$, were designed which would be adopted for the continuing experiment.

Finally, the target with inner part $Ni_{15}Nb_{20}Ti_{65}$ and outer part $Ni_{60}Nb_{40}$ was determined to deposit thin film sample for cutting test. The

roughness of cut surface had been measured. Although the best value of roughness is 21nm which is larger than the requirement for glass lens mold material 5nm, the result had proved the feasibility of the novel combinatorial method on machinability introduced in this research.

In Chapter 4, Nb-Ti alloy inner targets $Nb_{50}Ti_{50}$, $Nb_{66}Ti_{34}$ and $Nb_{83}Ti_{17}$, were combined with outer targets $Ni_{90}Nb_{10}$, $Ni_{80}Nb_{20}$, $Ni_{70}Nb_{30}$ and $Ni_{60}Nb_{40}$ to fabricate thin film samples. These twelve samples can almost cover the desired composition area with high thermal stability. The composition result of these samples manifest a tendency that the higher Ti content level is in inner target, the larger is Ti content range in the thin film sample. The thin film sample deposited by inner target $Nb_{50}Ti_{50}$, outer target $Ni_{70}Nb_{30}$ has the largest Ti content range and a good grading condition of Ti, which was decided to be the next cutting sample.

The composition result of cutting sample confirmed that long- time sputtering does not have a serious impact on the condition distribution. Roughness of the sample was measured to be larger than the requirement for glass lens mold material 5nm. Although the composition with good machinability has not been found, it confirmed the feasibility of the novel combinatorial method for evaluation of machinability proposed in this thesis.

Ti grading condition of the thin film sample made by combinatorial targets is symmetrical which means that only a few parts of sample can cover the Ti content range of the entire sample. This makes it possible to

further improve the combinatorial method by a cover mask. By using a cover mask, three samples can be deposited onto one substrate. The composition results of thin film libraries confirmed that the application of cover mask did not have serious influence on the composition distribution of samples.

Two more cutting samples were fabricated for cutting test, by using inner target $Nb_{50}Ti_{50}$ and $Nb_{66}Ti_{34}$, combined with outer targets $Ni_{90}Nb_{10}$; $Ni_{80}Nb_{20}$ and $Ni_{70}Nb_{30}$. After cutting test, surface roughness of cutting samples was examined. Finally, a composition $Ni_{51}Nb_{33}Ti_{16}$ was found to be with roughness less than 5nm which is the requirement for glass lens mold material.

Mechanical properties of $Ni_{51}Nb_{33}Ti_{16}$ were also measure. Hardness and tensile strength of it were evaluated to be 9.1GPa and 2.24GPa which meet the requirements for glass lens mold material.

In Chapter 5, the thermal property of $Ni_{51}Nb_{33}Ti_{16}$ with good machinability was evaluated. $Ni_{51}Nb_{33}Ti_{16}$ thin film sample was deposited on Alumina substrate. This sample was heated in a vacuum chamber up to 1023K at heating speed 12K/min. The real temperature of sample was measured by thermocouple while the apparent temperature of sample was measured by thermography.

The crystallization temperature of $Ni_{51}Nb_{33}Ti_{16}$ was measure to be 881K which is higher the molding temperature of glass lens 723K. However, even at lower temperature, crystallization can also happen as long as the heating time is long enough. Time is a very important factor other than

temperature for the evaluation of thermal stability. For TTT test, the temperature distribution of sample makes it possible to obtain TTT data with high throughput. The TTT curve of $Ni_{51}Nb_{33}Ti_{16}$ thin film sample explains that this material is with satisfying thermal stability.

The oxidation resistance experiment was carried out at temperature 723K for 20h in air. Moreover, another experiment was also carried out to measure adherence of $Ni_{51}Nb_{33}Ti_{16}$ to glass. The good results of those two experiments show that $Ni_{51}Nb_{33}Ti_{16}$ is qualified as glass lens mold material.

Finally, as explained before, the combinatorial evaluation method on machinability proposed in this thesis is feasible and an amorphous alloy $Ni_{51}Nb_{33}Ti_{16}$ was found to be with good machinability by using the combinatorial evaluation method. A high-throughput evaluation method was used to measure crystallization property of $Ni_{51}Nb_{33}Ti_{16}$. The result shows that $Ni_{51}Nb_{33}Ti_{16}$ has high thermal stability. The results of mechanical properties, oxidation resistance and adherence to glass prove that $Ni_{51}Nb_{33}Ti_{16}$ is qualified as glass lens mold material. Properties of it is shown in Table 6.1

Table 6.1 Properties of $Ni_{51}Nb_{33}Ti_{16}$ amorphous alloy

Machinability (Ra< 5nm)	Thermal stability (723K for 100h in vacuum)	Tensile strength (>1 GPa)	Hardness (> 7GPa)	Oxidation resistance (723K for 20h, in air)	Adherence to glass
OK (Ra=3nm)	OK (Amorphous)	OK (2.24GPa)	OK (9.1GPa)	OK	OK

6.2 Future works

By using the novel combinatorial evaluation method proposed in this research, it is efficient to find the material $Ni_{51}Nb_{33}Ti_{16}$ alloy which is qualified as glass lens mold material. In the future, the mold of glass lens with diffraction gratings will be fabricated by using $Ni_{51}Nb_{33}Ti_{16}$ amorphous alloy. Moreover, the TTT test explained in Chapter 5 will be improved in the future research to be able to detect the minor change of emissivity during crystallization.

Reference

[1] Yi, A. Y., Optical fabrication, in Encyclopedia of Applied Physics, P. K. Mallick, ed. (Dekker, 2003).

[2] Maschmeyer, R. O., et al., Precision molded glass optics, Applied Optics. 22, 2410–2412 (1983).

[3] Sakurai, J., Hata, S., Yamauchi, R., and Shimokohbe, A., Characterization of the Pt-Hf-Zr-Ni Thin Film Amorphous alloys for Precise Optical Glass Lens Mold, Journal of Solid Mechanical Materials Engineering., Vol.3, No.8 (2009) pp.1022-1032.

[4] Y. Liu, S. Hata, K.Wada and A. Shimokohbe: Jpn. J. Appl. Phys., 40, (2001), 5382.

[5] Blair et al., “Method of Molding Glass Elements and Element Made”, US Patent 4139677, 1979.

[6] Y. Taniguchi, et al. “Mold Having a Diamond Layer, for Molding Optical Elements”, US Patent 5380349, 1995.

[7] C. Leu, “Mold for Molding Optical Lenses”, US Patent Application 2006/0201205, 2006.

[8] Yi, A. Y., et al., Development of a compression molding process for three-dimensional tailored free-form glass optics, Applied Optics, Vol.45, No.25 (2006).

[9] Y.H. Kim, A. Inoue, and I.Masumoto: Mater. Trans., JIM, 31, 747(1990)

[10] H. Chen, Y. He, G. J. Shilet, and S. J. Poon: Scripta Met., 25, 1421 (1991)

[11] Y. Kawazoe, M. Hasegawa, A. Inoue, N. Kobayashi, T. Sakurai, L. Wille: Amorphous and Nanocrystalline Materials

[12] A. Inoue, B. L. Shen, H. Koshiba, H. Kato, A. R. Yavari: Acta Mater., 52, (2004),1631-1637.

[13] E.O.Hall: Proc. Phys. Soc., Ser. B, vol. 64, (1951) 747-753.

[14] N.J.Petch: J. Iron and Steel Institute, (1953) 25-28.

[15] Fujii, T., Hirano, M., Shibukawa, T., Ishida, T., and Takeuchi, Y., Study on Precision Machining of Glass Lens Mold with Minute Structure, Journal of Japan Society of Precision Engineering Vol.74, No.12 (2008) pp.1298-1302 (in Japanese).

[16] Pramanik, A., Neo, K.S., Rahman, M., Li, X.P., Sawa, M., and Maeda, Y., Cutting performance of diamond tools during ultra-precision turning of electroless-nickel plated die materials, Journal of Materials Processing Technology, Vol.140, No.1-3, (2003) pp.308-313.

[17] Junpei Sakurai, Seiichi Hata, Ryusuke Yamauchi, Hiroyuki Tachikawa, AkiraShimokohbe : MRS Proc., 1024E, A01-06 (2007.11, Boston, USA)

[18] Mitsuhiro Abe, Seiichi Hata, Ryusuke Yamauchi, Junpei Sakurai, Akira Shimokohbe,: MRS Proc., 1024E, A06-08 (2007.11, Boston, USA)

[19] Mitsuhiro Abe, Combinatorial Search for Glass Lens Mold Materials, M.S. Thesis, Tokyo Institute of Technology, 2009.

[20] Sakurai, J., Hata, S., Yamauchi, R., Abe, M., and Shimokohbe, A., Searching for Pt-Zr-Ni thin film amorphous alloys for optical glass lenses molding materials, Precision Engineering, Vol.34, No.3 (2010), pp.431-439.

[21] Hata, S., Sakurai, J., SHimokohbe, A., Experimental fabrication of glass lens molding die made of novel Pt based amorphous alloy. Trans Jpn

Soc Mech Eng Series C 2008;74:1020–5 (in Japanese).

[22] Yamauchi, R., Hata, S., Sakurai, J., Shimokohbe, A., Combinatorial search for a new amorphous alloys as mold materials for glass molding—evaluation of crystallization temperature and mechanical property. J Jpn Soc Prec Eng 2008;74: 252–7 (in Japanese).

[23] Sakurai, J., Abe, M., Ando, M., Aono, Y., and Hata, S., Searching for noble Ni-Nb-Zr thin film amorphous alloys for optical glass device molding die materials, Precision Engineering 35 (2011)537-546.

[24] Sakurai, J., Abe, M., Ando, M., Aono, Y., Shengxian, Jiang., Shimokohbe, A., and Hata, S., Effect of sputtering method on characteristics of amorphous Ni-Nb-Zr alloys for glass lenses molding die materials, J. Solid Mechanics and Mat. Eng. Vol.4, No.12 (2010) 1742-1753

[25] Sakurai, J., Abe, M., Ando, M., and Hata, S., Combinatorial searching for Ni-Nb-Zr amorphous alloys as glass lens molding die materials, Key Engineering Materials., Vol.447-448(2010)pp.661-665.

[26] Materials Science of Amorphous Metals

[27] Electrons, Atoms, Metals and Alloys

[28] X,Yang., C,R,Liu., Machining titanium and its alloys, Machining Science and Technology 3(1)(1999)107–139.

[29] C, R, Dandekar., Y, C, Shin., J, Barnes., Machinability improvement of titanium alloy (Ti-6Al-4V) via LAM and hybrid machining, International Journal of Machine Tools& Manufacture 50(2010) 174-182.

[30] S. Hata, R. Yamauchi, J. Sakurai and A. Shimokhobe:Jpn. J. Appl. Phys., 45, (2006),2708

[31] Y. Yamamoto, Y. Agawa, Y. Hara, S. Amano, A. Chayahara, Y.Horino and K. Fujii: Proc. Int. Conf. Ion Implantation Technology,1998, Vol. 2, p.

1148.

[32] Yuko Aono, Junpei Sakurai, Tetsuo Ishida, Akira Shimokohbe, Seiichi Hata. High-Throughput Measurement Method for Time-Temperature-Transformation Diagram of Thin Film Amorphous Alloys, Appl. Phys. Express, Vol. 3, No. 12, 125601, Dec. 2010.

Acknowledgement

I would like to express my heartfelt gratitude to Professor Seiichi Hata, who gave me the possibility to complete my research for Doctor course, by his financial support, his wise advice when some trouble happened, and to Professor Takeshi Hatsuzawa, Professor Toshiharu Kagawa, Professor Shinichi Yokota, and Associate Professor Hayato Yoshioka, for being as the reviewers for my doctor thesis.

I also extend my sincere thanks to Mr. Masayuki Ando who taught me all the equipments and relative knowledge of my research, to Ass. Prof. Junpei Sakurai who supported me in my research work and gave me profound opinions about my research, to Dr. Yuko Aono who helped me not only with my research but also with my new life here in Japan

Thanks to all the present and past members of Hata laboratory for all their assistance, support and valuable advice. I appreciate the happy time with Miss Yui Ishida for whose kind help with Japanese, Mr. Kota Takagaki for whose generous share of manga, Mr. Hiroshi Kozako for the interesting conversation in English and Chinese. I am grateful to the happy time with Ms. Nastaran Tamjidi talking about all the things, family, research, traditions and secrets.

Finally I would like to take this opportunity to express my grateful thanks to my parents and my husband Tao Wang, for whose patient love and support which enabled me to complete this research.